Aptamer-Facilitated Biomarker Discovery of Leukemia Cells with Mass Spectrometry and Their Detection with Luminescent Nanoparticles

Yaroslav Grechkin

This Thesis is submitted to the Faculty of Graduate and Postdoctoral Studies in partial fulfillment of the requirements for Master's Degree in Chemistry and Biomolecular Sciences

Department of Chemistry and Biomolecular Sciences

Faculty of Science

University of Ottawa

© Yaroslav Greckin, Ottawa, Canada, 2019

TABLE OF CONTENTS

Preface

This thesis is an original intellectual product of Yaroslav Grechkin. No part of this thesis has been previously published.

Chapter I was written by Yaroslav Grechkin and summarizes recent advances and existing challenges in aptamer-target identification methods along with the employment of aptamer-conjugated nanoparticles for leukemia cell detection. Mr. Emil Zaripov prepared **Figure 1.2** and contributed to manuscript edits. Dr. Zoran Minic has prepared **Figures 1.3, 1.4, 1.5 and 1.6** and contributed to manuscript edits.

Chapter II was written by Yaroslav Grechkin. Mrs. Svetlana Grechkina (*A.E. Arbuzov Institute of Organic and Physical Chemistry, Kazan Scientific Center, Russian Academy of Sciences, Kazan, Russia*) performed the synthesis of luminescent Tb (III)-doped silica nanoparticles and their surface modification. Yaroslav Grechkin performed the conjugation of Sgc8-apatamer with luminescent Tb (III)-doped silica nanoparticles and all instrumental analyses. Dr. Svetlana Fedorenko (*A.E. Arbuzov Institute of Organic and Physical Chemistry, Kazan Scientific Center, Russian Academy of Sciences, Russia*) and Dr. Maxim Berezovski were involved throughout the project in concept formation and manuscript edits. Mr. Emil Zaripov prepared **Figure 2.4,** and **Figure 2.1** was prepared and provided by Dr. Svetlana Fedorenko.

Chapter III was written by Yaroslav Grechkin under the supervision of Dr. Maxim Berezovski. Yaroslav Grechkin performed flow cytometry, aptamer-protein complexes pull-down and in-solution digestion and mass spectrometry sample preparation experiments. All mass spectrometry analyses were performed by Dr. Zoran Minic. Mr. Nico Huttmann and Mr. Emil Zaripov performed statistical and bioinformatics analyses.

Scope of the thesis

Aptamers have displayed numerous advantages over antibodies, which made them attractive for various biological applications. Nevertheless, there is a number of factors, which limit their wide usage in biomedicine, such as tedious selection process, non-specific binding due to electrostatic interactions and low nuclease resistance. Moreover, aptamer-based imaging probes may have the decreased efficiency (either as a result of the loss of the aptamer binding, or the decreased sensing efficiency of a probe) after the conjugation as well as aptamer-target identification associated challenges. This thesis is focused on two aforementioned aspects, which have great importance for further use of aptamers as diagnostic probes and aptamer-based biomarker discovery. Particularly, Chapter II is dedicated to the development of the luminescent aptamer-based probes for leukemia cell detection, using Sgc8-aptamer conjugated with silica Tb-doped nanoparticles, while Chapter III is focused on the improvement of the aptamer molecular target identification approach, using AptaBiD. Thus, this Thesis is aimed to answer the following questions:

1. Would Sgc8-aptamer remain its strong binding with leukemia cells after the conjugation with silica Tb-TCAS nanoparticles? Would luminescent properties of silica Tb-TCAS nanoparticles be affected by the conjugation with the aptamer? How aptamer-conjugated nanoparticles will affect the cell viability of leukemia cells? (Chapter II)
2. Does Sgc8-aptamer bind exclusively leukemia cells, or its target can be found on non-malignant lymphocytes? Could AptaBiD target identification approach be used for Sgc8-aptamer molecular target identification? Could formaldehyde cross-linking facilitate the aptamer target identification? (Chapter III)

Abstract

Aptamers have shown a great potential due to their cheaper synthesis and easy chemical modification compared to antibodies, and have been employed in various biological assays and applications throughout the last two decades. Despite of their limitations, such as non-specific binding and low nuclease resistance, aptamers could be successfully used in the biomarker discovery and for the development of the aptamer-based imaging probes for *in vitro* assays.

In this thesis, luminescent aptamer-conjugated nanoparticles were developed and utilized for leukemia cell detection with fluorescent microscopy. It was shown that for the bioconjugation of an aptamer with luminescent nanoparticles it is more beneficial to use carboxyl-modified nanoparticles, which results in a stable luminescence after the conjugation and the absence of unsaturated and unstable conjugates, unlike with amino-modified nanoparticles. Moreover, a cell viability assay was performed and it was revealed that aptamer-conjugated nanoparticles did not induce spontaneous apoptosis and necrosis of leukemia cells, which can be further explored with additional cytotoxicity tests, whether the aptamer-conjugated nanoparticles are biocompatible, or not.

Aptamer-based biomarker discovery implies disease biomarker identification, and most commonly used methods are tedious and require a relatively high concentration of captured aptamer-target complexes. For that, AptaBiD was used in order to optimize aptamer-target identification method. Using Sgc8-aptamer, it was first shown with flow cytometry that it binds to both, healthy and malignant T lymphocytes, which requires further improvements for this aptamer to be used for leukemia detection. Among three tested detergents for the aptamer-target purification, DDM happened to be the most suitable one, due to its gentle cell lysis and solubilization properties. However, the cross-linking with formaldehyde has not positively affected the results obtained and could be replaced with photocross-linking in future experiments, which would allow to selectively

cross-link an aptamer with a photomodified nucleobase with its target. Lastly, a high number of intracellular proteins identified within samples could be associated with the aptamer non-specific binding and internalization, which could be improved in future with an alternative cell fractionation with a membrane isolation approach used for the identification of transmembrane target protein.

Acknowledgments

I want to express my sincerest gratitude to my family, especially, to my mother and grandmother, who have been always supporting me throughout the life. I owe you my success and all my achievements because without you I would not be the person I am now.

I would like to thank my scientific advisor, Dr. Maxim Berezovski, for his warm support and guidance throughout my graduate studies at the University of Ottawa. Thank you for being more than just a great supervisor, and giving me all the opportunities to achieve my career goals. I have learned a lot of skills and techniques, and most importantly, realized what I would like to focus on later in life.

I have to thank Dr. Eva Hemmer for her sincere support and advice with my studies and research. You have been my source of inspiration and I am grateful for your guidance and supervision.

I want to express my genuine gratitude to Dr. Shahrokh Ghobadloo, who helped me a lot with my research as well as always could find a way to cheer me up and open my eyes wider on certain things. I need to thank Dr. Zoran Minic for his motivational feedback and assistance with my experiments as well as all the skills and knowledge I have obtained.

I am very grateful for my friends and lab mates, who always managed to be around and played a huge role in my success at the university. Thank you, Emil, for being helpful, caring and kind friend. Thank you, Nico, for being a great example, in both, science and social life. Thank you Yuchu, Suttinee and Ahmed for supporting me, listening to my stories and giving me your advice and critics, and being people I will always look up to.

List of abbreviations

2D-GE – two-dimensional gel electrophoresis

5-dUI - 5-iodo-deoxyuridine

7-AAD – 7-aminoactynomycin D

AB – antibody

ALL – acute lymphoblastic leukemia

AML – acute myeloid leukemia

AptaBiD – Aptamer-Facilitated Biomarker Discovery

Apt – aptamer

APC – allophycocyanin

AP-MS – affinity purification mass spectrometry

APTES – (3-aminopropyl)triethoxysilane

ATP synthase – adenosine triphosphate synthase

AgNPs – silver nanoparticles

AuNPs – gold nanoparticles

bFGF – basic fibroblast growth factor

BrU - 5-bromo-2'-deoxyuridines

CD3 – cluster of differentiation 3

CD4 – cluster of differentiation 4

CD109 – cluster of differentiation 109

CD117 – cluster of differentiation 117, mast/stem cell growth factor receptor

CD62L - – cluster of differentiation 62L, L-selectin

CD49d – cluster of differentiation 49d, alpha integrin 4

CID – collision-induced dissociation

CMC – critical micelle concentration

CLL – chronic lymphocytic leukemia

CML – chronic myeloid leukemia

CT – computer tomography

DAPI - 4′,6-diamidino-2-phenylindole

DDM – n-dodecy-β- maltopyranoside

DNA – deoxyribonucleic acid

DPBS – Dulbecco's Phosphate Buffer Saline

Dsh – dishevelled protein

EDAC – 1-ethyl-3-(3-dimethylaminopropyl) carbodiimide

EDTA – ethylenediaminetetraacetic acid

ELISA – enzyme-linked immunosorbent assay

EMSA – electrophoretic mobility shift assay

EPR – enhanced permeability and retention effect

FAM – 6-carboxyfluorescein

FDA – Federal Drug Administration

FITC – fluorescein isothiocyanate

FS – forward scatter

GSH-Px – glutathione peroxidase

HIV – human immunodeficiency virus

HPLC – high-performance liquid chromatography

K_d – dissociation/binding constant

LC-MS – liquid chromatography-mass spectrometry

MS – Mass Spectrometry

mRNA – messenger ribonucleic acid

MRI – magnetic resonance imaging

NPs - nanoparticles

PBS – phosphate buffer saline

PCR – polymerase chain reaction

PCP signaling – planar cell polarity signaling

PD1 – programmed cell death protein 1

PD-L1 - programmed death-ligand 1

PE – phycoerythrin

PEG – polyethylene glycole

PI – Propidium Iodide

PKCδ1 – protein kinase C delta

PTK7 – protein tyrosine kinase 7

PMBC – peripheral blood mononuclear cells

RNA – ribonucleic acid

SELEX – Systematic evolution of ligands by exponential enrichment

SDS-PAGE – sodium dodecyl sulfate polyacrylamide gel electrophoresis

SNs – silica-coated Tb-TCAS nanoparticles

SS – side scatter

ssDNA – single-stranded DNA

T-ALL – acute lymphoblastic leukemia

TCAS - thiacalix[4]arenesulfonate

TEOS – tetraethyl orthosilicate

TEM – transmission electron microscopy

tRNA – transfer ribonucleic acid

UV – ultraviolet

VEGF – vascular endothelial growth factor

Wnt signaling – wingless/integrated signaling

List of figures

(b) in water. Zeta potential values of Sgc8 aptamers, SNs-COOH, SNs(COOH)-Sgc8 (c) and Sgc8 aptamers, SNs-NH_2 and SNs(COH)-Sgc8 (d) measured in water.

Figure 2.6. (a) Fluorescamine fluorescence spectra after interaction with various concentration of Sgc8-aptamer (1.5 μM, 0.75 μM, 0.375 μM, 0.15 μM, 0.075 μM, 0.0375 μM) and SNs-NH_2, SNs-COOH, SNs(COH)-Sgc8 (0.34 g L^{-1}) and SNs(COOH)-Sgc8 (0.34 g L^{-1}). All spectra were obtained in 50 mM borate buffer under excitation wavelength – 390 nm. (b) Calibration curve.

Figure 2.7. Emission spectra of SNs-COOH (a) and SNs-NH_2 (b) before and after conjugation with Sgc8-aptamer, and a schematic representation of Tb(III)-TCAS-SiO_2 energy levels (c). Solid line represents radiative transitions, dotted line – non-radiative transitions, and * represents $^5G_6$, $^5L_{10}$, $^5G_5$, $^5D_2$, $^5L_9$ energy levels. All spectra were obtained in water media under excitation wavelength – 330 nm; concentration of nanoparticles – 0.5 g L^{-1}.

Figure 2.8. Flow cytometry analysis with Sgc8 aptamer binding with CCRF-CEM and Jurkat cell lines (positive), and Raji cell line (negative control).

Figure 2.9. Fluorescent microscopy images of CCRF-CEM cells treated with DAPI, SNs-COOH (control sample), SNs(COOH)-Sgc8 and SNs(COH)-Sgc8. Excitation wavelength – 340 nm.

Figure 2.10. Fluorescent microscopy images of Jurkat cells treated with DAPI, SNs-COOH nanoparticles (control sample), SNs(COOH)-Sgc8 and SNs(COH)-Sgc8. Excitation wavelength – 340 nm.

Figure 2.12. Cell viability assay with Annexin V-FITC and PI after 48 hours of incubation. SNs(COOH)-Sgc8 concentration: 0 μg/mL (a), 25 μg/mL (b), 50 μg/mL (c) and 100 μg/mL (d).

Figure 3.1. Flow cytometry graphs, representing the gating strategy based on PI signal. All cells stained with PI (necrotic) were discarded from further analysis, and gates were adjusted on single-cell viable cell subpopulation.

Figure 3.9. Venn diagrams, representing the amount of proteins identified with MS within each sample. In the following experiment we optimized all the previous conditions (including the incubation at 4 C^{o}), and n-dodecyl-β-D-maltopyranoside was used as a detergent. MS results were obtained in triplicates for each sample, and only mutual proteins found in each of triplicates were used for further analyses.

List of tables

Chapter I: General Introduction

Aptamers for biomarker discovery

Researchers around the globe were always interested in the discovery of specific molecular signatures that will allow them to predict, treat, or even prevent many of the known and unknown diseases. These molecular signatures, or biomarkers, contain the unique information regarding our body state, and in case of any adverse changes inside the organism they immediately indicate such alterations, and, as a result, any illness can be detected, or even treated during its initial stage. Biomarkers are broadly determined as biomolecules that indicate any alterations in expression or state of genes and proteins in cells. When these changes are detected, there is a clinical correlation with the disease pathogenesis, individual susceptibility to disease, and even with the probability for the success of a given restorative regimen[1]. Nowadays, there are over than 35 oncology biomarkers have been approved by FDA for the diagnosis or therapy, and some of the antibody-based drugs are being successfully used in clinical settings, such as recently approved Pembrolizumab (PD-L1 Antibody) and Nivolumab (Anti-PD-1 Antibody). Hence, biomarker discovery is a vital biomedical application because it allows developing our knowledge of various diseases' treatment and diagnosis.

Even though there was a number of developments in cancer therapy during the last three decades, it still remains as the major public health problem worldwide[2]. The most common method for cancer treatment is the chemotherapy; however, it does not hit malignancies with the strong specificity, damaging healthy tissues and organs. Discovery of new biomarkers and their further study is a promising application because using biomarkers it is possible to detect cancer on the cellular, or molecular level at the very early stage, whilst a patient does not have any obvious cancer-related symptoms[3]. Many metabolites and proteins are secreted into the blood pool from malignant cells or

tissues, and then the blood screening (plasma or serum) allows to non-invasively detect cancer biomarkers[4]. Moreover, patient survival directly depends on the early detection, and, therefore, the utilization of biomarkers would greatly ease the disease prognosis.

Nevertheless, biomarker discovery is a challenging application due to a number of factors. First, biomarkers are usually found at the low-abundance, and their detection method should be highly sensitive and accurate. In addition, this method should have the potential to distinguish among the numerous post-translational modifications and isoforms of the same protein[5]. Secondly, widely spread methods for biomarker discovery, such as Western blotting, mRNA screening using quantitative PCR or hybridization arrays, and two-dimensional gel electrophoresis combined with MS[6,7] have an influential disadvantage: they usually tend to distort positive and negative results[8-10]. Indeed, commonly used approaches for identification of protein biomarkers present on the plasma membrane, such as genetic and proteomics methodologies, are mainly designed to identify differences in protein expression patterns of cancer cell samples compared with healthy ones[11,12]. Particularly, proteomics methods include the analysis of complex protein samples using two-dimensional gel electrophoresis and shotgun techniques that employ various membrane solubilization approaches, such as isotope-coded affinity tagging, multidimensional protein identification technique and surface enhanced laser desorption-ionization combined with MS analysis of complex biological mixtures. These methods quite helpful for the analysis of a large number of proteins in their expression patterns; however, identification of specific biomarkers, which are strongly correlated with a specific disease, remains as a complicated task[13]. Finally, antibodies that were widely used for biomarkers discovery[14-16] have several limitations including difficulties in their production due to the biological complexity and the high cost of the procedures. Also, antibodies usually require a

"sandwich system" for the target biomarker detection[17], which means two different antibodies should be capable of recognizing the target, and this makes large-scale biomarker screening impractical[18].

Due to the described downsides of the methods and techniques used for biomarker discovery, a combined approach has emerged termed Aptamer-Facilitated Biomarker Discovery (AptaBiD, **Fig. 1.1**) that implies the aptamer employment for biomarker discovery, and further target identification with MS[19]. Aptamers, called also as "chemical antibodies", are short oligonucleotides that generated specifically for the target molecule recognition[20]. Aptamers showed a plethora of advantages over antibodies; they can be easily synthesized and chemically modified; their conformational changes are usually reversible, making it possible to restore their original structures after the denaturation. In addition, they have a small size, lack of immunogenicity, and fast tissue penetration. Thus, aptamers production is much cheaper and has a higher reproducibility rate than for the antibodies[21], and this approach has gained great popularity these days because of the aforementioned benefits.

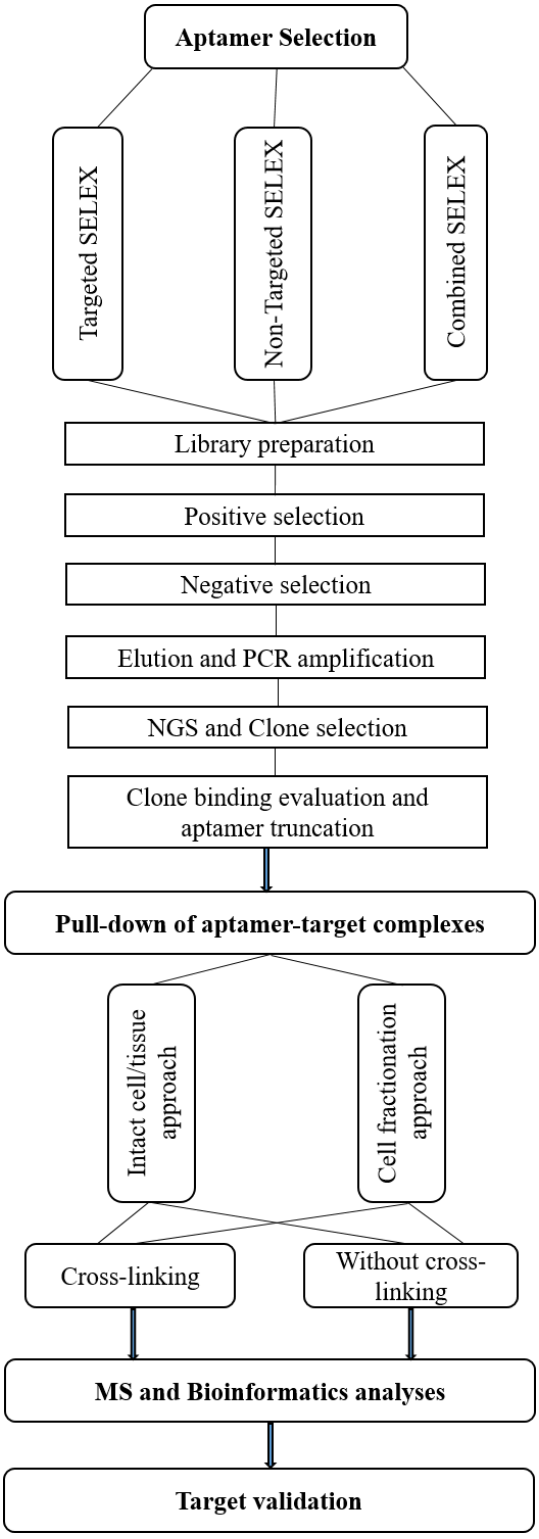

Figure 1.1. Aptamer-Facilitate Biomarker Discovery: a general scheme.

AptaBiD consists of four major stages: the selection of short oligonucleotides, aptamers, to the specific target such as a transmembrane protein, or even a whole cell **(Fig. 1.2)**; and further identification of the target with MS, preceded by the pull-down of biotinylated-aptamer-protein complexes using biotin/avidin affinity isolation system on magnetic beads, which is followed by the mass spectrometric analysis and target validation experiments. Using counter-selection rounds with non-tumor cells, it is possible to select a pool of aptamers recognizing solely the exclusive targets present on the cellular membrane of cancer cells, and therefore, explore new cancer biomarkers.

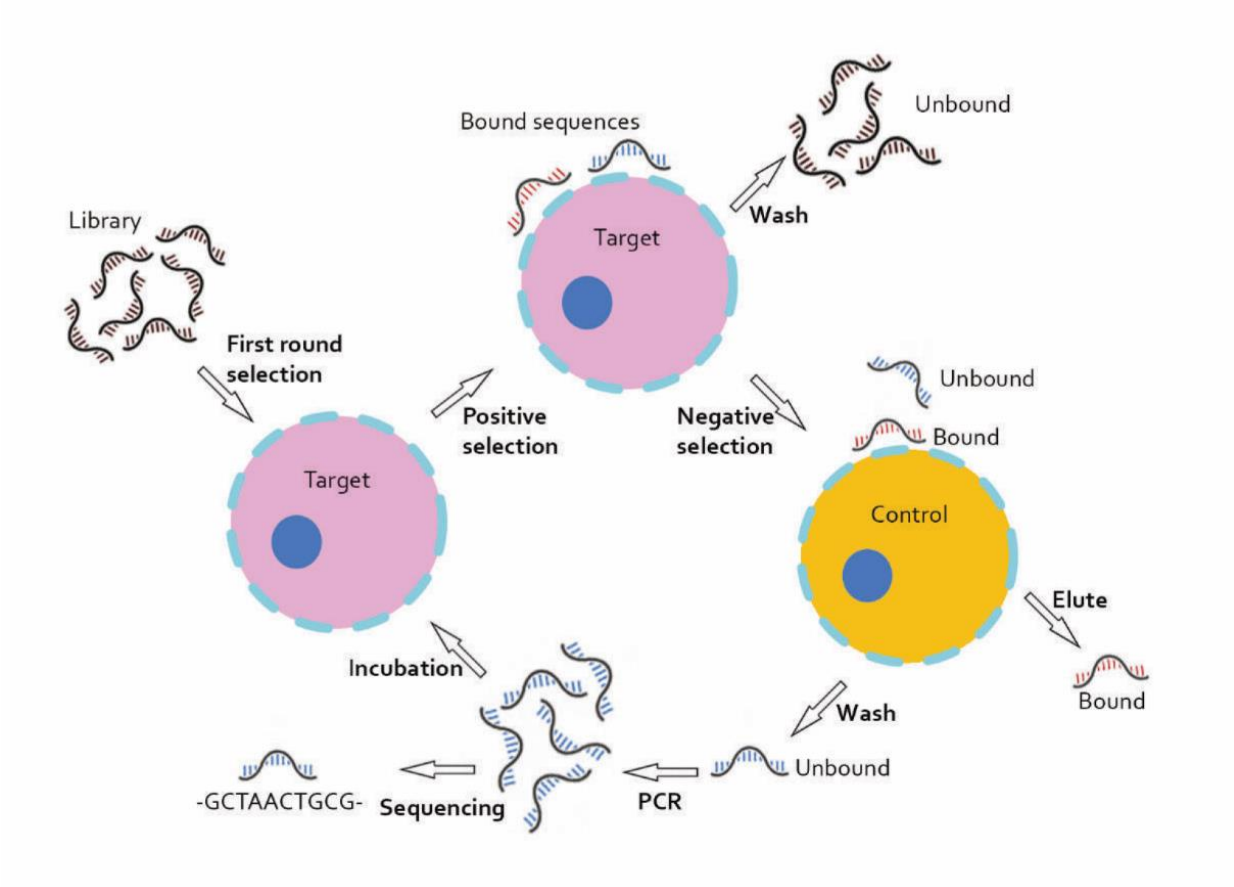

Figure 1.2. Cell-SELEX Scheme

Aptamer target isolation and identification with mass spectrometry: recent advances and remaining challenges

Identification of a molecular target is a vital step towards the application of aptamers for the drug delivery and targeted therapeutics. Although numerous aptamers have been developed over the past two decades, binding partners for only a very limited number of these aptamers have been identified[22]. The identification of the target protein of an aptamer is a challenging task because aptamer-target protein interactions require a native conformation of both, the aptamer and target protein. Moreover, aptamers are usually being selected to transmembrane proteins, and their transmembrane domains are hydrophobic, poorly soluble in water, and of relatively low abundance. Affinity chromatographic separation technologies based on aptamer-biotin/streptavidin interactions played a crucial role in the development of successful methods for confident identification of protein targets. Hence, aptamer-biotin/streptavidin affinity system combined with mass spectrometry (AP-MS) is the most widely employed technique to identify protein target from the complex membrane protein mixture. An integrated workflow for identifying target proteins for aptamer is shown in **Figure 1.3**.

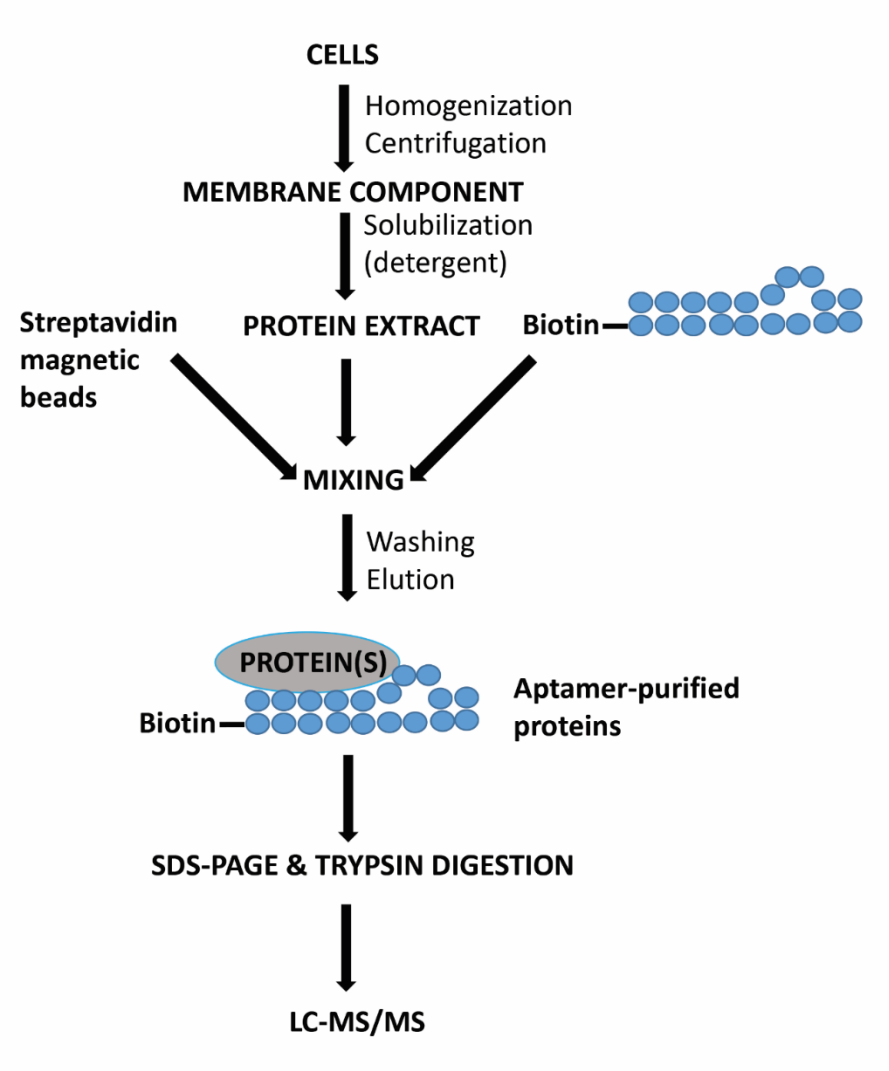

Figure 1.3. General workflow for identification of an aptamer target protein using affinity chromatography based on the biotin-streptavidin system. Membranes are first isolated from cells or tissues and then proteins are solubilized in detergent-containing lysis buffer. Obtained membrane proteins are incubated with a biotinylated aptamer and streptavidin magnetic beads. The beads are first washed, and bound proteins are then eluted. Eluted aptamer-purified proteins are separated by SDS/PAGE, digested and analysed by LC-MS/MS.

Among all the approaches, the most popular is the **intact cell/tissue approach** followed by the pull-down of aptamer-protein complexes using affinity chromatography separation. Briefly, it implies biotinylated aptamer incubation with the cell line or tissue, which were used during the SELEX, and further cell lysis with subsequent pull-down with streptavidin/avidin-coated magnetic beads. Despite the advantages of this method, it requires utilization of an excess of masking DNA/RNA (masking tRNA, salmon sperm, or scrambled DNA) that would block non-specific interactions as well as sophisticated post-experimental analyses, employing bioinformatics assays, as a great number of irrelevant DNA/RNA binding proteins could be pulled-down and identified within samples. For example, Yang M. et al.[23] lysed cells with the lysis buffer containing 0.1 % Triton X-100. After the lysis, cell lysate was centrifuged and the supernatant was incubated with streptavidin-coated magnetic beads and aptamer-protein complexes were captured. Among all the candidate DNA/RNA binding proteins identified with MS, the only membrane protein was Siglec-5, and MS data showed 5 unique peptides as the sequence of Siglec-5. Jia W. et al.[24] used a similar approach: cells were lysed in RIPA buffer containing three non-ionic and ionic detergents (1% Tergitol-type NP-40, 1% sodium deoxycholate and 0.1% SDS) on ice. After centrifugation, proteins were incubated with the biotinylated aptamer S3, and then protein-aptamer complexes were extracted with streptavidin-coated sepharose beads. MS results showed that the candidate protein target for S3 aptamer was CD109, and that was confirmed with EMSA and other validation assays.

Another promising method employs **cell fractionation with the isolation of the membrane component**. The vast majority of aptamers generated through Cell-SELEX interacts with their binding partners, which present on the cellular membrane. Hence, the isolation of the plasma membrane and further lysis and pull-down experiments would facilitate the target identification procedure improving the confidence level of obtained results. Daniels, D. et al.[25] used affinity

purification procedures in order to identify the GBI-10 target on U251 cells. Briefly, stripped cells were homogenized on ice in a sucrose solution, and whole cells and nuclei were removed using centrifugation. It should be noted, that this approach is advantageous, as GBI-10 aptamer was selected to the cellular membrane, and since all the irrelevant DNA/RNA binding and other intracellular proteins were discarded from the further analysis, it was easier to identify its authentic target. Then, the membrane component was solubilized with extraction buffer containing 0.1 % Triton X-100, and cell-surface extracts were incubated with biotinylated aptamers immobilized on streptavidin beads. After that, these complexes were washed and bound targets were then eluted and resolved using electrophoresis prior to silver staining. The digestions were analyzed by automated microcapillary LC-MS/MS. By using this approach, it was revealed that the molecular target of GBI-10 aptamer is tenascin-C.

Table 1.1. List of commonly utilized detergents for aptamer target identification

Identified target proteins	Detergent used	Reference
tenascin-C	0.1 % (vol/vol) Triton X-100	Daniels, D. et al.[25]
CD109	RIPA buffer containing three non-ionic and ionic detergents (1% Tergitol-type NP-40, 1% sodium deoxycholate and 0.1% SDS)	Jia W. et al.[24]
Siglec-5	0.1 % (vol/vol) Triton X-100	Yang M. et al.[23]
ALPPL-2	0.1 % (vol/vol) Triton X-100	Dua P. et al.[26]
α-subunit of mitochondrial ATP synthase and Filamin A	0.1% sodium deoxycholate	Kolovskaya O.L. et al.[27]
Vimentin	0.1% sodium deoxycholate	Zamay G. et al.[28] and Zamay T. et al.[29]
IHMC (Immunoglobin Heavy Mu Chain)	0.1% Nonidet P-40, 1.25 % cholesteryl-hemisuccinate and 2.5% n-dodecyl-β-d-maltoside.	Mallikaratchy P., Tan W. et al.[13]
Vimentin	Pierce lysis buffer that contains 1% Tergitol-type NP-40	Recently, Wang Y. et al.[30]
selectin L (CD62L) and integrin α4 (CD49d)	2% (vol/vol) Triton X-100 and 0.4% (w/v) SDS	Bing T. et al.[31]

Membrane protein solubilisation is crucial for future identification of a target protein by using liquid chromatography-mass spectrometry (LC-MS)-based approach. Detergent-based lysis buffers showed higher efficiencies and yields in the solubilisation of membrane proteins[32]. Nevertheless, the majority of the commercially-available detergents are usually poorly compatible with MS, and sometimes detergent removal is mandatory. Detergents used for the identification of a molecular target of the aptamer are presented in **Table 1.1**, and the most commonly used detergents for this application are non-ionic surfactants, which allow gently isolating transmembrane proteins, not disrupting the protein naïve state. Nevertheless, the selection and implementation of a detergent for the solubilisation of membrane proteins still remains as a challenging task. For instance, Dua P. et al.[26] washed pancreatic cells twice with chilled hypotonic buffer and incubated with the same buffer containing protease inhibitors. Then, the buffer was removed, and cells were washed again two times and homogenized with membrane lysis buffer containing 0.1 % Triton X-100. Afterwards, the lysate was centrifuged and concentrated membrane lysate was incubated with biotinylated aptamer-SQ-2. SQ-2-protein complex was captured by the incubation with pre-blocked streptavidin-agarose beads, and this complex was collected by centrifugation and washed four times with lysis buffer. ALPPL-2 was identified as a target membrane protein, and authors confirmed that with several validation assays. Triton X-100 remains one of the most popular non-ionic detergents in many studies, mostly due to its cost and properties, allowing proteins to retain their native structure. In another study, Kolovskaya O.L. et al.[27] incubated biotinylated aptamers with cells, and streptavidin-coated magnetic beads. Then, this mixture was used to extract targets bound with aptamers. Sodium deoxycholate in phosphate buffer was used as a detergent for gentle cell lysis. Detergent choice plays a big role in aptamer-bound target pull-down experiments, and this is associated with the chemical nature of a surfactant along with the localization of an aptamer target. The ionic surfactants completely disrupt

cellular membranes and denature proteins by breaking protein-protein interactions, whether non-ionic surfactants have milder solubilization properties, disrupting lipid-lipid or protein-lipid interactions within the cellular membrane, which allows proteins to remain structurally intact in their biological state. Thus, using a "soft" non-ionic detergent it is possible to capture aptamer-protein complexes, avoiding irrelevant proteins from the intracellular compartment. After the washing, the precipitate of proteins bound with the aptamers to magnetic particles was diluted with freshly prepared urea, filtered and incubated for dissociation of aptamers from bound proteins. After that, magnetic particles with the aptamers were removed by a magnet, and the supernatant containing the target proteins for the aptamers was harvested for the digestion with trypsin and subsequent sample preparation for MS analysis. According to the MS analysis, potential target proteins of the AS-14 aptamer could be α-subunit of mitochondrial ATP synthase and Filamin A as they both play an important role in carcinogenesis. Zamay G. et al.[28] pre-incubated cells with masking DNA and ssDNA library. Then, cells were incubated with a biotinylated aptamer or biotinylated ssDNA library as a control. Afterwards, cells were lysed with 0.1% sodium deoxycholate in DPBS, and protein targets were separated from aptamer-coated beads by urea solution. Purified target proteins were digested with porcine trypsin, and the peptide mixture was desalted and analysed by nanoflow ultra high-pressure liquid chromatography and tandem MS. Thus, vimentin was identified with MS as a candidate protein target for the LC-18 aptamer. Zamay T. et al.[29] used sodium deoxycholate and performed affinity purification procedures in order to avoid any non-specific aptamer binding, including incubation cells with scrambled DNA and naïve library to cover organelles and mask proteins. Pull-down procedures were performed with a biotinylated NAS-24 aptamer and streptavidin-coated magnetic beads. The biotinylated library was used as a negative control in order to diminish false positive results of non-

specific DNA-binding. MS analysis was performed, and vimentin was identified as a target protein of NAS-24.

Importantly, the target identification step with pull-down procedures can be eliminated if the pool of oligonucleotides was initially selected to the recombinant target protein through SELEX. For instance, Prodeus A. et al.[33] and Lai W-T et al.[34] used PD-1 recombinant chimera consisting of the mPD-1 extracellular domain fused to a histidine-tagged human Fc domain and PD-L1 protein, respectively, as a target during the positive selection step.

Cross-linking approaches for identification of a target protein

In general, affinity chromatographic fractionation can lead to the loss of interactions between the aptamer and target protein during biochemical manipulation under native conditions. To avoid these problems, *in vivo* or *in vitro* chemical cross-linking have been successfully employed to stabilize aptamer-protein interactions in cells or tissues prior to cell lysis. The resulting covalent bonds formed between interacting partners can provide information about the protein-nucleic acid interaction interface. Cross-linking can be accomplished chemically and photochemically, and the latter often has the advantage of causing minimal perturbation to the protein–nucleic acid interface[35]. The sequencing of proteins cross-linked to oligonucleotides can be performed using a mass spectrometer[36-40].

First demonstration of MS sequencing of a cross-linked protein–nucleic acid complex by CID has been reported using basic fibroblast growth factor bFGF[41]. The workflow for the identification of protein target using this strategy is shown in **Figure 1.4**. The bFGF photoaptamers and the photoaptamer specific to the HIV coat protein $gp120_{MN}$ have been evaluated for both the equilibrium binding constant and the relative rate of cross-linking to target proteins. The results of this study showed that the cross-linking significantly enhanced probe specificity in the case where affinity

specificity was weakest and had a small, but positive effect compared to the case, when affinity specificity was the strongest.

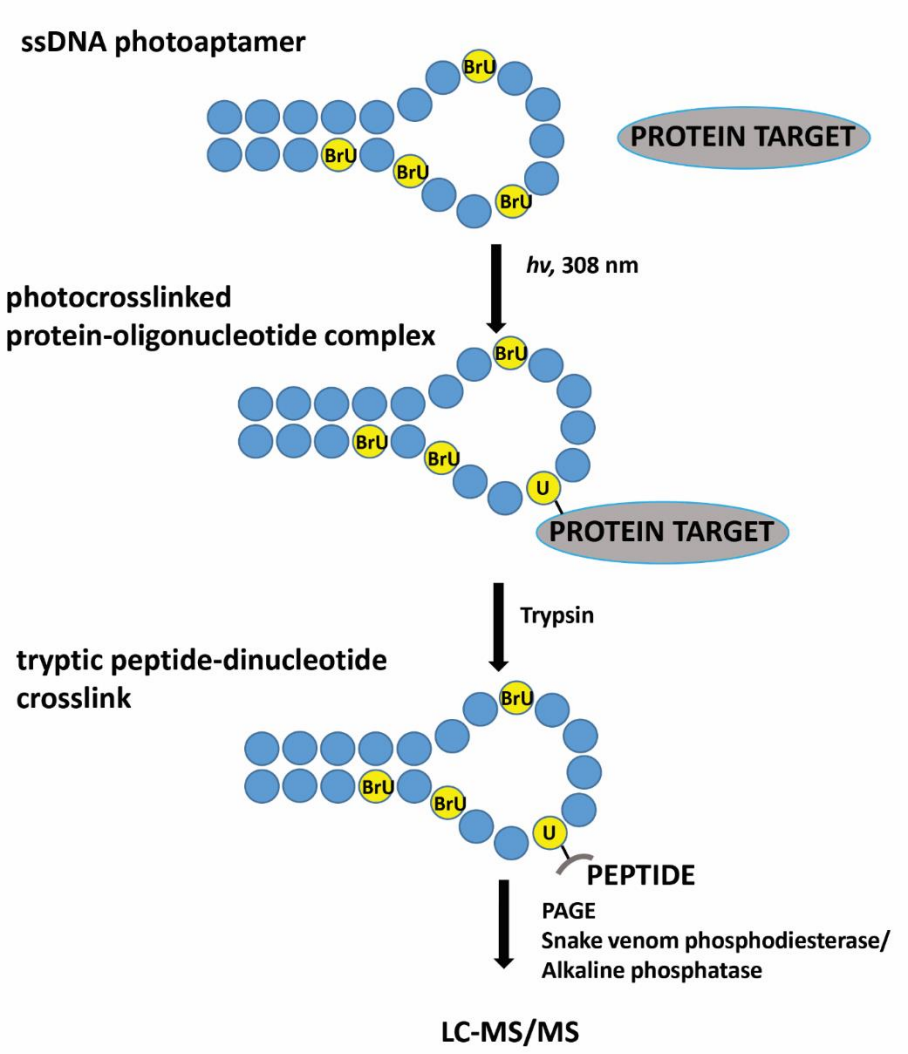

Figure 1.4. Workflow for identification of peptide crosslinks with photo-active 5-bromo-2'-deoxyuridines (BrU) aptamer.

Mallikaratchy P., Tan W. et al.[13] developed a novel strategy for identifying a membrane protein target by using the covalent cross-linking of the photochemically modified aptamer to its target, using a whole cell. DNA aptamers have been generated using Cell-SELEX technique with different cell lines. The identification of a target from Burkitt's lymphoma cells using the aptamer named TD05 was achieved in a seven-step process **(Figure 1.5)**. First, the aptamer-probe was chemically modified with a photoactive uracil derivative for covalent binding of the aptamer with cells. Second, the target protein was purified by the streptavidin-based affinity chromatography. Finally, IHMC (Immunoglobin Heavy Mu Chain) protein was identified by MS followed by a database search. In that study, cells were lysed only after binding and UV-induced covalent cross-linkage between the protein target and modified aptamer. Cells were lysed with the buffer containing three detergents: 0.1% Nonidet P-40, 1.25 % cholesteryl-hemisuccinate and 2.5% n-dodecyl- β-d-maltoside. Also, introduced disulfide bonds between the aptamer and biotin facilitated the effective extraction of the aptamer-protein complex.

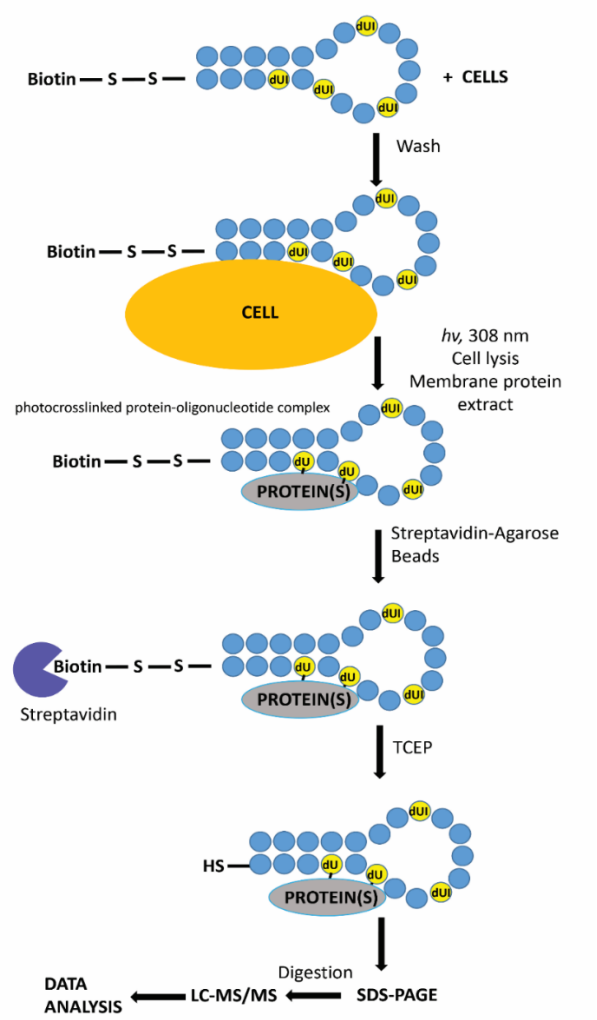

Figure 1.5. Workflow for the identification of a target protein by using the modification of an aptamer with photo-active 5-iodo-deoxyuridine (5-dUI) nucleotides.

Recently, Wang Y. et al.[30] presented morphology-based tissue aptamer selection method or Morph-X-Select technique for aptamers selection against ovarian cancer tissue. This method combines image-directed laser microdissection with a thiophosphate-modified DNA aptamer library that allows to dissect specific regions, which were detected by the thioaptamer library, and, therefore, to identify targeted proteins. Briefly, this method based on general principles of the SELEX procedure and starts with a negative control step when the DNA library incubated with normal ovarian tissue. Further, all the unbound DNA sequences collected and incubated with ovarian cancer tissue, and the bound aptamer sequences then eluted and PCR-amplified. More interestingly, in this study authors performed cross-linking with 1% formaldehyde at ambient temperature. Cells then were harvested, washed, lysed with Pierce lysis buffer that contains 1% Tergitol-type NP-40. After ten rounds of selection, aptamers that showed the highest affinity with ovarian cancer tissue were sequenced, and obtained results were evaluated. By using this approach, vimentin was identified as a target protein of V5 aptamer.

Bing T. et al.[31] have developed stable-isotope labeling by amino acids in cell culture (SILAC)-based quantitative proteomic method for identification of cell-surface target proteins termed target discovery of cell-binding aptamers **(Figure 1.6)**. In this study, aptamers were incubated with cells in PBS buffer containing 2% formaldehyde to induce cross-linking. After incubation, cells were washed with washing buffer containing PBS and EDTA, and incubated in a lysis buffer containing 2% Triton X-100 and 0.4% SDS. Then, cell lysate was centrifuged, and the supernatant was transferred to a new tube for incubation with high-capacity streptavidin agarose resin. For pull-down procedures, streptavidin beads and biotin-saturated streptavidin beads were employed to pull-down heavy and light lysates. In the reverse experiment, streptavidin-beads and biotin-saturated streptavidin beads

were used to pull-down light and heavy lysates, respectively. With this method, selectin L (CD62L) and integrin α4 (CD49d) have been identified as the targets of Sgc-3b and Sgc-4e aptamers.

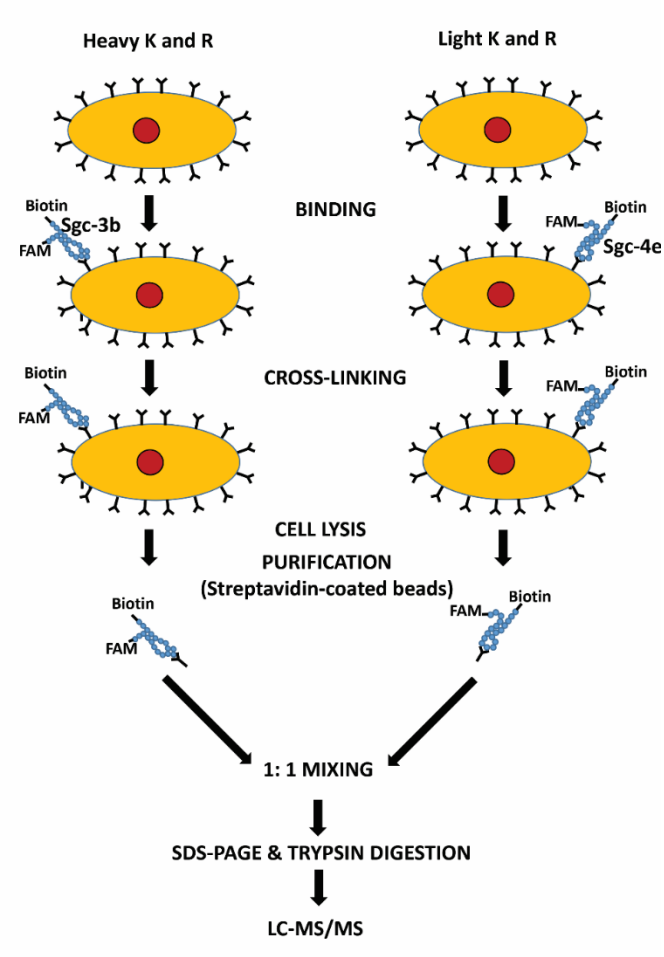

Figure 1.6. SILAC-based quantitative proteomics workflow for the identification of cell-surface target proteins of two previously reported aptamers, Sgc-3b and Sgc-4e.

Bioinformatics analysis of MS results

AptaBiD pull-down, even following formaldehyde crosslinking, yields a lot of non-specific proteins that are released during cell lysis. Even mild detergents, which keep the nucleus membrane intact, result in hundreds of proteins that bind to the aptamer non-specifically, and as a result produce a very long list of proteins, which may be difficult to analyse and pinpoint the real aptamer target. Even the most optimized protocol must be complemented with the respective bioinformatics analysis, which can be performed in specialized software such as Orange Data Mining, or in general programming environment such as R. While software may be user-friendly at first, R provides substantially higher flexibility and allows to tailor the analysis for the data. A general workflow should include removal of the proteins that contain the DNA binding motif. For example, histone proteins have high affinity to any DNA and most certainly bind to the aptamer and get pulled-down on the beads, appearing on the target list. After removal of the proteins with DNA binding domains, it might be beneficial to remove the proteins that are not localized on the plasma membrane. Consulting a database such as UniProt, proteins that are only encountered in the cytoplasm should be removed, as they were unable to interact with the aptamer on the cell surface, and thus, are an artifact of the pull-down experiment.

Proteins that are present in the pull-down experiments but absent in control experiments are generally good candidates for the target; however, at least 3 replicates are required for statistical significance. Statistical tests that can be used include normality test which will show if the protein in all replicates is normally distributed. In case of normal distribution, parametric t-test may be performed to identify significance, if any. In other cases, a non-parametric test can be performed to assess significance.

Some aptamers might be internalized by the cells after their binding to the surface receptor. For example, Sgc8, an aptamer that binds to PTK7 receptor on Jurkat cells is internalized after the binding. In this case, it is also important to consult interactome databases and identify the proteins that are a part of this pathway, as they may be also pulled-down along with the target protein.

Aptamer-facilitated leukemia diagnostics and therapy

Leukemia is a disease that involves the production of abnormal white blood cells in the bone marrow, and it is classified as a heterogeneous group of hematopoietic malignancies. There are two major categories of leukemia that comprise Myeloid and Lymphoid, depending on the affected type of white blood cells. Leukemia is also formed of four principal subgroups, which consist of acute lymphoblastic leukemia (ALL), acute myeloid leukemia (AML), chronic lymphoblastic leukemia (CLL), and chronic myeloid leukemia (CML). Leukemia causes death in many patients worldwide, making it one of the most lethal types of cancer[42,43]. The primary method of leukemia therapy involves chemotherapy and bone marrow transplantation. However, these therapeutic approaches have proven to be more beneficial for solid tumors rather than leukemia. In solid tumors, cancer cells accrue at tumor sites, allowing anticancer drugs to access tumor sites through the enhanced permeation and retention effect, which does not apply to leukemia cells, which constantly circulate within the blood pool. In addition, leukemia cells are surrounded by normal blood cells, which makes it challenging to selectively target malignant cells and not affect healthy ones. Thus, an alternative method is required, which would allow to hit leukemia cells with higher specificity without inducing side cytotoxic effects.

Antibodies have shown to be promising agents for leukemia treatment and diagnostics; however, their production and chemical modification is relatively expensive and complicated. Aptamers have a high binding affinity and specificity for a broad range of targets, such as small organic molecules, phospholipids, viruses, proteins, toxins, and to the extent of whole cells and tissues. In contrast to the conventional antibodies, aptamers can be chemically modified with various tags as well as possess lower immunogenicity and an extended half-life[44,45].

Advances in the selection of aptamers, targeting leukemia. Throughout the last 10 years, a number of aptamers targeting leukemia cells have been developed, possessing high affinity and binding constant in the nanomolar range. For instance, using Cell-SELEX, Shangguan and his colleagues developed a group of aptamers, known as Sgc-aptamers, for the detection of leukemia cells (CCRF-CEM, T-cell lines, human acute lymphoblastic leukemia) with the presence of normal bone marrow aspirates. Among all the selected aptamers, Sgc8-aptamer (88-mer) demonstrated the greatest affinity towards its target (K_d=0.80±0.09nM)[46].

Afterwards, a shortened form of Sgc8-aptamer, called Sgc8c (41-mer), was developed through the truncation with the identical affinity and strong binding[47]. By employing two-dimensional gel electrophoresis (2D-GE) and MS, the binding partner of Sgc8-aptamer on the surface of CCRF-CEM was found to be the protein tyrosine kinase 7 (PTK7). It has been also revealed that both, Sgc8 and Scg8c aptamers are being internalized via receptor-mediated endocytosis[48], and previous studies have shown that PTK7 could be a possible biomarker for T cells acute lymphoblastic leukemia[49].

Yang and his coworkers have selected three DNA aptamers against NB4 AML (human promyelocytic leukemia cell line) cells through the Cell-SELEX procedure. The target of NB4 aptamer was identified as sialic-acid-binding immunoglobulin-like lectins (Siglec05). This aptamer was further employed for the selective detection of AML cells in human bone marrow samples and can be possibly utilized for targeted treatment of AML due to its strong binding and high affinity[23]. In addition, Sefah et al developed two other aptamers, KH2C12 and KHG11, which showed strong binding with AML cell line (HL60, Human promyelocytic leukemia cells) with a great selectivity[50].

Nianxi Zhao et al. selected a DNA aptamer targeting CD117, a transmembrane receptor, which is overexpressed on AML cells, utilizing the hybrid SELEX method. It was shown that the aptamer binds to CD117 with a low dissociation constant in the nanomolar range (K_d < 5nM), and also could be internalized through the endocytosis into CD117-expressing cells[51].

Aptamer-based diagnostic probes for leukemia detection. Diagnostics and treatment of cancer at the early stage is of high importance and could be accomplished by using outstanding properties of nanomaterials. Previously, advances in the synthesis of an array of nanomaterials, along with metallic, silica, magnetic, hydrogel, and polymeric nanoparticles, as well as carbon nanotubes have been reported, which have distinct characteristics, such as large surface area, and exceptional optical and magnetic properties[52,53]. Currently, a wide variety of aptamers coupled with nanomaterials have been developed for the detection of cancer cells.

Silica-coated nanoparticles have gained great popularity in the biomedicine due to a number of advantages, such as biocompatibility and absence of cytotoxicity, high hydrophilicity, inexpensiveness, along with silica matrix serving as a strong fluorescence enhancer[54]. In a previous study, a technique for sensitive and accelerated imaging of cancer cells utilizing dye-doped silica nanoparticles was developped[55]. The biotinylated Sgc8-aptamer was attached to the surface of neutravidin-coated silica nanoparticles, and to inhibit non-specific interactions, nanoparticles were also PEGylated. It has been reported, that this assay could improve the sensitivity in flow cytometry analyses between 10- and 100-fold in comparison to the classical approach.

In order to develop a detection system for the imaging of T-cell leukemia cells along with B-cell lymphoma cells in the developing stages, Chen and his group employed the sensitivity of fluorescence resonance energy transfer of dye-doped (FAM-RG6-ROX) silica nanoparticles and specificity of aptamers[56]. FAM dye was used as an energy donor, whilst RG6 and ROX dyes were

used as acceptors. In another study, Tan et al. have successfully conjugated two aptamers with magnetic nanoparticles and the fluorescent dye for the selective recognition and isolation of leukemia cells. Briefly, they conjugated two previously selected DNA aptamers (88-mer), with low dissociation constants (K_d=5 nM) and high affinity to CCRF-CEM acute leukemia cells, to magnetic iron-oxide nanoparticles and Rubpy dye (2,2'-bipyridyl)dichlororuthenium(II) hexahydrate-silica nanoparticles) to develop an efficient system for the extraction and recognition of leukemia cells from the whole blood cell mixture[57]. It was noted that the aptamer-conjugated nanoparticles allowed isolating target cells with a greater selectivity compared to the centrifugation, avoiding any unbound components and undesired aggregates.

Aptasensors for leukemia detection and treatment. Biosensors are broadly determined as sensors, which integrate a biological identification mechanism along with a physical transduction method, allowing to improve analytical measurements on the molecular level[58]. Malignant cells present the specific intra- or extracellular biomarkers, which make them distinct from normal cell lines. Therefore, the development of new techniques for sensitive and particular biomarker-based detection of cancer cells is of high interest.

Among the numerous biosensing techniques, the colorimetric method has been widely used because of its inexpensiveness and the ability to observe the color change by the naked eye[59]. Recently, gold nanoparticles (AuNPs) have been widely utilized in the development of various forms of aptasensors, due to their great characteristics, such as facile synthesis and chemical modification, biocompatibility, chemical stability, outstanding optical and electrical characteristics, large surface area and high extinction coefficient[60,61].

Ye and colleagues developed an iodide-responsive copper-gold nanoparticle-based colorimetric device for ultrasensitive detection of target cancer cells. In this aptasensor, the Sgc8c-

aptamer was conjugated with Cu-Au nanoparticles, and its efficiency was examined for CCRF-CEM cancer cells. The aptamer-Cu-Au nanoparticles sensor was employed for the selective and ultrasensitive recognition of cancer cells with a linear response range from 50 to 500 cells/mL and detection limit of 5 cells in 100μL binding buffer[62].

A variety of other aptasensors has been produced, using surface plasmon resonance (SPR), surface acoustic wave (SAW), microchannel cantilever sensors as well as quartz crystal microbalance (QCM)[45]. Recently, QCM has been outstandingly utilized to examine the anchorage-independent mammalian cells by controlling cell-surface interactions in a dynamic and non-invasive manner. However, for the anchorage-dependent cells such as leukemia, QCM, is usually coupled with the immune phenotyping[63,64]. For instance, Pan and colleagues, have reported a novel detection technique for leukemia cells, utilizing aptamer-conjugated magnetic beads combined with the QCM method[65]. In the following system, CCRF-CEM cells were captured by Sgc8c-aptamer-conjugated magnetic beads in the complex matrix, and a magnet-QCM system was employed for quantitative cell detection with a detection limit of $8x10^3$ cells/mL.

Since silver nanoparticles (AgNPs) possess a greater extinction coefficient than AuNPs, they have been frequently used for the development of aptamer-based fluorescent sensing techniques[66]. The premier silver decahedral nanoparticles-enhanced FRET sensor for the cell imaging with great sensitivity and specificity towards CCRF-CEM cells was developed by Li et al.[67] Fluorophore-functionalized aptamer (Sgc8-FITC) was coupled with Ag_{10}NPs through the thiol group on the aptamer, and, therefore, quencher-carrying strands (BH1-1) were hybridized with Sgc8-FITC to produce Ag_{10}NPs-based FRET sensor (Ag_{10}Sgc9-F/Q). Binding of the sensor to the CCRF-CEM cells will trigger the release of F/Q at the time of the interaction of the aptamer

with PTK7, resulting in the fluorescence. It has been established that the aptamer binds to its complementary target with the greater binding constant compared to its complementary strand.

Electrochemical biosensors have gained great popularity due to various features, including faster response and lower cost for their production compared to the optical sensors. Furthermore, electrochemical aptasensors demand a fewer quantity of the analyte for its detection.

Yao and his colleagues[65] constructed a label-free electrochemical aptasensor based on steric hindrance for sensitive recognition of CCRF-CEM cells. Thiolated Sgc8c-aptamer was self-assembled onto the gold electrode with the formation of an Au-S bond. The function of the electrochemical aptasensor was based on cyclic voltammetry and electrochemical impedance spectroscopy using Fe $(CN)_6^{3-/4-}$ as a redox probe. 6-Mercapto-1-hexanol (MCH) solution was used to block the free sites of gold surface and to allow the aptamer to maintain in the upright position rather than being placed down on the surface of the electrode. Once the target is present, aptamer binds to the CCRF-CEM, so that the redox probe will not have entry to the surface of the electrode due to the steric hindrance. On the other hand, in the absence of CCRF-CEM, Fe $(CN)_6^{3-/4-}$ has a greater ability to access the surface of the electrode. The produced sensor possesses high selectivity and sensitivity for the recognition of CCRF-CEM cells with the comparison to non-target cell line, Raji cells (Cultured human Burkitt lymphoma cells, $PTK7^-$) with a linear range from 10^4 to 10^7cells/mL, and the detection limit was calculated to be $6x10^3$ cells/mL[65].

An innovative electrochemiluminescence device was introduced for ultrasensitive and selective recognition of K562 (human erythroleukemic cell line) constructed around aptamers and ZnO@carbon quantum dots (ZnO@CQDs)[68]. In this device, screen-printed carbon electrode (SPCE) was taken advantage of along with being altered with nanoporous gold to obtain a favorable passage for the electron transfer, and also to raise the number of aptamers. The carbon

quantum dots (CQDs) covered ZnO (ZnO@CQDs) were used as an ECL label. The aptamer and concanavalin A (Con A) conjoined ZnO@CQDs were utilized to arrest cells and selectively detect the cell surface of carbohydrate, respectively. The greater sensitivity could be achieved by merging of a double signal amplification based around a high surface-to-volume ratio of ZnO for a greater capacity of CQDs and Con A, and the enhanced electrical connectivity of the nanoporous gold. The procedure could linearly encounter K562 cells which range from 1.0x102 to 2.0x107 cells/mL with a recognition limit of 46 cells/mL[68].

A system for facile detection of leukemia cancer cells with a detection limit of 10 cells/mL was developed by Mehrgardi and Khoshfetrat using an ultrasensitive, simple and selective electrochemical aptasensor. The thiolated Sgc8c-aptamer was attached on the gold nanoparticles-coated magnetic Fe_3O_4 nanoparticles (Apt-GMNPs) in the sensing platform. The redox agent, ethidium bromide, was embedded into the stem of the hairpin structure of the aptamer and contributed to the read-out signal for measuring aptamer-target interactions. Once leukemia cells are added onto the Apt-GMNPs, the aptamer loses its secondary structure, allowing the ethidium bromide molecules to escape, which results in the decline of the electrochemical signal. In addition, the nitrogen-doped graphene was utilized to enhance the readout signal[69].

In the past two decades, a wide variety of aptamers have been selected to oppose leukemia such as Sgc8-aptamer, which can selectively recognize and be internalized into PTK7- expressing cells; or AS1411, a therapeutic aptamer that is currently undergoing clinical trials for the therapy of leukemia cells. However, it should be noted that the properties of aptamers require additional improvements for their biomedical application due to their vulnerability to nuclease-mediated degradation. Moreover, there is a plethora of challenges for the utilization of aptamers in biomedicine, such as their small size that causes them to become liable to renal filtration. In order

to resolve this problem, aptamers could be coupled with biodegradable polymers such as PEG, what at the same time can cause an increase in the cost of the procedure along with the processing time. In addition, the selection of new aptamers is mostly based on SELEX, which is a laborious and costly process. Despite all the existing challenges, aptamers offer a great number of benefits due to their unique features and they can become a greatly advantageous platform for clinicians in the upcoming years.

Challenges and limitations of aptamers for biomarker discovery

Although a variety of biomarker-discovery methods exists and is being currently employed in biomarker research, many of them have intrinsic disadvantages such as the requirement of expensive equipment, lack of reproducibility or necessity of extensive data analysis in order to produce validated and reliable data. Additionally, no previously used methods allowed for a combination of both, discovery and targeting, which undoubtedly aptamers are capable of. Nevertheless, there is a list of challenges exist, which limit aptamer utilization for biomarker discovery.

First, RNA and DNA aptamers are unstable in blood, mostly due to the poor nuclease resistance and non-specific interactions with non-target biomolecules. In addition, the selection process could take a long time, up to 3-6 months depending on the target system's complexity and experimental goals. Even though different variations of SELEX exist, most require multiple rounds of positive selection interchanged with rounds of negative selection to build up the pool's specificity to the target. SELEX protocol may be tailored in a way to allow for very precise discrimination between targets such as cells with a minute difference, for example, a few membrane surface proteins. To achieve this, a number of positive or negative selection rounds, in addition to selection conditions, need to be adjusted if one desires such specificity. Moreover, only a very low number of aptamers have been selected against non-protein biomolecules such as lipids, glycans, which also play a vital role in biological processes.

Final aptamer product allows for very specific binding to the target, however, the binding partner is unknown, unless a recombinant protein was used as a target of SELEX. Following the binding event and DNA-protein crosslinking, the target can be pulled down and identified with various methods such as western blot or MS; yet, a comprehensive bioinformatics analysis is required due to a large number of proteins identified in order to accurately establish a true target. In case if the

aptamer is specific enough to discriminate between very similar phenotypes of the cell, the interactor protein (biomarker) can be attributed to a potentially miniscule difference between targets, leading to high specificity and reproducibility. Additionally, once the target is identified, the aptamer may be used for targeted drug delivery or protein binder inhibition. Finally, it is still challenging to identify binding sites on proteins and aptamers as well as to establish a 3D structure of the aptamer and its binding partner due to the complexity and multiple interactions and forces involved.

Despite all the remaining challenges and limitations, aptamers exhibit a wide variety of remarkable properties, which attract researchers and make them as promising agents for a great number of applications. Aptamers can be selected to complex targets according to the design of the SELEX procedure. All previously selected aptamers with their identified targets in the have been summarized in **Table S1**. Additionally, facile synthesis and chemical modification create a number of opportunities for their utilization in biomedicine. Hence, aptamer facilitated biomarker discovery is a promising method which combines biomarker discovery aspect, as well as future implications related to its high specificity, whether it be diagnostic purposes or even treatment.

Chapter II: Aptamer-conjugated Tb(III)-doped silica nanoparticles for efficient luminescent leukemia cells detection

Objective of the study

The objective of this study was to synthesize luminescent Tb (III)-doped silica nanoparticles and to conjugate them with Sgc8-aptamer. In addition, we aimed to examine the capacity of Sgc8-SNs probes to detect leukemia cells as well as to reveal whether Sgc8-SNs induce apoptosis or necrosis of leukemia cells.

Introduction

Nowadays, cancer remains the second cause of death worldwide after cardiovascular diseases, and it became a major cause of mortality in North America[70]. Among various types of cancers, leukemia is still recognized as one of the most common lethal cancers, even though a lot of advancements have been made for its diagnosis at early stages as well as efficient therapy[2]. Indeed, leukemia mainly affects children at a very early age, unlike other cancers that have a correlation with a specific age group. Leukemia can be determined as a heterogeneous group of hematopoietic cancers in which bone marrow produces malignant white blood cells. There are two most popular types of leukemia: myeloid (whether granulocytes or monocytes became malignant) and lymphoblastic (abnormal lymphocytes are being produced) that are also classified into two groups: acute or chronic[43]. One of the major problems that make leukemia hard to diagnose or cure is the fact that all abnormal white blood cells are surrounded by healthy blood cells, and it is quite challenging to distinguish between them. Moreover, during chemotherapy, the majority of normal white blood cells will be damaged that could cause the immune system downregulation provoking several infectious diseases. Thus, an efficient and targeted method undoubtedly could facilitate both, diagnosis and therapy of leukemia; and, to overcome these challenges, therapeutic agent should be biocompatible and biodegradable, and most importantly should have a high affinity and specificity to leukemia cell[71,72].

Aptamers have shown a lot of benefits over antibodies[73], which make them promising agents for cancer diagnostics or treatment, as they act as nanocarriers and can be conjugated with drugs for targeted drug delivery[48,74], magnetic or fluorescent nanoparticles for imaging (MRI, CT, Flow Cytometry, etc.), or even magnetic nanoparticles inducing hyperthermia[75-78].

Weihong Tan and his colleagues from the University of Florida are pioneers of aptamer selection against leukemia cells, and in 2006 they presented a panel of selected oligonucleotides for specific recognition of human acute lymphoblastic leukemia cells, using human bone marrow aspirates as a negative control during selection process[46]. Among their aptamers, Sgc8 aptamer had the highest affinity against its target with a low dissociation constant in the nanomolar range (K_d = 0.80±0.09 nM), making Sgc8 aptamer a powerful weapon for targeted detection of malignant T cells. Sgc8 aptamer showed great potential as a promising agent and was employed in many studies for efficient detection of leukemia cells using nanoparticles or aptamer-based biosensors[62,65,67,69,79]. Thus, it was decided to use Sgc8 aptamer in this study, as its ability to specifically recognize leukemia cells gives a number of opportunities for the design of functional nanomaterials that could be used for diagnostic and therapeutic purposes.

Lanthanide-based nanoparticles have gained a great attraction for many biological applications. Lanthanide-doped nanoparticles offer unique optical characteristics over commonly-used fluorophores that are crucial for bioimaging and biosensing: they emit in the UV, visible and NIR regions (depending on the lanthanide ion), and possess large Stokes shifts and anti-Stokes shifts as well as sharp and well-resolved emission peaks[80-83]. In addition, a ligand-to-metal energy transfer is the cause of the composition of lanthanide ion-based complexes[84]. Interestingly, lanthanide ions within complexes with a completed first coordination sphere possess longer-lifetime emission; therefore, ligand choice, as well as the design of complexes, both play a big role for enhanced luminescence. Those ligands, which provide a larger number of coordination sites within a complex, will shield a lanthanide ion from coordinating water molecules, as stretching vibrations of OH quench the excited state of a lanthanide (III)[85]. Calix[n]arenes have gained attention due to their ability to coordinate lanthanide ions through covalently attached functional

groups acting as antennae, enhancing both, luminescence and magnetic relaxation properties of lanthanides[86]. Indeed, terbium complexes with thiacalix[4]arenesulfonate (TCAS) have the most intensive luminescence among other lanthanide-sulfocalixarene complexes. TCAS coordinates Tb through sulfonate groups of the upper rim in acidic/weakly acidic media, and by phenolate groups of the lower rim in neutral/weakly basic media[87].

Silica-coating became a standard procedure for nanomaterials as it is being widely used; however, it offers many benefits among other matrices. First of all, it is biocompatible and not toxic as well as has high hydrophilicity. It is relatively cheap due to the geochemical abundance of silicon, and most importantly, and in several studies it was shown that silica acts as an enhancer for fluorescent materials since it shields fluorescent complexes[54,88]. Silica-coated luminescent nanoparticles have lower photodegradation and photobleaching,[89] as well as enhanced luminescence due to the silica shielding the whole luminescence complex[80].

In this study, we conjugated Sgc8 aptamer with luminescent [Tb(TCAS)]-doped silica nanoparticles with immobilized carboxyl and amino groups through the well-known Michael addition-Schiff base reaction. Aptamer-modified nanoparticles were examined with UV-absorbance and zeta potential analysis in order to show that the conjugation was successful, as well as it has been revealed that Sgc8-conjugated [Tb(TCAS)]-doped silica nanoparticles can selectively target leukemia cells (acute lymphoblastic leukemia, T-ALL), using Fluorescent Microscopy.

Results and Discussion

Synthesis of SNs and their further modification with -NH_2 and –COOH groups

For our experiments, [Tb(TCAS)]-doped silica-coated nanoparticles with immobilized amino- and carboxyl groups were used, and were further conjugated with Sgc8-aptamer. It has been reported previously that terbium complexes with TCAS have higher luminescence intensity compared to other lanthanide-doped nanoparticles with TCAS[84]. At the same time, silica enhances the luminescence by shielding the Tb-TCAS complexes from photodegradation, as well as it allows to chemically modify the surface of nanoparticles with carboxyl, amino or thiol groups, which could be used for the conjugation with various biomolecules. According to the previously published data, silica can either decrease or increase the lanthanide-centered luminescence compared to the luminescence intensity of lanthanide complexes in aqueous solutions, due to the concentration-induced self quenching, or the restricted quenching by oxygen and water molecules[90]. Nevertheless, the comparison of emission spectra of Tb-TCAS complexes in water compared to Tb-TCAS-doped silica-coated nanoparticles reveals that Tb-TCAS silica coated nanoparticles luminescence approximately 6 times higher compared to Tb-TCAS complexes in water[90]. This can be explained by the fact that silica also protects Tb-TCAS from the quenching by water molecules or self-quenching. Hence, amino-functionalized [Tb(TCAS)]-doped silica nanoparticles (SNs-NH_2) were synthesized through the water-in-oil reversed microemulsion method, which is being widely used for the synthesis of a wide range of nanoparticles having a core-shell structure[91-93]. Core-shell structure of [Tb(TCAS)]-doped silica-coated nanoparticles has been achieved through the water-in-oil microemulsion method, which implies TEOS basic hydrolysis with ammonium hydroxide in the presence of surfactant and co-surfactant (Triton X-100 and n-heptanol, respectively) and aqueous dispersion of Tb-TCAS complexes as well as oil

phase – cyclohexane. As it was described previously[92], aqueous phase, containing Tb-TCAS complexes, formed numerous water droplets by the action of the surfactant and co-surfactant. Hence, each nanodroplet serves as a nanoreactor for the synthesis of nanoparticles, forming the shelf on nanoparticles, whilst silica coating is formed by the basic hydrolysis and polymerization of TEOS around each nanodroplet **(Fig. 2.1)**. Furthermore, (3-aminopropyl)thriethoxysilane (APTES) was used in order to immobilize amino groups on the surface of silica nanoparticles according to the published protocol[94].

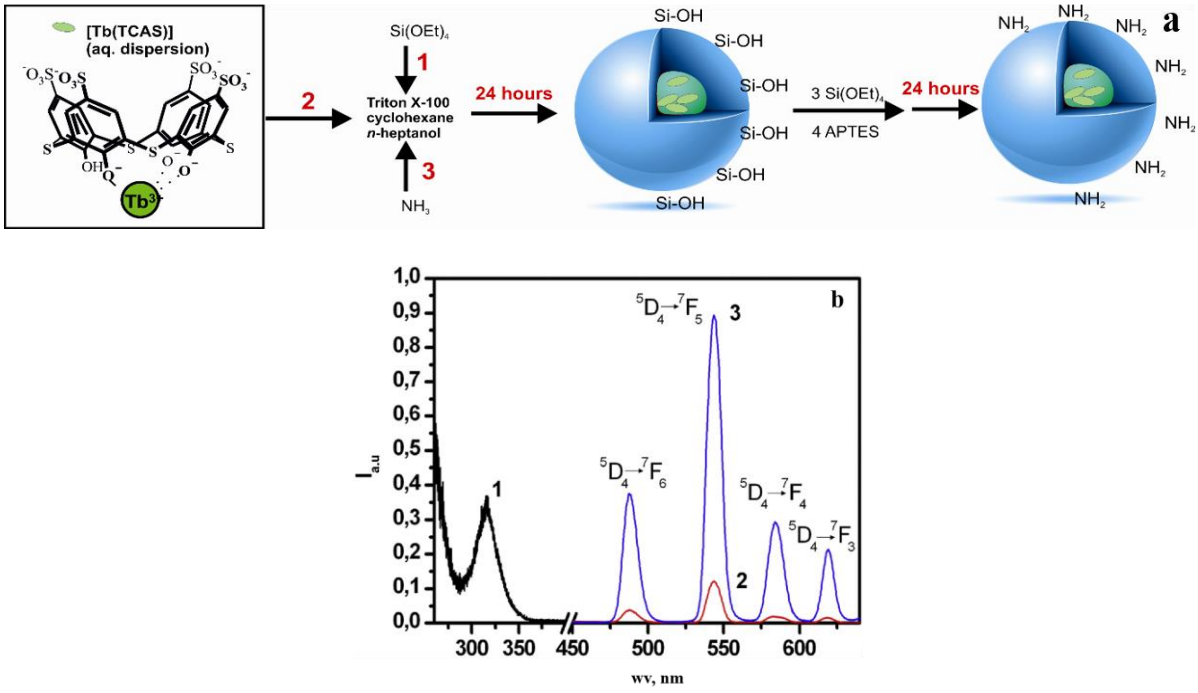

Figure 2.1. Synthesis of [Tb(TCAS)]-doped silica nanoparticles and their modification with amino groups (SNs-NH_2), (a), excitation (b, 1), and luminescence spectra of SNs-NH_2 with d=20 nm (2) and d=35 nm (3) at 0.05 g/L^{-1}.

As it was revealed with TEM, Tb-TCAS silica-coated nanoparticles with immobilized amino groups have quasi-spherical shape and diameter d=39±12 nm **(Fig. 2.2, b)**. The amount of

immobilized amino groups per one SNs (4291 amino groups) with a diameter 39 nm was determined using a standard fluorescamine method, considering the mass of a single SNs **(Fig. 2.3.)**. [Tb(TCAS)]-doped silica nanoparticles with carboxyl groups (SNs-COOH) with a diameter 39 nm were synthesized through the treatment of SNs-NH_2 with succinic anhydride **(Fig. 2.2, a)**. The amount of immobilized carboxyl groups per one SNs determined with fluorescamine method was 1716 (conversion rate – 40%, **Fig. 2.3**). The excitation wavelength used for fluorescamine (390 nm) could not trigger the luminescence of Tb-TCAS nanoparticles considering their excitation spectrum, which allowed to perform the quantitative analysis of immobilized carboxyl and amino groups. Overall, having nanoparticles with different surface modification, it is possible to utilize two approaches of bioconjugation with Sgc8-aptamer and evaluate SNs luminescent properties after the conjugation.

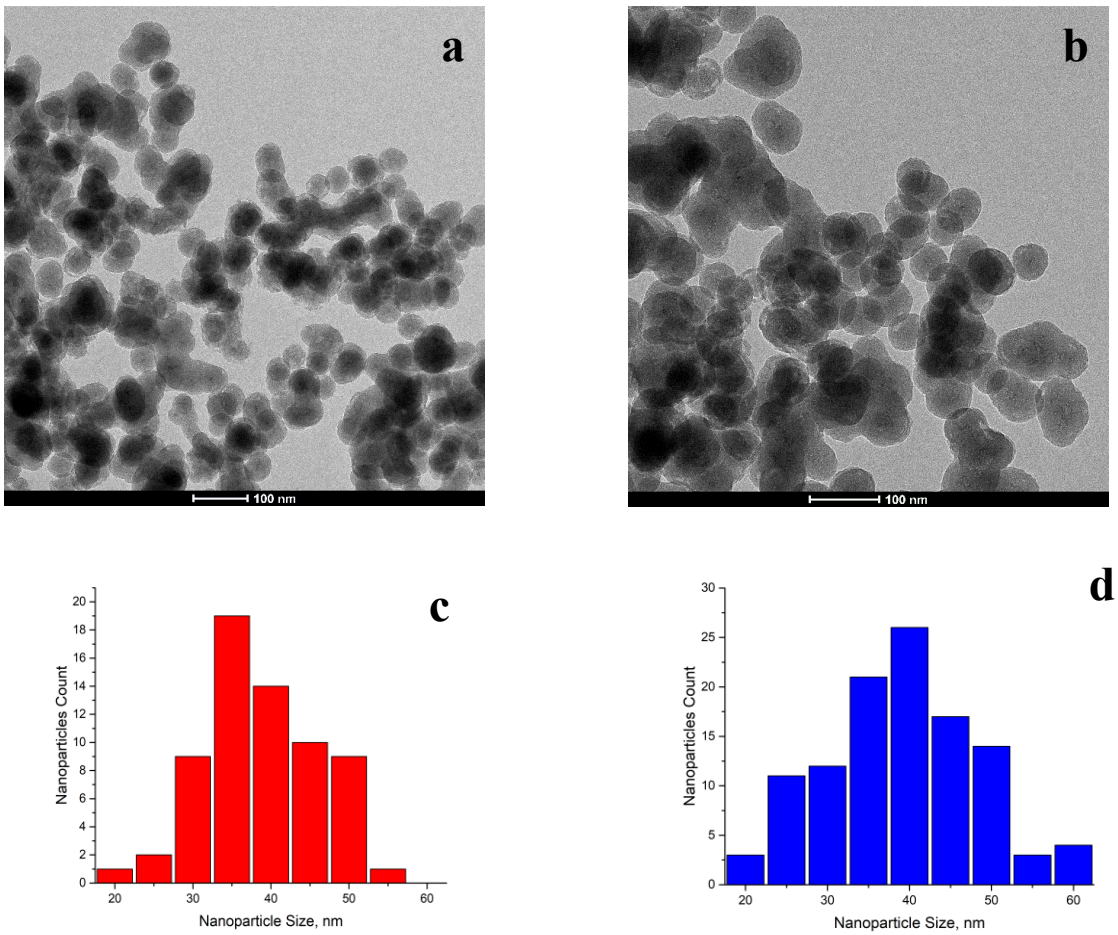

Figure 2.2. TEM images of SNs-COOH and SNs-NH_2 (a, b) and nanoparticles size distribution (c, d). Average diameter of SNs-COOH – 39±10 nm, SNs-NH_2 – 39±12 nm.

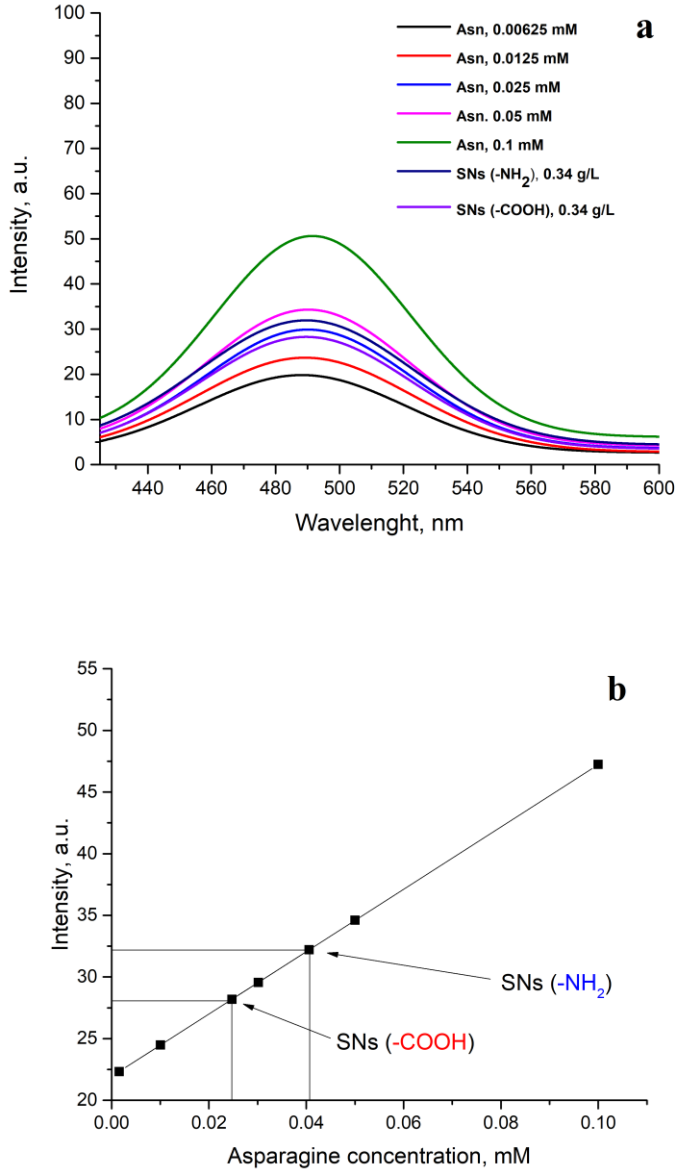

Figure 2.3. (a) Fluorescamine emission spectra with various concentration of asparagine (0.00625 mM, 0.0125 mM, 0.025 mM, 0.05 mM, 0.1 mM) and SNs-NH_2 (0.34 g L^{-1}) and SNs-COOH (0.34 g L^{-1}). All spectra were obtained in 50 mM borate buffer, [Fluorescamine] = 0.924 M under excitation wavelength – 390 nm. (b) Calibration curve.

Conjugation SNs-NH_2 and SNs-COOH with Sgc8 aptamer

We used two approaches for bioconjugation of SNs with the aptamer Sgc8: using the reaction of SNs-NH_2 with glutaraldehyde and the reaction of SNs-COOH with EDAC in the presence of sulfo-NHS according to the published protocol[94]. In order to conjugate Sgc8-aptamer with SNs-COOH, we induced covalent bonding through Michael addition Schiff Base reaction with the formation of the amide bond between carboxyl groups on the nanoparticles and an amino group on the 5' end of Sgc8 aptamer. The second approach is based on a transformation of amino- to aldehyde-groups (SNs-COH) via interaction with glutaraldehyde, and implies further interaction of SNs-COH with the terminal amino group on the 5' end of Sgc8 aptamer. Michael addition Schiff Base reaction is one of the most popular methods used for immobilization of biomolecules with thiol or carboxyl groups. The reaction scheme is illustrated in **Fig. 2.4**.

Between two approaches used for the bioconjugation, the coupling of carboxyl-modified nanoparticles with the aptamer is more favorable. According to the previous findings[95], the coupling of amino-modified Tb-TCAS nanoparticles with Sgc8-aptamer with glutaraldehyde could lead to the cross-linking of two adjacent nanoparticles with available amino groups. Glutaraldehyde itself can polymerize at acidic and basic pH in aqueous solutions, which would affect the efficiency of the aptamer-nanoparticle conjugation. In addition, the final aptamer-nanoparticle composite is relatively unstable due to the formation of an unsaturated conjugate with two double bonds, which are attractive to other nucleophilic centers.

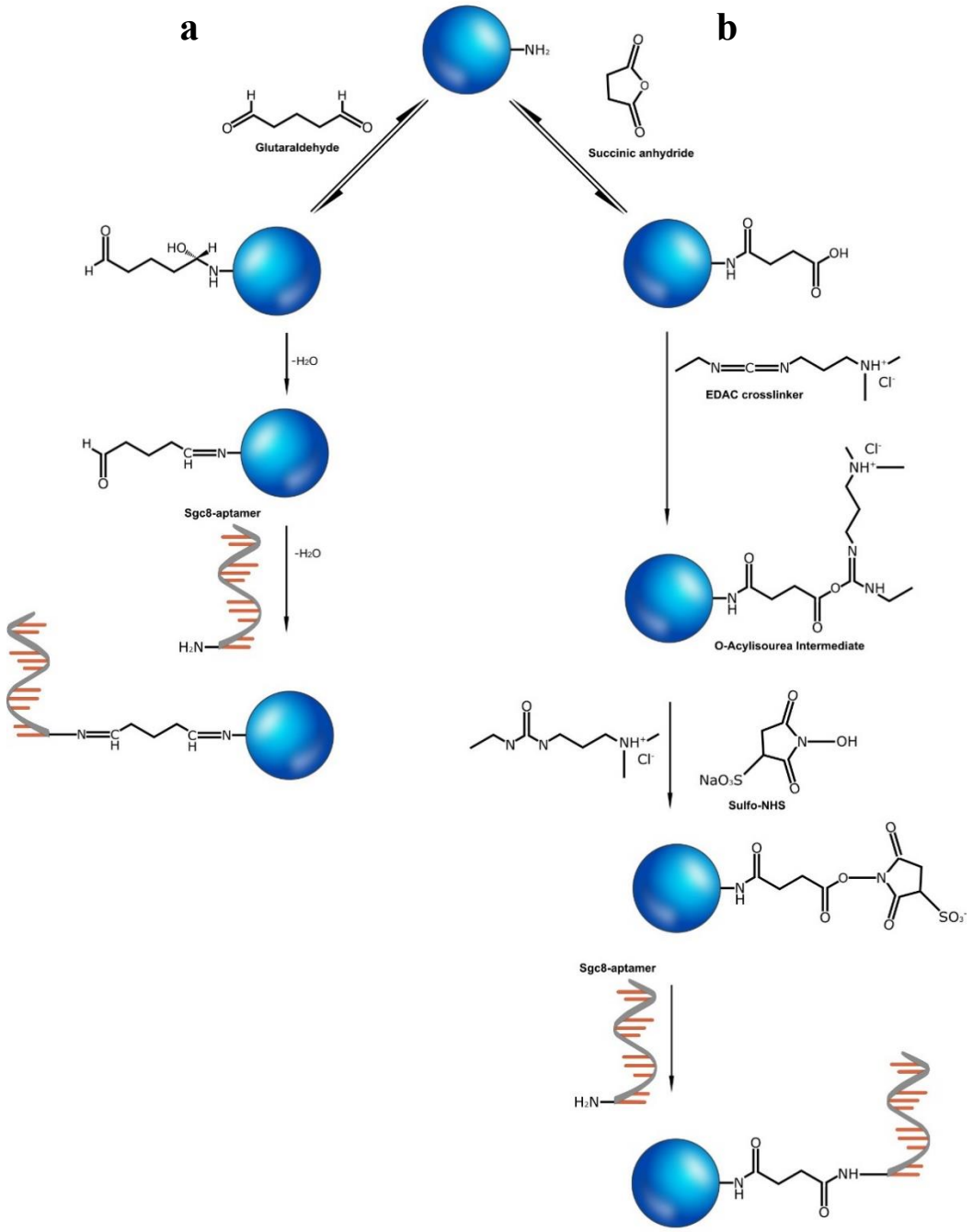

Figure 2.4. SNs-COH (a) and SNs-COOH (b) conjugation with Sgc8 aptamer.

UV-absorbance spectra **(Figure 2.5)** were obtained for nanoparticles before and after conjugation, and it was found that the DNA absorbance peak at 260 nm was present for Sgc8 aptamer, Sgc8-SNs(COOH) and Sgc8-SNs(COH) samples that proves once again that Sgc8 aptamer was conjugated with SNs successfully.

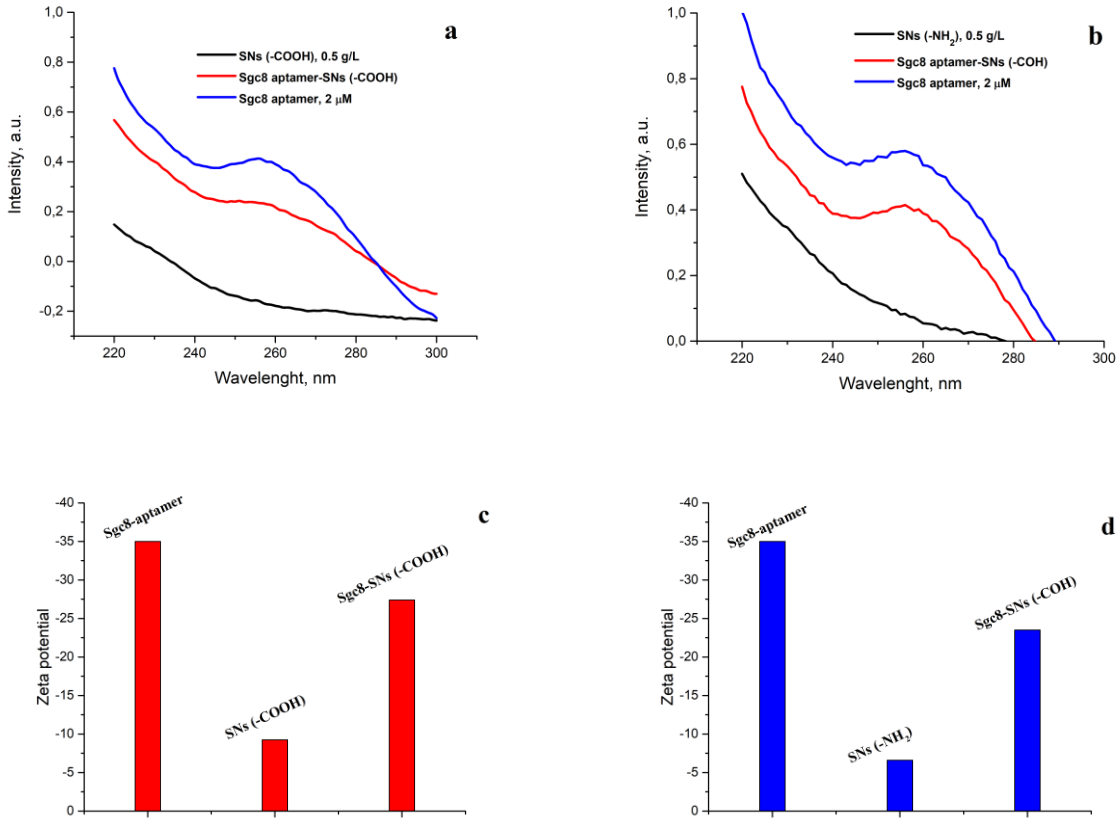

Figure 2.5. UV-absorbance spectra of Sgc8 aptamers (2 μM), SNs-COOH (C=0.5 g L^{-1}), Sgc8-SNs-(COOH) (C=0.5 g L^{-1}) (a) and SNs-NH_2 (C=0.5 g L^{-1}), Sgc8-SNs-(COH) (C= 0.5 g L^{-1}) (b) in water. Zeta potential values of Sgc8 aptamer, SNs-COOH, Sgc8-SNs-(COOH) (c) and Sgc8 aptamer, SNs-NH_2 and Sgc8-SNs-(COH) (d) measured in water.

Figure 2.5 (c, d) represents the zeta potential of Tb(III)-doped silica nanoparticles with immobilized amino and carboxyl groups. As it was expected, the zeta potential of Sgc-8 aptamer have negative values due to the phosphate backbones within DNA structure, and SNs-NH_2 zeta potential was higher than for SNs-COOH due to the partial negative charge on carboxyl groups. It should be noted that the modest difference in zeta potential between SNs-COOH nanoparticles and SNs-NH_2 nanoparticles could be due to the fact that some amino groups have not been substituted completely during the synthetic procedure, thus, remaining on the surface of nanoparticles and increasing zeta potential value. However, successful conjugation can be explained by the decrease of zeta potential for Sgc8-SNs(COOH) and Sgc8-SNs(COH) samples due to the phosphate backbones contribution. Zeta potential values as well as the concentration of all samples presented in **Table 2.1.**

Quantitative analysis of covalently bound Sgc8-aptamer was performed utilizing the fluorescamine method **(Fig. 2.6)**. For the calibration curve we used aqueous solutions of Sgc8-aptamer in the concentration range 0.0375 – 1.5 μM at pH=9. As some of the primary amino groups remained unreacted (≈2575 in case of SNs-COOH), which could also react with fluorescamine, the amount of the conjugated Sgc8-aptamer was determined as a difference between luminescence spectra, and was 0.66 μM for Sgc8-SNs-COH, and 0.55 μM for Sgc8-SNs-COOH.

Table 2.1. Zeta potential values and concentration of Sgc8-aptamer, SNs-COOH, SNs-NH_2, Sgc8-SNs (-COOH) and Sgc8-SNs (-COH) in water.

Sample	Concentration of NPs, g L^{-1}	Concentration of aptamers, μM	ξ-Potential, mV
Sgc-8-NH_2 aptamer	-	0.1	-35
	-	0.5	-29
SNs-NH_2	0.01	-	-7
	0.05	-	-4
Sgc8-SNs(COH)	0.01	-	-24
	0.05	-	-22
SNs-COOH	0.01	-	-9
	0.05	-	-9
Sgc8-SNs(COOH)	0.01	-	-27
	0.05	-	-23

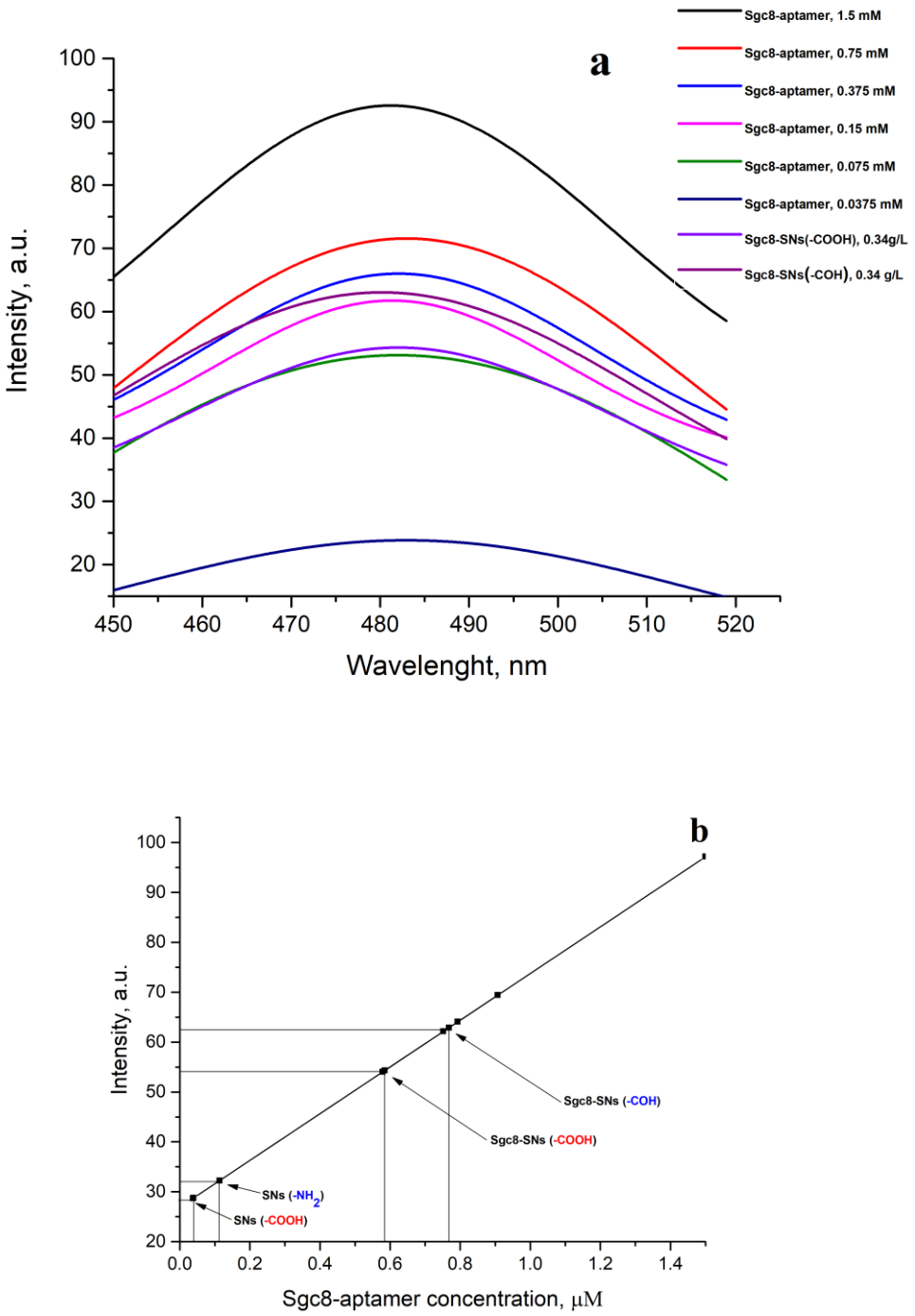

Figure 2.6. (a) Fluorescamine fluorescence spectra after interaction with various concentration of Sgc8-aptamer (1.5 μM, 0.75 μM, 0.375 μM, 0.15 μM, 0.075 μM, 0.0375 μM) and SNs-NH_2, SNs-COOH, Sgc8-SNs(COH) (0.34 g L^{-1}) and Sgc8-SNs(COOH) (0.34 g L^{-1}). All spectra were obtained in 50 mM borate buffer under excitation wavelength – 390 nm. (b) Calibration curve.

Indeed, to show that fluorescence properties of nanoparticles after modification have not been changed, we obtained luminescence spectra for all the samples. **Fig. 2.7 (a, b)** represents luminescence spectra of amino- and carboxyl-modified silica nanoparticles before and after Sgc8-aptamer conjugation. SNs-NH_2, SNs-COOH, Sgc8-SNs(COOH) and Sgc8-SNs(COH) possess 4 sharp and well-resolved emission peaks at 488 nm ($^5D_4 \rightarrow {}^7F_6$), 543 nm ($^5D_4 \rightarrow {}^7F_5$), 588 nm ($^5D_4 \rightarrow {}^7F_4$) and 621 nm ($^5D_4 \rightarrow {}^7F_3$).

The emission peaks observed within the luminescence spectrum is the result of the radiative transitions of $^5D_4$ to ^7F_j (where j=0,1,2…6) levels, which is the common attribute of Tb(III)-centered luminescence (**Fig. 2.7, c**), possessing the emission band with the higher intensity at 543 nm. Tb(III) luminescence arises from 4f-4f forbidden electron transitions, which are shielded by 5s and 5p electrons; hence, the ligand with an efficient antenna effect would be beneficial for the enhanced luminescence. The three-dimensional structure of TCAS with pre-organized donor groups on both, lower and upper rims allow this ligand to serve as an antenna for Tb-centered emission, absorbing light at 330 nm, which is followed by the energy transfer from the triplet energy level of the ligand (T_1) to the excited state of Tb(III)[96].

Luminescence intensity of Sgc8-SNs(COOH) at 543 nm has slightly decreased compared to SNs(COOH); although we have not observed any other significant changes in luminescence properties after nanoparticles modification. Nevertheless, SNs-NH_2 showed decreased luminescence intensity that could be also due to the interactions between amino groups and silica shell that caused aggregation of nanoparticles and widely influenced on optical properties.

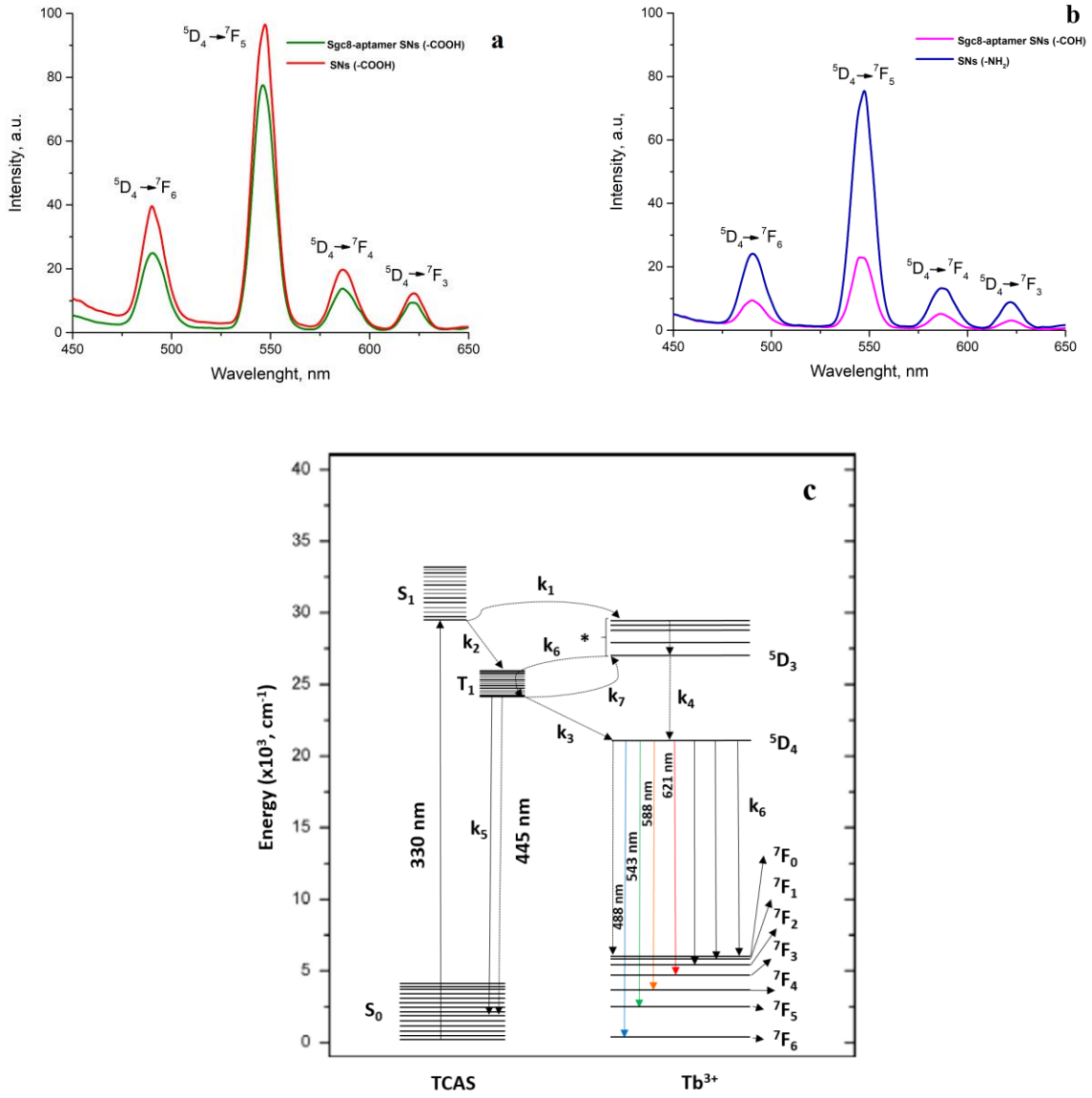

Figure 2.7. Emission spectra of SNs-COOH (a) and SNs-NH_2 (b) before and after conjugation with Sgc8-aptamer, and a schematic representation of Tb(III)-TCAS-SiO_2 energy levels (c). Solid line represents radiative transitions, dotted line – non-radiative transitions (k_1-k_7), and * represents $^5G_6$, $^5L_{10}$, $^5G_5$, $^5D_2$, $^5L_9$ energy levels. All spectra were obtained in water media under excitation wavelength – 330 nm; concentration of nanoparticles – 0.5 g L^{-1}.

Detection of leukemia cells with flow cytometry and fluorescence microscopy

Prior to the conjugation of SNs-NH_2 and SNs-COOH with Sgc8 aptamer, we decided to confirm its binding with CCRF-CEM (CCL-119, T lymphoblasts, acute lymphoblastic leukemia) cell line, as well used Jurkat cells (TIB-152, Clone E6-1, T lymphocytes, acute T cell leukemia) and Raji cell line as a negative control (CCL-86, Burkitt's lymphoma, B lymphocytes), **Figure 2.8**. Sgc8 aptamer showed strong binding with CCRF-CEM cell line as well as with Jurkat cell line; although the shift of fluorescence intensity was stronger for CCRF-CEM cells. Jurkat cells could also be used as a model for all the further experiments. It was reported previously[97] that the Sgc8 aptamer target is a tyrosine protein kinase 7 (PTK7), or colon carcinoma kinase 4 (CCK4), which is involved in transduction of extracellular signals across the cellular membrane. Stronger shift of fluorescence intensity for CCRF-CEM is related to the higher amount of the Sgc8 aptamer molecular targets presented on the cellular membrane than for Jurkat cells; however, both CCRF-CEM and Jurkat cell lines are PTK7 positive as it was shown in our experiments with anti-human PTK7 antibody **(see Chapter III, Fig. 3.3).**

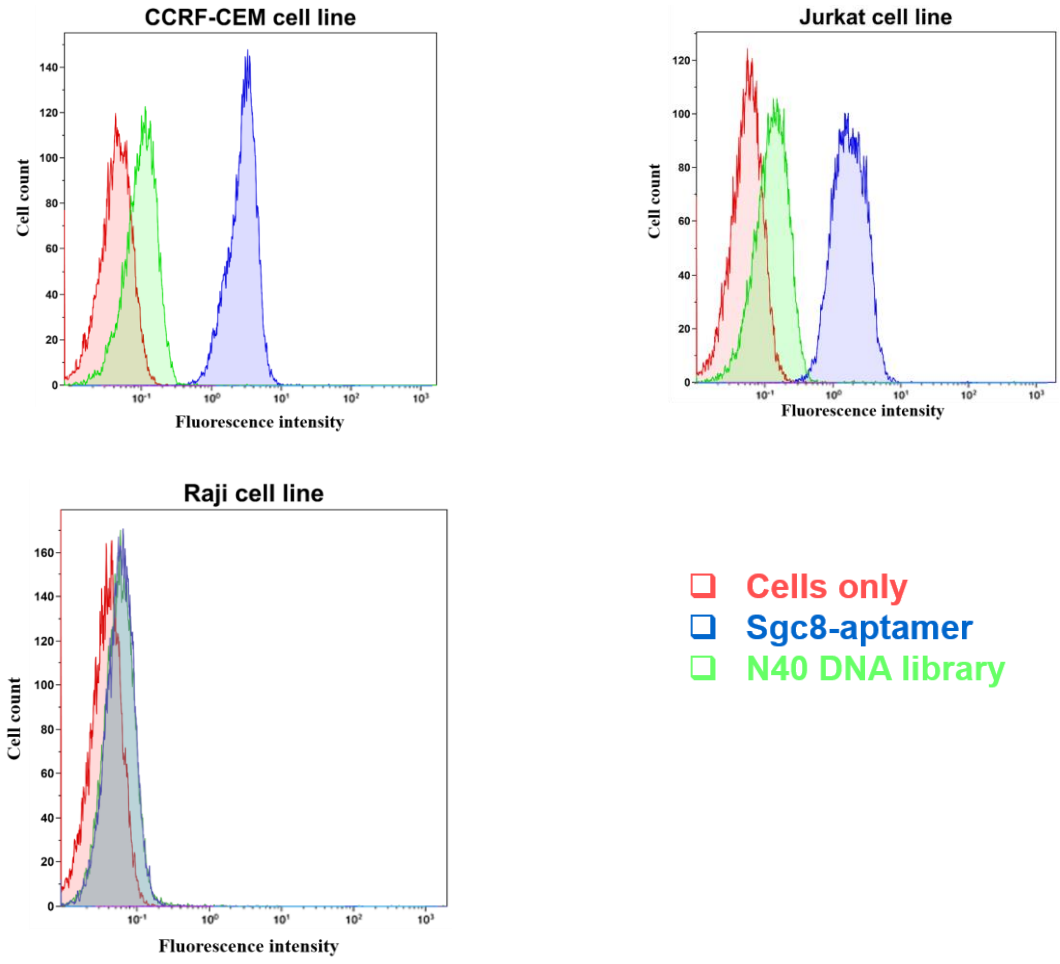

Fig 2.8. Flow cytometry analysis with Sgc8 aptamer binding with CCRF-CEM and Jurkat cell lines (positive), and Raji cell line (negative control).

In order to examine the ability of Sgc8-SNs to efficiently detect leukemia cells, we could not use flow cytometry as SNs have their excitation maximum peak at 330 nm, and this requires excitation sources in the far-UV range that could not be meet with commonly used flow cytometers. For that, we used fluorescence microscopy with the excitation source at 340 nm.

Figures 2.9 and 2.10 show fluorescence microscopy images of CCRF-CEM and Jurkat cells with SNs-COOH (control samples), Sgc8-SNs(COOH), Sgc8-SNs(COH) and DAPI. Sgc8-SNs(COOH) and Sgc8-SNs(COH) labelled CCRF-CEM and Jurkat cells; however, since there was no binding obtained between Sgc8-aptamer and Raji cell line (PTK7-negative) with flow cytometry, it was decided to exclude the negative cell line from fluorescence microscopy experiments. Considering emission spectral overlap between DAPI and Tb(III)-centered luminescence, it is quite challenging to use them simultaneously within one sample; and therefore, other DNA-staining dyes could be used along with SNs, such as 7-AAD, which has its emission maximum at 650 nm[98], or ethidium monoazide bromide with the emission maximum at 610 nm[99]. Moreover, for our experiments, we decided to use non-fixed cells as it could show the difference between DAPI staining (that shows all cells with damaged membrane), and all cells detected by Sgc8-SNs(COOH) nanoparticles.

Interestingly, while DAPI stained only cells with a damaged cellular membrane (presumably, necrotic cells), SNs-COH and SNs-COOH conjugated with Sgc8 aptamer labeled all cells. Moreover, due to the wide emission spectrum of Tb-TCAS-doped SNs with maximum intensity peaks at 489 and 541 nm, they were observed in two fluorescence channels.

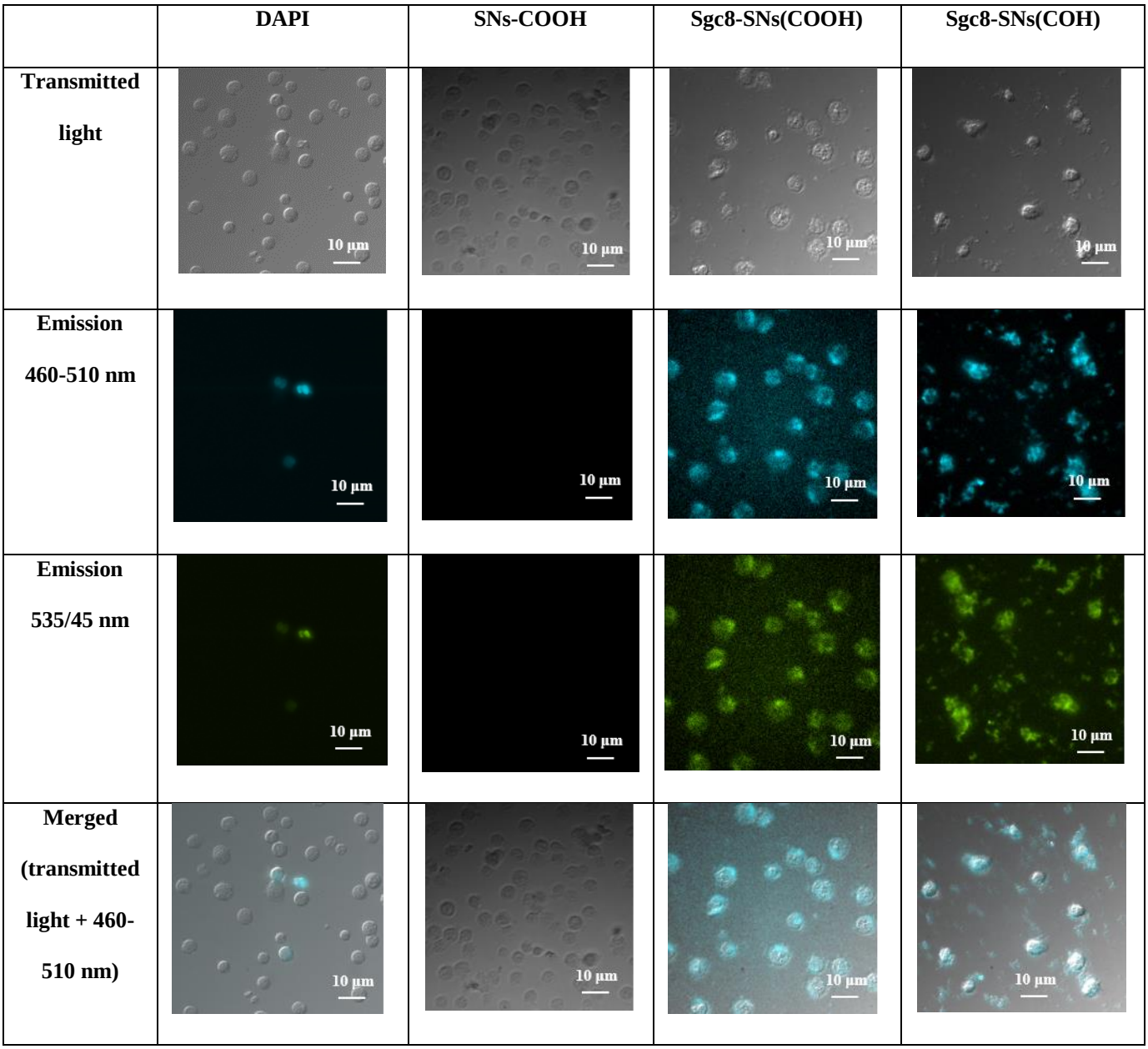

Figure 2.9. Fluorescent microscopy images of CCRF-CEM cells treated with DAPI, SNs-COOH (control sample), Sgc8-SNs(COOH) and Sgc8-SNs(COH). Excitation wavelength – 340 nm.

	DAPI	SNs-COOH	Sgc8-SNs(COOH)	Sgc8-SNs(COH)
Transmitted light	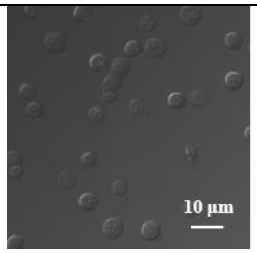	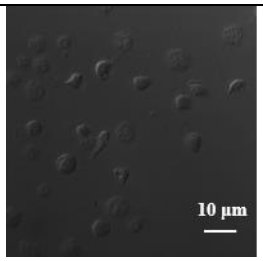	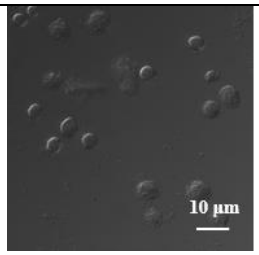	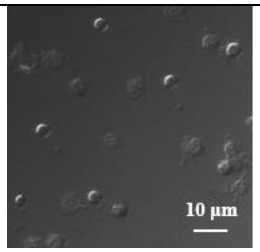
Emission 460-510 nm	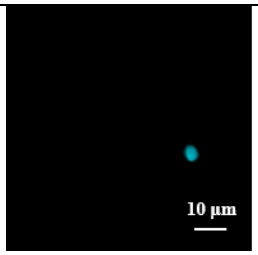	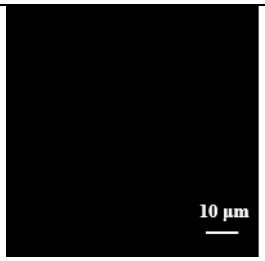	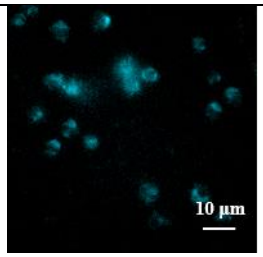	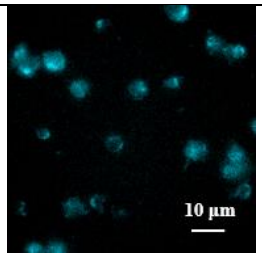
Emission 535/45 nm	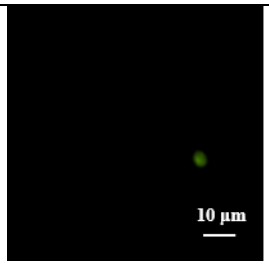	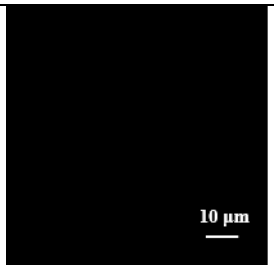	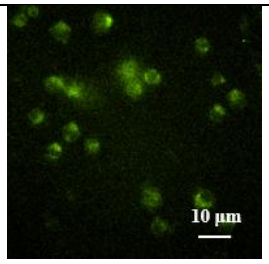	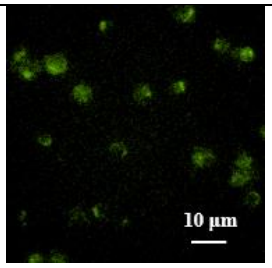
Merged (transmitted light + 460-510 nm)	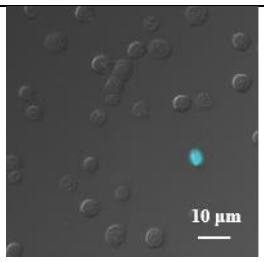	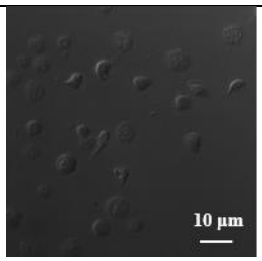	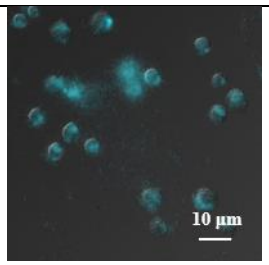	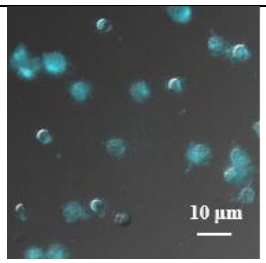

Figure 2.10. Fluorescent microscopy images of Jurkat cells treated with DAPI, SNs-COOH nanoparticles (control sample), Sgc8-SNs(COOH) and Sgc8-SNs(COH). Excitation wavelength – 340 nm.

Even though we have observed that the luminescence intensity of SNs-COOH is higher compared to Sgc8-SNs(COH), we could not notice the same trend for aptamer-conjugated nanoparticles with fluorescence microscopy. Moreover, as it has been previously revealed with flow cytometry that Sgc8-aptamer possesses stronger binding[47] with CCRF-CEM cell line compared to Jurkat cell line; however, fluorescence microscopy data shows that there is no significant difference between the aforementioned cell lines, which could be due to the non-specific binding of Sgc8-aptamer.

It would be beneficial to test aptamer-conjugated nanoparticles with other methods, such as flow cytometry; however, the absorbance of Tb-TCAS silica coated nanoparticles in far UV-range limits their application. In order to improve that, other lanthanide ions or ligand could be used, which would allow obtaining a lanthanide-based complex, absorbing in the visible or near-IR region. In addition, to reveal whether the aptamer-conjugated nanoparticles detect leukemia cells due to the cellular uptake of Sgc8-aptamer conjugated nanoparticles, an antibody blocking experiment could be used since Sgc8-aptamer has non-competitive binding with its target compared to Anti-PTK7 antibody. If Sgc8-aptamer is attracted to the same epitope on the target as Anti-PTK7 antibody, it should lose its binding upon the addition of the antibody. In this case, there should be no signal obtained from Sgc8-aptamer conjugated nanoparticles with fluorescence microscopy. However, if Sgc8-aptamer and Anti-PTK7 antibody bind to two different epitops of the target, it would be more challenging to evaluate, whether Sgc8-aptamer binds selectively leukemia cells, or non-specifically. For this, siRNA silencing of PTK7, or cDNA-transfection of PTK7 gene of PTK7-negarive cell line could be used, which would elicit the selectivity of Sgc8-aptamer binding.

Cell viability assay

For the biomedical application of Tb-TCAS silica coated nanoparticles, it is essential to evaluate aptamer-conjugated nanoparticles cytotoxicity and possible side effects that they may cause in living organisms. It has been reported previously that silica itself and silica-coated materials may induce some cytotoxic effects, and should be carefully evaluated prior to being widely used as a matrix for targeted drug delivery and other biological applications[100,101]. In addition, lanthanide nanoparticles as rare earth elements could be a reason for multiple cellular perturbations simply due to their absence in biological systems, and terbium, specifically, has no biological role in our bodies. At the same time, there is no sufficient data published regarding Tb compounds cytotoxicity, even though it has attractive optical properties that could be employed in a number of biological applications[102]. In addition, even if Tb compounds do not induce any cellular perturbations, size-dependent cytotoxicity of Tb-based nanoparticles could be another problem that should be taken into consideration and evaluated for the further employment of Tb-TCAS nanoparticles in biomedicine.

In 1994, a number of experiments with yttrium group fluorides on animals and peritoneal macrophages (rat) was conducted. Authors mentioned, that it is crucial to control the level of yttrium, terbium and lutetium fluorides in the air of the workplace with a maximum admissible concentration of fluorides – 2.5 mg/m^3 (maximum individual concentration). Later, in 1996, pulmonary toxicity of systemic Tb was examined using mice. It was concluded that intravenous administration of Tb causes pulmonary lipid peroxidation at early stages as well as that SOD, CAT and GSH-Px could be acting as possible modulators of lipid peroxidation induced by Tb ions[103]. On the other hand, effects of lanthanum, cerium, yttrium and terbium ions on the respiratory burst

of peritoneal macrophages were studied, and it was stated that lanthanide ions can inhibit production of active oxygen species at high concentration.

We decided to use the cell viability assay with Annexin V-FITC and PI[104] in order to determine the percentage of viable, apoptotic, necrotic and viable cells with a damaged cell membrane. Annexin V acts as a ligand to phosphatidylserines that are overexpressed on a cellular membrane for the apoptotic cell, whilst PI is used for staining all cells with a damaged cellular membrane as it can easily penetrate into cells and bind to double-stranded DNA similarly to DAPI and 7-AAD[98].

Thus, cells that were stained with both PI and Annexin V-FITC are necrotic. CCRF-CEM cells were treated with various concentrations (0 µg/mL, 25 µg/mL, 50 µg/mL and 100 µg/mL) of Sgc8-SNs(COH) and Sgc8-SNs(COOH) conjugates and left for 24 and 48 hours incubation. Afterwards, cells were centrifuged and washed with PBS and stained with Annexin V-FITC and PI for further analysis with flow cytometry.

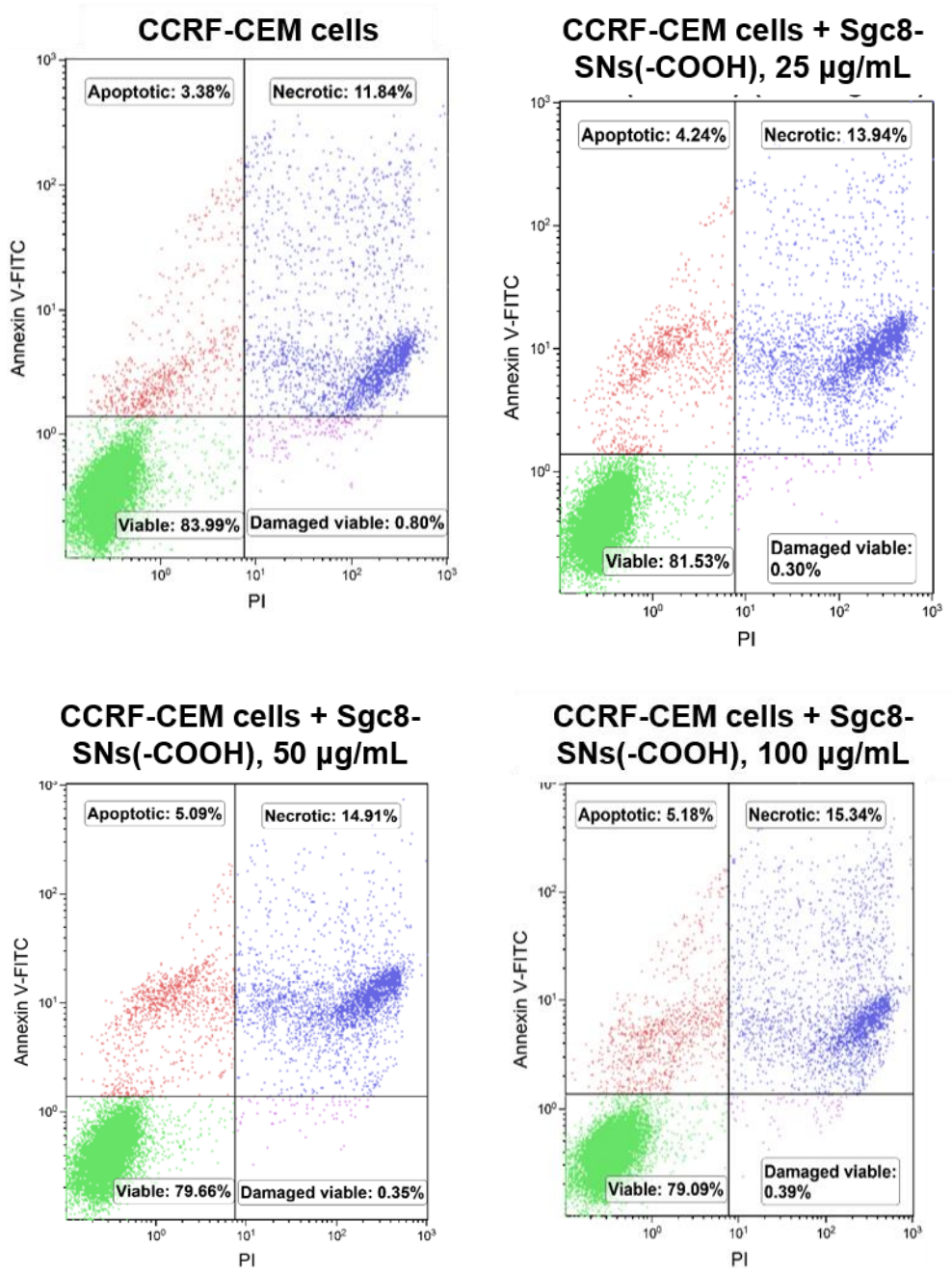

Figure 2.11. Cell viability assay with Annexin V-FITC and PI after 24 hours of incubation. Sgc8-SNs(COOH) concentration: 0 µg/mL (a), 25 µg/mL (b), 50 µg/mL (c) and 100 µg/mL (d).

Figure 2.11 shows that the amount of CCRF-CEM cells that underwent apoptosis and necrosis has slightly increased after 24 hours incubation with Sgc8-SNs(COOH) comparing to the control sample (0 μg/mL). Indeed, the increase of nanoparticles concentration from 25 μg/mL to 100 μg/mL only had a modest effect on cells' viability. The similar pattern was observed after 48 hours of incubation **(Fig. 2.12)** with roughly 5% of cells turning necrotic. Our results show that Sgc8-SNs(COOH) do not significantly induce apoptosis or necrosis; however, in order to reveal the impact of Tb-based nanoparticles on cell viability, other assays should be performed, such as a traditional MTT cytotoxicity test.

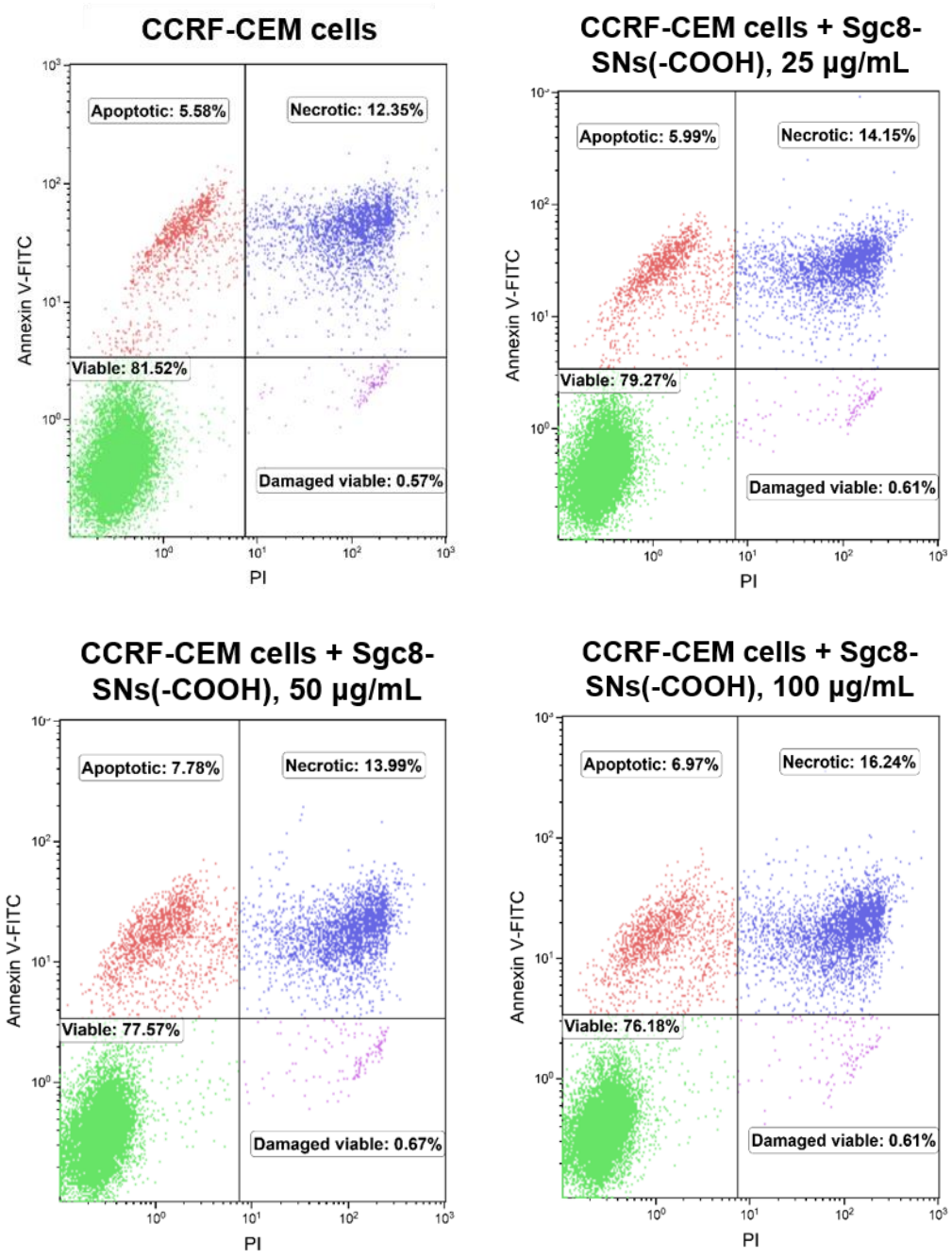

Figure 2.12. Cell viability assay with Annexin V-FITC and PI after 48 hours of incubation. Sgc8-SNs(COOH) concentration: 0 µg/mL (a), 25 µg/mL (b), 50 µg/mL (c) and 100 µg/mL (d).

Conclusions

In the present study, a rapid and facile way for conjugation of Tb-TCAS-doped silica nanoparticles with immobilized carboxyl and amino groups with Sgc8-aptamer using Michael addition-Schiff base reaction was employed. In a simple manner, the synthetic procedure allows to conjugate biomolecules with functional nanomaterials, such as fluorescent nanoparticles, in three steps. It should be noted, that nanoparticles remained their luminescent properties, although SNs-NH_2 conjugated with Sgc8-aptamer possessed less intensive luminescence, compared to nanoparticles prior to the conjugation. In addition, the conjugation of SNs-NH_2 nanoparticles with Sgc8-aptamer results in the formation of an unstable conjugate, which requires further reductive amination as well as glutaraldehyde used as a cross-linker can polymerize in aqueous media and induce cross-linking of the adjacent SNs-NH_2[95]. Hence, it is more favorable to use carboxyl-modified SNs for the conjugation with aptamers.

Sgc8-aptamer was chosen for modification with SNs, since it showed a high affinity to its target, having the binding constant in the nanomolar range. We have confirmed Sgc8-aptamer ability to selectively bind CCRF-CEM and Jurkat cell lines with flow cytometry, but not the control cell line (Raji cell line, PTK7-negative). Indeed, we showed that Sgc8-SNs(COOH) and Sgc8-SNs(COH) can detect leukemia cell lines using fluorescent microscopy. However, additional experiments are needed in order to reveal, whether Sgc8-SNs(COOH) and Sgc8-SNs(COH) bind their target specifically to PTK7, such as an antibody-blocking experiment, or PTK7-gene transfection with the control cell line. Alternatively, Tb-TCAS could be conjugated with the anti-PTK7 antibody, which would allow enhancing selectivity and efficiency of the detection of leukemia cells.

Moreover, we assessed Sgc8-SNs(COOH) nanoparticles impact on cell viability using the assay with Annexin V-FITC and PI, and it was revealed that the aptamer-conjugated nanoparticles do not induce apoptosis or necrosis of leukemia cells. On the other hand, there is no sufficient evidence, whether the aptamer-conjugated nanoparticles are not cytotoxic and an alternative method, as MTT assay could be performed in order to understand if aptamer-conjugated nanoparticles induce any cytotoxic effects.

Despite all the advantages of Tb-TCAS silica coated nanoparticles, the main drawback is their excitation in the far UV range, which limits their usage in biological applications. Even if Sgc8-aptamer-conjugated nanoparticles would be used in the future for *in vitro* blood screening for the diagnostics of leukemia, UV light is harmful to viable cells, and this affects the results of the screening. In order to improve it, another lanthanide-ligand system could be used, with the absorbance in visible or near-IR range. For instance, erbium or holmium complexed with fleroxacin possess absorption bands in the visible range, once present as trivalent ions in aqueous solutions[105]. Moreover, lanthanide-based upconverting nanoparticles (e.g. Y_2O_3: Er^{3+}, Yb^{3+} or Gd_2O_3: Er^{3+}, Yb^{3+}), absorbing and emitting light in near IR-range could be another beneficial example for the bioconjugation with Sgc8-aptamer[106].

Chapter III: Sgc8-aptamer molecular target confirmation using AptaBiD

Objective of the study

The objective of this study was to confirm and validate Sgc8-aptamer binding with leukemia and non-malignant T-lymphocytes. In addition, AptaBiD pull-down approach was employed to identify Sgc8-aptamer binding partner. In order to improve the aptamer-target identification approach, we aimed to investigate the impact of a detergent choice and cross-linking with formaldehyde.

Introduction

For the last two decades, aptamers have shown to be promising agents for various fields, including medicine, pharmacology and agriculture[45]. Aptamers advantages over antibodies are tremendous: they can be easily synthesized and chemically functionalized according to the specific application, they possess low immunogenicity and have low dissociation constants in the nanomolar range to their targets[73]. Moreover, the cost of the synthesis is much cheaper compared to the production of antibodies, which allows them to substitute antibodies in a number of biomedical assays. Most importantly, using counter selection rounds, it is possible to select aptamers against those molecular signatures, which are not present in healthy tissues or cells; thus, aptamers can be utilized for new disease biomarker discovery in a simple and elegant manner[5].

In 2006, Shangguan et al. selected a panel of aptamers targeting T-ALL leukemia cell line with Sgc8-aptamer having the lowest binding constant[46]. Sgc8-aptamer was utilized for a number of applications due to its high affinity to the target: it was coupled with magnetic and fluorescent nanoparticles and served as a biosensor[107]. Sgc8-aptamer target identification was conducted by the same group, and it was revealed that its target is protein tyrosine kinase 7 (PTK7). Moreover, a number of validation assays was performed, which confirmed that Sgc8-aptamer targeting the transmembrane protein, and viral transfection of PTK7-negative cell line proved that PTK7 is the binding partner of Sgc8-aptamer[97].

PTK7 is a defective transmembrane protein kinase-like protein that is expressed in many cells of the human body[108]. It is also referred to as colon carcinoma kinase 4 (CCK4) because of its elevated expression in colon carcinoma tissue. While the exact function of PTK7 remains unknown, it has the potential to be a biomarker for certain cancer cells as it has been reported to be upregulated in the lung, gastric and, as previously mentioned, colon cancers[109,110]. Shin et al. investigated the role of

PTK7 in angiogenesis[111], and with the knowledge that PTK7 is upregulated in cells of various forms of cancer, the authors analyzed PTK7's role in angiogenesis by using expressed and purified PTK7 as a decoy receptor. Human umbilical vascular endothelial cells (HUVECs) were analyzed and the authors observed a dose dependent "inhibition of vascular endothelial growth factor (VEGF)-induced tube formation, migration and invasion of HUVECs[111]. They also determined that PTK7 expression in HUVECs is associated with the paralleled tube formation and that PTK7 knockdown inhibits VEGF-induced capillary-like tube formation in HUVECs.

Undoubtedly, aptamer interaction with its target as well as the binding mechanism are crucial to understand in order to use them for disease diagnostics or treatment[18]. However, the identification of the aptamer binding partner remains as a tedious and challenging task, despite all the advances made throughout the last two decades[17]. The most commonly used methods for the aptamer target identification are Affinity-Chromatography based aptamer-target pull-down followed by MS analysis or Immunoblotting[31]. In addition, detergent and affinity purification system choice plays a vital role in the aptamer-target isolation and identification[112].

In 2008, Aptamer-facilitated Biomarker Discovery (AptaBiD)[19] approach was developed by Berezovski et al. which consists of four major steps: aptamer selection, aptamer target isolation, MS analysis, and target validation assays. The aptamer-target complexes pull-down and further isolation allows employing AptaBiD for the aptamer binding partner identification, but most importantly, for the discovery of new disease biomarkers. In the present study, aptamer-target complexes pull-down approach was utilized in order to confirm Sgc8-aptamer target and to find optimal conditions in order to optimize the aptamer-target identification.

Results and Discussion

Sgc8-aptamer binding confirmation with Flow Cytometry

In the first set of experiments, binding of Sgc8-aptamer was confirmed with human acute lymphoblastic leukemia cell line – CCRF-CEM (CCL-119), T lymphoblasts, which were utilized during the selection rounds. In addition, it was decided to use Jurkat cells, which are mature T lymphocytes, as it is noteworthy to understand, whether Sgc8-aptamer target is found in both mature and immature malignant T cells. It should be also noted that it is vital for the biomarker discovery applications that an aptamer is capable of specific recognition of the target it was selected to, so Raji (CCL-86, B lymphocytes) cell line was employed, as it obviously possesses different proteome, and can act as a negative control in this study.

Flow cytometric analysis allows evaluating the aptamer interaction with its binding partner by measuring the fluorescence intensity of a fluorophore conjugated to the 5' or 3' end of the oligonucleotide. Typically, aptamer solution is incubated with the target, and after the incubation, samples were washed by centrifugation in order to discard all the unbound oligonucleotides, excluding false positive signal from the unbound fluorescently-labelled sequences. Thus, bound aptamer will result in the shift of fluorescent intensity, compared to the control samples.

For the following reason, Sgc8-aptamer labelled with FAM dye was used along with two controls: N40-DNA library labeled with FAM and Anti-PTK7 Antibody labelled with APC dye. Propidium Iodide (PI) was used as a marker of viability since it is highly important to include only viable cells for our analyses. PI enters the cell once it has lost the cellular membrane integrity, and PI intercalates with the double-stranded DNA, resulting in an increase of the fluorescence intensity. Apoptotic and necrotic cells with a damaged cellular membrane could non-specifically uptake both the aptamer and antibody, which results in false positive results; therefore, we

excluded all PI-positive cells and gated viable single-cell population for further analyses with all three cell lines used (**Fig 3.1**). In addition, based on the forward scatter (FS, cell size) and side scatter (SS, cellular complexity and granularity), we gated single-cell population, excluding all aggregated cells, or cells, undergoing mitosis.

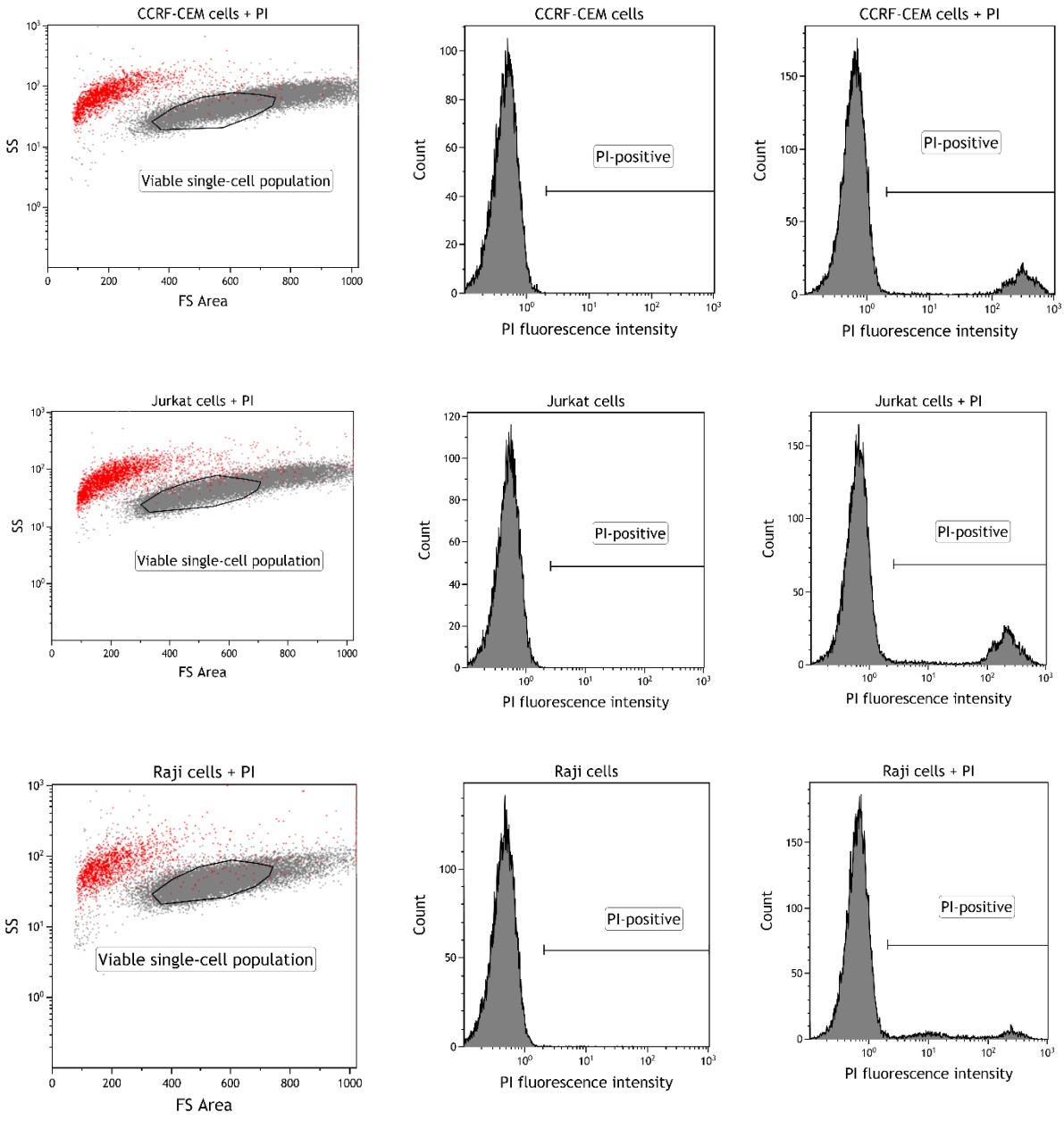

Figure 3.1. Flow cytometry graphs, representing the gating strategy based on PI signal. All cells stained with PI (necrotic) were discarded from further analysis, and gates were adjusted on single-cell viable cell subpopulation. SS stands for the side scatter and FS is the forward scatter.

Fig. 3.2 represents flow cytometry analysis of CCRF-CEM, Jurkat and Raji cells treated with Sgc8-aptamer, N40-DNA library, and a negative blank control sample. According to the data obtained, we observed a significant shift in fluorescent intensity for the sample treated with Sgc8-aptamer, whether the sample treated with DNA library showed only a modest change in the fluorescent intensity, which is associated with either unwashed oligonucleotides, or non-specific binding. Similar results were obtained for samples, containing Jurkat cells; however, Sgc8-aptamer showed weaker binding compared to the results with CCRF-CEM cell line, which could be related to the lower expression level of Sgc8-aptamer target within T lymphocytes. Lastly, using negative control - Raji cell line, we confirmed that Sgc8-aptamer can recognize T cells, but does not bind B lymphocytes. According to the previously published results, protein tyrosine kinase 7 (PTK7) was identified as a potential target of Sgc8-aptamer[97]. Moreover, Raji and Toledo cells, which naturally do not possess PTK7, were transfected with PTK7 cDNA and analyzed with flow cytometry. Flow cytometry results showed that Raji and Toledo cells before transfection did not show any binding with both, Sgc8-aptamer and Anti-PTK7 Antibody; however, cDNA transfection of Raji and Toledo resulted in binding with the aptamer and antibody, which confirms that PTK7 could be a potential target of Sgc8-aptamer[97].

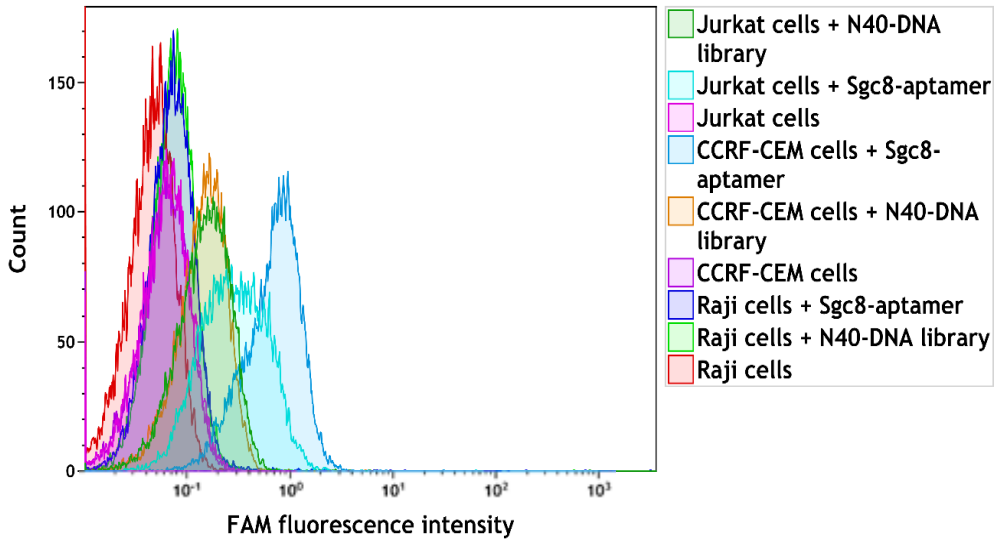

Figure 3.2. Flow cytometric analysis of Sgc8-aptamer binding with CCRF-CEM, Jurkat and Raji cells. Y-axis shows a cell count and X-axis represents FAM fluorescence intensity. Samples, containing cells only and cells, incubated with N40-DNA library were used as negative controls.

As Sgc8-aptamer showed binding with Jurkat and CCRF-CEM line, it was essential to confirm, whether two abovementioned cell lines possess PTK7. Jurkat, CCRF-CEM and Raji cell lines were treated with Anti-PTK7 Antibody and analyzed with flow cytometry. Similarly to our results with Sgc8-aptamer, stronger binding was observed for APC-labelled Anti-PTK7 Antibody with CCRF-CEM cell line, and a weaker shift in fluorescence intensity for Jurkat cell line; however, no binding has been detected for Raji cells (**Fig. 3.3**). It was reported earlier, that Sgc8-aptamer does not compete with PTK7 antibody, once they are used together within the same sample, which could be due to the simultaneous binding of the aptamer and antibody to different sites of PTK7[97], or Sgc8-aptamer binds to the molecule, which is tightly associated with PTK7. In order to further reveal the role and binding of Sgc8-aptamer, additional experiments with a recombinant PTK7 and Sgc8-aptamer could be performed. For instance, aptamer-based ELISA[113]

with a fluorescently-labeled Sgc8-aptamer and recombinant PTK7, immobilized on the solid support could clarify, whether Sgc8-aptamer binds specifically to PTK7 or not. In addition, competitive ELISA with Sgc8-aptamer and Anti-PTK7 Antibody could confirm if there is no competition in binding between the aptamer and antibody to PTK7. Another method that could be used is flow cytometry with the fluorescently-labelled Sgc8-aptamer, Anti-PTK7 Antibody and a recombinant PTK7, conjugated with beads of the appropriate size, suitable for flow cytometric analysis. Considering that Anti-PTK7 Antibody and Sgc8-aptamer showed non-competitive binding, additional direct investigation of Sgc8-aptamer binding with the recombinant PTK7 is of great importance and would allow to exclude other targets from the analysis, which could be attracting Sgc8-aptamer.

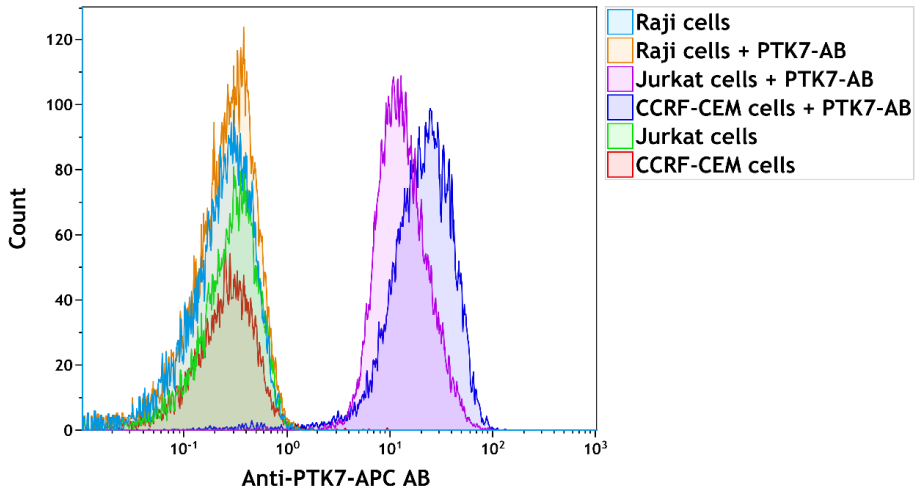

Figure 3.3. Flow cytometric analysis of APC-labelled Anti-PTK7 Antibody binding with CCRF-CEM, Jurkat and Raji cells. Y-axis shows a cell count and X-axis represents APC fluorescence intensity.

Overall, we have confirmed that Sgc8-aptamer binds both CCRF-CEM and Jurkat cells, but not the control cell line (B lymphocytes), which could be due to the fact that both CCRF-CEM and Jurkat cells possess the same target, attracting Sgc8-aptamer. Nevertheless, further study of Sgc8-aptamer binding with PTK7 should be considered in order to confirm if the aptamer binds specifically to its previously assigned target, or there could be another candidate, tightly associated with PTK7 or having similar motifs within the structure.

Sgc8-aptamer targets human non-malignant PMBC

Furthermore, we decided to investigate if Sgc8-aptamer target presented only on malignant T cells by conducting flow cytometry experiment with non-malignant human peripheral mononuclear blood cells (PMBC). For that, we isolated white blood cells according to the protocol, and incubated cell suspension with Sgc8-aptamer and N40-DNA library (control sample). It was published earlier that PTK7 does not act as a cancer biomarker, and it could be found in healthy tissues; however, the expression rate in malignant cells and tissues is immensely higher is compared to healthy ones[108]. Thus, we first detected T cell subpopulation by using CD3 antibody **(Fig. 3.4)**, followed by the detection of CD4+ T cells with CD4 antibody (T-helpers). Then, adjusting the gating on T cells only, we revealed that Sgc8-aptamer binds to healthy T cells, which could be associated with Sgc8-aptamer target is found in both, healthy and malignant samples, or non-specific binding of Sgc8-aptamer. It could be suggested that for efficient detection or treatment of leukemia cells it is vital to conduct additional experiments in order to reveal the specificity of Sgc8-aptamer binding, and couple Sgc8-apatmer with an additional probe, which can facilitate recognition of cancerous T cells. Since Sgc8-aptamer can bind to both, malignant and non-malignant T lymphocytes, it cannot be used solely for the diagnostics of leukemia cells, and in order to improve that, the rate of PTK7-expression for malignant cells should be established

for malignant and non-malignant cells. As it was noted, PTK7 is overexpressed in cancer cells compared to healthy ones and using this, it would be possible to distinguish between malignant and non-malignant T cells. Additionally, another aptamer could be selected through counter selection rounds, which could be exclusively binding to leukemia cells, and not targeting healthy cells. This aptamer could be conjugated with an imaging probe along with Sgc8-aptamer for the enhanced recognition of leukemia.

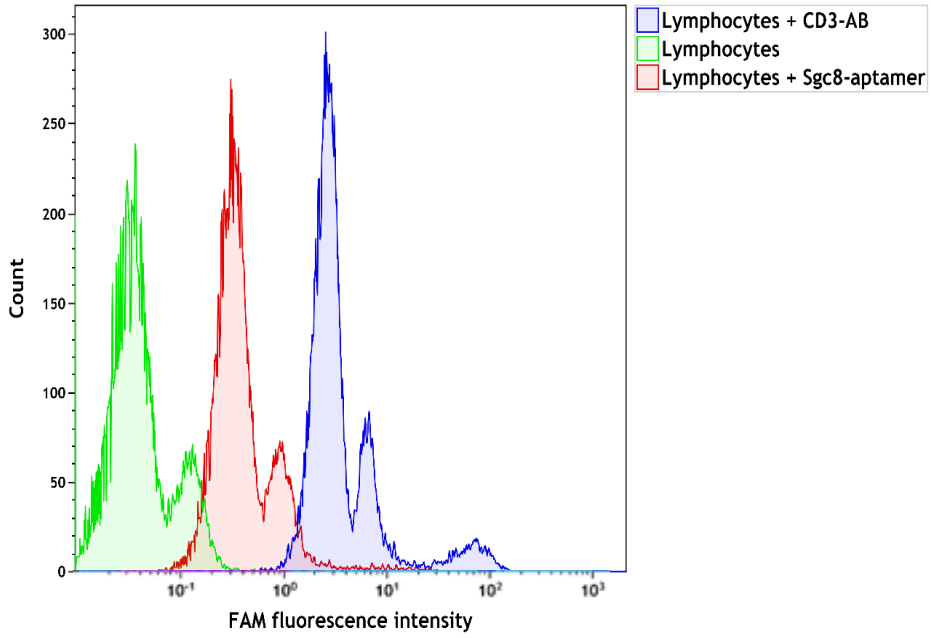

Figure 3.4. Flow cytometric analysis of FAM-labelled CD3-Antibody and Sgc8-aptamer binding with human lymphocytes. Y-axis shows a cell count and X-axis represents FAM fluorescence intensity.

Sgc8-aptamer molecular target identification

Modern medicine indispensably leads to the diagnostics and therapy of any disease on the molecular level. Biomarker discovery and their further utilization in biomedicine could beneficially facilitate many aspects of commonly established treatment procedures and protocols; in other words, using disease biomarkers, it is possible to target abnormal tissues or cells with high precision and specificity, not hitting healthy ones[1]. Therefore, it is essential to investigate possible intrinsic pathways and interactions between a biomarker and its ligand, which could serve either as a diagnostic probe, or a carrier for the drug delivery applications.

Aptamer-facilitated biomarker discovery approach offers the selection of aptamers to the targets, which are only present in diseased cells or tissues, and could serve as biomarkers for further therapy and detection applications[19]. At the same time, using aptamer target affinity purification procedure, or aptamer-target complexes pull-down with magnetic beads/affinity chromatography columns, it is possible to identify an aptamer binding partner with MS[9]. Moreover, bioinformatics tools can ease the analysis of MS data, and it allows comparing the obtained results for the aptamer of interest and control samples.

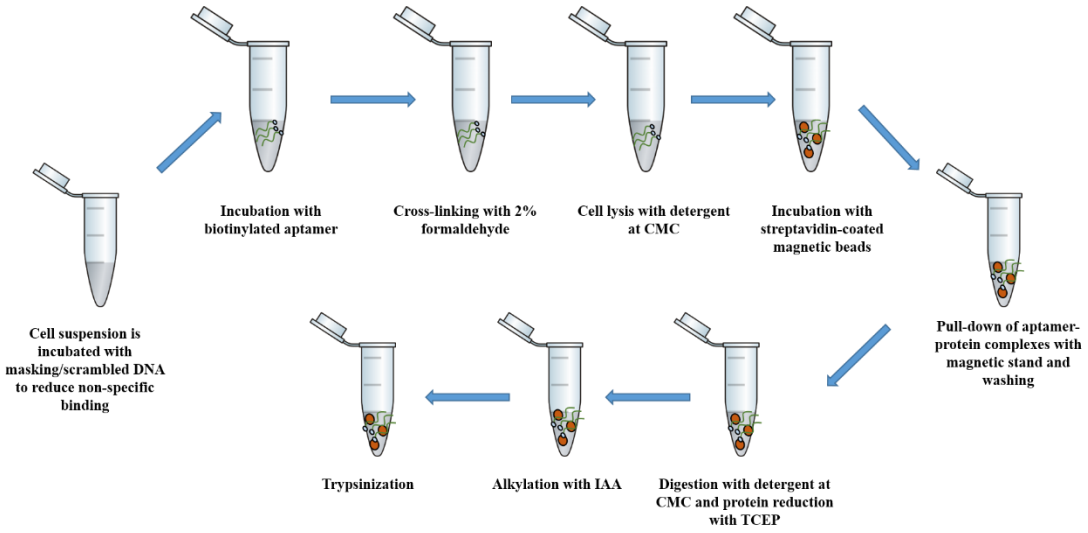

Figure 3.5. Pull-down scheme including in-solution digestion of samples for subsequent MS analysis.

The core part of this study is the pull-down of aptamer-target complexes, which implies a careful and appropriate choice of all the reagents and conditions used. **Fig. 3.5** shows subsequent steps of the pull-down, including further in-solution digestion and sample preparation for MS analysis. In our study, we used two cell lines: CCRF-CEM and Jurkat cells, which showed strong binding with Sgc8-aptamer with flow cytometry. Cell suspension (with approximately 10^6 cells/mL for both cell lines) was incubated with masking scrambled DNA, which is a random, non-labeled oligonucleotide with the same length of the sequence as the aptamers used in the experiment. This step enables to diminish the occurring non-specific binding, since usually scrambled DNA is used in 3-fold excess compared to the concentration of the aptamer. For aptamer-target isolation, we used biotinylated Sgc8-aptamer and Apt9, which was used as a control. Both Sgc8-aptamer and the control were incubated with the cell suspension, and afterwards we used 2% formaldehyde in order to induce cross-linking. The cross-linking allows to form covalent bonds between the aptamer and its binding partner; therefore, it facilitates the

detection of the target. Lastly, detergent plays a vital role in protein purification. Detergents are amphiphilic molecules, bearing a hydrophilic polar group, and a hydrophobic non-polar tail. This structure allows detergent to insert its hydrophobic tail into the lipid cellular membrane, disrupting the lattice, and, therefore, extracting the proteins. At the critical micelle concentration (CMC), or above it, detergent molecules form micelles, and extracted proteins become a part of the micelle complexes, in some cases, with the complete loss of the surrounding lipids/proteins. All detergents are classified as either ionic, non-ionic or zwitterionic, and non-ionic detergents are the most commonly used, whether it is crucial to retain the naïve state of the extracted protein[114].

Thus, it was important to elucidate the impact of different detergents, choice of the system for the pull-down of aptamer-protein complexes as well as other conditions such as the concentration of the masking DNA, temperature on the aptamer target identification on the final results.

Sgc8-aptamer target identification with digitonin

Digitonin is a non-ionic detergent with a steroid-like saposin structure. It has a CMC value of 0.02-0.03% (0.25-0.5 mM) with the micelle size of approximately 70-75 kDa. Digitonin is a naturally extracted detergent from the plant *Digitalis Purpurea*, which could cause the batch-to-batch variations within the chemical structure, and it remains its major drawback[115]. Digitonin has gained great popularity for the structural studies of transmembrane proteins with cryogenic electron microscopy over the last decade, and we decided to evaluate its capacity for the aptamer target identification[116].

Fig. 3.5 represents Venn diagrams, which are commonly used in proteomics analyses, facilitating comparison of identified proteins, in samples with Sgc8-aptamer and a control aptamer (Apt9). For CCRF-CEM cell line we identified 22 common proteins in both, control and Sgc8-

aptamer samples; however, 120 proteins were present only in the sample with Sgc8-aptamer. Among them, we did not identify PTK7 protein; however, we identified its interactor Phosphoglycerate kinase (*P00558*), which also has common motifs within the primary structure. Bioinformatics analysis in a similar manner was performed for the samples containing Jurkat cell suspension. Within the sample with Sgc8-aptamer, we identified 67 unique proteins, and PTK7 (*P43403*) was the most enriched protein. In addition, we have identified its indirect binding partner - Thyroid hormone receptor-associated protein 3 (*Q9Y2W1*).

To sum up, our results with digitonin showed that it could be used for the aptamer target identification assays. Indeed, we have obtained more proteins for samples with Jurkat cell line, which could be due to the difference in the internal cellular complexity of immature T lymphoblasts – CCRF-CEM cell line and mature T lymphocytes – Jurkat cell line[117]. Nevertheless, CCRF-CEM cell line was used for Sgc8-aptamer selection and further target identification, and it was revealed that PTK7 is the most relevant candidate, and it was confirmed afterwards with gene transfection experiments. Within the results obtained, we could not identify Sgc8-aptamer target for CCRF-CEM cells with digitonin, as well as obtained a lot of irrelevant proteins, which implies that further optimization of the protocol with digitonin should be considered. All the intracellular proteins could be identified as a result of non-specific binding of Sgc8-aptamer: no matter how selectively it binds to its target, a negatively-charged DNA/RNA aptamer would be attracted by positively charged lysine amino groups of proteins at physiological pH, which is a fundamental limitation of aptamers. In addition, digitonin itself could have induced “harsher” cell lysis than it was expected, which resulted in the pull-down of various intracellular proteins. For the aptamer-target identification, which is a transmembrane protein, it is not necessary to lyse cells completely, but to gently isolate the aptamer bound to its binding partner from the cellular membrane. Lastly,

the number of washing rounds could be increased in order to prevent the identification of non-specifically bound proteins.

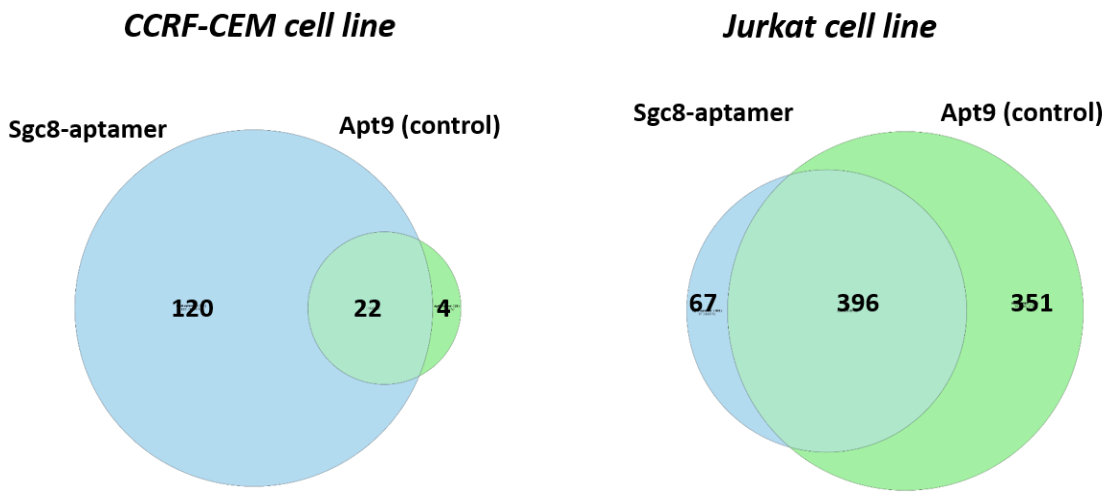

Figure 3.5. Venn diagrams, representing the amount of proteins identified with MS within each sample. In the following experiment, digitonin was used as a detergent. MS results were obtained in triplicates for each sample, and only mutual proteins found in each of triplicates were used for further analyses.

Sgc8-aptamer target identification with Triton X-100

Triton X-100 (octyl phenol ethoxylate) is one of the most commonly used detergents in proteomics. It is a non-ionic detergent, with low CMC value of 0.1% (0.2 mM) and the size of micelles within the range from 60 to 90 kDa[118]. The micelle formation process is a temperature-dependent in case of Triton X-100, which limits its applications, whether low temperatures should be maintained. Moreover, the presence of benzene rings, which strongly absorb light within UV range, interferes with protein quantitation[119]. Nevertheless, Triton X-100 is currently being used in a wide variety of applications, and we were interested to evaluate, whether it is a suitable detergent for our approach.

In addition, considering our previous results with digitonin, we decided to introduce cross-linking with 2% formaldehyde, as it could positively impact on the enrichment of the molecular target of Sgc8-aptamer, and to maintain consistency, we utilized both cell lines and the same aptamer-control. **Fig. 3.6** depicts the number of proteins identified for samples containing CCRF-CEM cells. Interestingly, we have obtained more proteins for the samples, where the cross-linking was induced, which could be due to the formation of covalent bonds within adjacent proteins, and their further isolation within pull-down with streptavidin-coated magnetic beads; however, we could not identify PTK7 within samples with CCRF-CEM cells. In contrast, for samples with Jurkat cells, we identified PTK7 within both, cross-linked and non-crosslinked samples (**Fig. 3.6**) that confirms our previous findings with digitonin. Similarly to what we saw with digitonin, Triton X-100 could be responsible for the complete cell lysis and the pull-down of numerous intracellular proteins due to its solubilization properties. Moreover, the results obtained question the specificity of Sgc8-aptamer binding to its target as well as the stability of the aptamer-target complexes during

the pull-down. Nevertheless, understanding the nature and biological role of Sgc8-aptamer target, PTK7, could explain these findings.

According to the previous study, PTK7 is a transmembrane protein which was identified as a potential target of Sgc8-aptamer[97]. Later, it was confirmed with fluorescence microscopy that after the treatment with trypsin, Sgc8-aptamer lost its binding with CCRF-CEM cells (incubation at 4 C^o); however, it showed a strong binding inside the cell (incubation at 37 C^o), which could be due to the cellular uptake, or specific internalization[120]. PTK7 protein is a member of the Wnt signaling family, which functions as a promoter of PCP signaling pathway[121]. PTK7 recruits Dsh proteins to the membrane, which causes the activation of PCP signaling. PTK7-Dsh interaction is mediated by the adaptor protein – RACK (receptor of activated protein kinase C). Then, RACK supports Dsh recruitment by interacting with PKCδ1[122]. Interestingly, PTK7 acts as a transmembrane receptor: once it has its ligand bound, it undergoes internalization, which is followed by either clathrin- or caveolin-mediated endocytosis, with subsequent lysosomal degradation. Dynamin is a GTPase, which plays a major role in the scission of newly formed intracellular vesicles from the plasma membrane of one cellular compartment and their targeting to another cellular compartment. At the same time, Ras-related proteins - Rab5, Rab7 and Rab 9 drive the formation of the early and late endosomes, with a final degradation in lysosomes or transport of the endosomes to Golgi complex **(Fig. 3.7)**. This could be the major reason, why we have identified a lot of irrelevant intracellular proteins, as Sgc8-aptamer binds PTK7, the whole complex being internalized through the formation of endosomes, and all due to the presence of biotin many of intracellular protein could be attracted. Most of the products are being degraded in lysosomes, and remaining ones are being isolated with magnetic beads and digested for MS

analysis. Thus, it is crucial to understand the role of the aptamer-target and choose appropriate conditions and method for its identification.

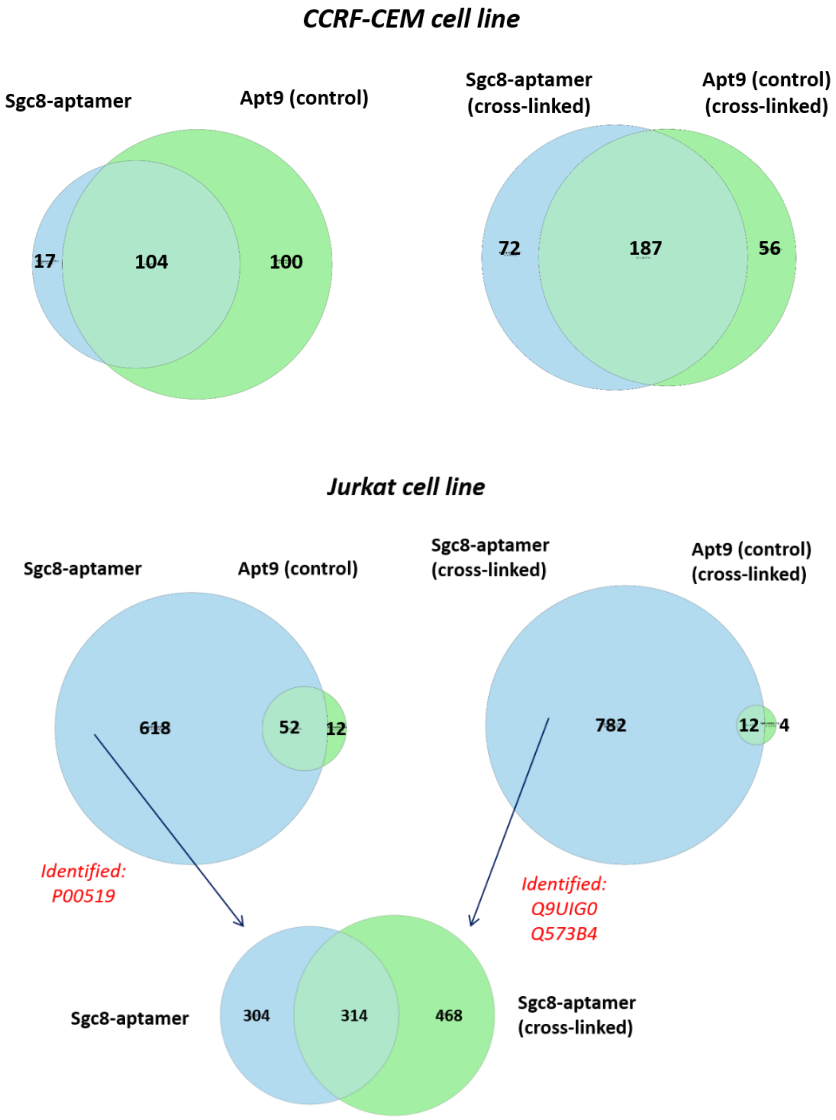

Figure 3.6. Venn diagrams representing the number of proteins isolated in AptaBiD and identified with MS. Triton X-100 was used as a detergent in AptaBiD. MS results were obtained in triplicates for each sample, and only mutual proteins found in each of triplicates were used for further analyses.

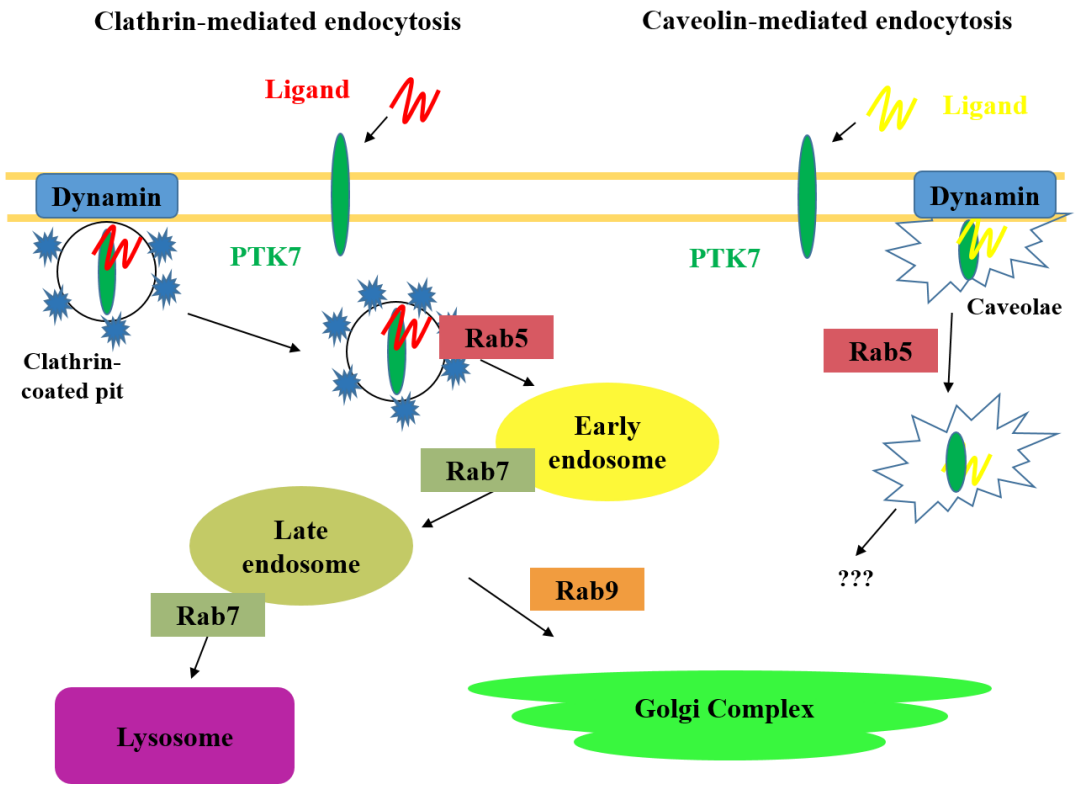

Figure 3.7. Clathrin- and caveolin-mediated endocytosis, and PTK7 involvement in canonical Wnt and PCP signaling. Rab5, Rab 7 and Rab9 defined in the text.

Sgc8-aptamer molecular target identification with n-dodecyl-β-D-maltopyranoside

N-dodecyl-β-D-maltopyranoside (DDM), is also known as layrul maltoside, a non-ionic, "mild" detergent, which has a maltose hydrophilic head and hydrophobic alkyl tail. Due to its advantages over other detergents, such as low CMC value (approximately 0.0087%/0.17 mM), cheaper cost, and ability to maintain a stable native state of many proteins, it is currently the most popular detergent used for protein extraction studies[123]. However, it has two disadvantages, including the relatively big micelle size (around 65-70 KDa) and the formation of "substantial non-mobile belt" around proteins, which could be detrimental for crystallogenesis studies[124]. Thus, inspired by previous advances, we used DDM as a detergent for Sgc8-aptamer target identification.

Fig. 3.8 represents results obtained with the experiment with DDM for both cell lines. Using DDM, we could identify PTK7 in both sets of samples (except samples with CCRF-CEM cells, where the cross-linking was induced). As it was suggested, the number of proteins identified corresponds to the internalization of PTK7 with subsequent endocytosis of Sgc8-aptamer-PTK7 complexes. Another possible reason could be non-specific interactions between Sgc8-aptamer and intracellular proteins during the cell lysis. This could be improved by increasing the amount of washing rounds during the pull-down with magnetic beads as well as conducting the incubation of the aptamer with cell suspension at 4 C^o.

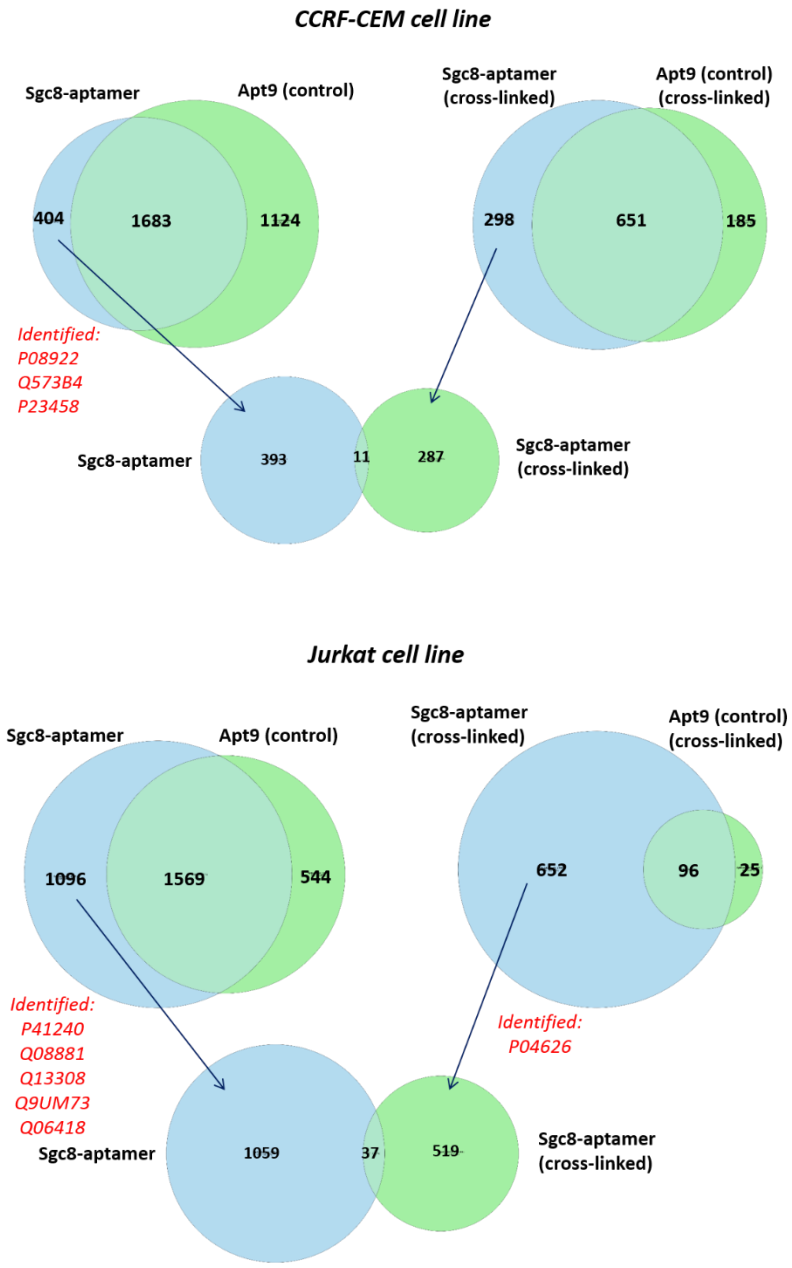

Figure 3.8. Venn diagrams representing the number of proteins isolated in AptaBiD and identified with MS. n-Dodecyl-β-D-maltopyranoside was used as a detergent in AptaBiD. MS results were obtained in triplicates for each sample, and only mutual proteins found in each of triplicates were used for further analyses.

The number of proteins identified is a result of either internalization of PTK7 with the bound aptamer that leads to the pull-down of numerous intracellular proteins, attracted non-specifically, or the inaccurate selectivity profile of Sgc8-aptamer. Even though it has been shown that Sgc8-aptamer possesses binding with PTK7-negative cell lines (Raji and Toledo cells) after the transfection with PTK7 cDNA[97], it is of great importance to confirm its target with additional experiments, such as the evaluation of Sgc8-aptamer binding with the recombinant PTK7. However, if the results obtained caused by the internalization of PTK7 with the bound aptamer, it would be quite challenging to identify the target of Sgc8-aptamer as it undergoes endocytosis with the subsequent lysosomal degradation[120]. In order to improve the target identification approach for internalizing aptamers, cell fractionation with the isolation of a membrane component could be used prior to the pull-down.

MS results obtained with digitonin, Triton X-100 and n-dodecyl-β-D-maltopyranoside suggest that the selectivity of the approach used requires further improvements. Previously assigned target of Sgc8-aptamer has not been identified in most cases, which either is due to the internalization, non-specific binding of Sgc8-aptamer, or misinterpretation of Sgc8-aptamer target. It was decided to analyze the results obtained with n-dodecyl-β-D-maltopyranoside in order to see, whether we could find any direct or indirect interactors of PTK7, or proteins with similar motifs within the primary structure. Comparison of datasets with the identified proteins between Sgc8-aptamer and the control aptamer revealed that some of the major PTK7 interactors were identified within the sample with Sgc8-aptamer, but not within the control aptamer sample. This could be due to fact that these interactors were pulled-down along with the target; however, the overall number of proteins identified does not allow us to draw a conclusion, whether those interactors were pulled-down selectively, or not. Moreover, these results are insufficient to conclude that the

target of Sgc8-aptamer is PTK7, or that the target undergoes internalization; however, additional experiments could be conducted to clarify the role and nature of Sgc8-aptamer binding.

Detergent plays a crucial role in aptamer-target isolation experiments, and among three detergents utilized, n-dodecyl-β-D-maltopyranoside showed that the previously assigned target of Sgc8-aptamer has been identified almost in all samples with Sgc8-aptamer, excluding the sample with CCRF-CEM cells and formaldehyde cross-linking; however, it has not been identified within samples with the control aptamer. In addition, it is essential to use proper bioinformatics tools for comparison of the obtained results. As it was confirmed earlier that Sgc8-aptamer target is present on the cellular membrane, all the intracellular identified proteins could be discarded from further analyses, and analysis of the role of PTK7 explained the amount of identified proteins as well as the presence of its interactors found within samples. Lastly, in order to inhibit the internalization of Sgc8-aptamer-PTK7 complexes, it is vital to conduct the incubation at 4 C^{o} as well as to utilize a higher concentration of the masking DNA.

Sgc8-aptamer molecular target identification with n-dodecyl-β-D-maltopyranoside: inhibition of PTK7-internalization

In the final part of the study, we implemented all our previous findings for the optimization of the aptamer-target identification. N-dodecyl-β-D-maltopyranoside was used as a detergent due to its capacity to gently denature proteins of interest. We also used the incubation of the aptamer with the cellular suspension at 4 C^{o}, as it has a direct impact on the inhibition of the internalization. Indeed, we kept the same control samples and cross-linking in order to maintain consistency, even though the cross-linking did not enhance our results in previous experiments.

Fig. 3.9 represents the results of the comparison of all identified proteins for both cell lines. Even though the incubation of Sgc8-aptamer at 4 C^{o} with samples did not result in a decreased number of proteins identified; results with n-dodecyl-β-D-maltopyranoside were consistent, and we identified PTK7 in all samples (excluding the samples with CCRF-CEM cell line with cross-linking). Indeed, cross-linking with 2% formaldehyde could not improve our results, which can be associated with the non-specific binding of Sgc8-aptamer as well as with the internalization of Sgc8-aptamer-PTK7 complexes. In addition, formaldehyde could induce cross-linking of adjacent proteins via lysine residues, or the cross-linking of Sgc8-aptamer with other non-target transmembrane proteins. In order to enhance the specificity of the cross-linking, photocross-linking[35] could be used instead, which allows to form a cross-link between the aptamer with a modified photoactive nucleobase, such as 5-bromouracil, or 5-iodouracil, and its binding partner. Nevertheless, we have identified several intracellular interactors of PTK7, including PHLPP1, PHLPP2, WNT5A and ACACB, which has a correlation with the internalization of PTK7 with the bound Sgc8-aptamer and further endocytosis.

Aptamer-target identification is a challenging and sophisticated task, mostly due to the biological complexity of the cell, and naturally occurring non-specific interactions between an aptamer and positively charged biomolecules. It is vital to reveal, whether the aptamer binds to the target on the cellular membrane, or its target is found inside the cell, in order to design the target isolation experiments. This could be achieved through treating cells with trypsin and comparing it with an untreated control: an aptamer, binding to a transmembrane protein should either lose its binding or possess a weaker signal, which can be evaluated with flow cytometry and fluorescence microscopy. Once the aptamer has been selected to a transmembrane protein, it would be beneficial to perform a cell fractionation and utilize the plasma membrane for the aptamer target identification; therefore, excluding irrelevant intracellular proteins which could be attracted to the aptamer through electrostatic interactions.

According to the results obtained, the method used requires major optimization due to the number of proteins identified with various detergents, even with the induced formaldehyde cross-linking. Sgc8-aptamer itself could have induced non-specific binding; thus, causing the pull-down of numerous intracellular proteins through electrostatic interactions. Alternative methods, such as cell fractionation prior to the pull-down as well as photocross-linking could be used in future in order to improve the selectivity of this approach as well to clarify the target and specificity of Sgc8-aptamer binding. In addition, Western blot of the samples with Sgc8-aptamer and control aptamers after the pull-down could be utilized followed by the in-gel digestion and MS analysis, in order to enhance this method. Moreover, HPLC-based approach for the aptamer-target identification[125] was shown to be more beneficial compared to classic SDS-PAGE-based techniques, and could be used to substitute streptavidin-biotin pull-down of the aptamer-target complexes.

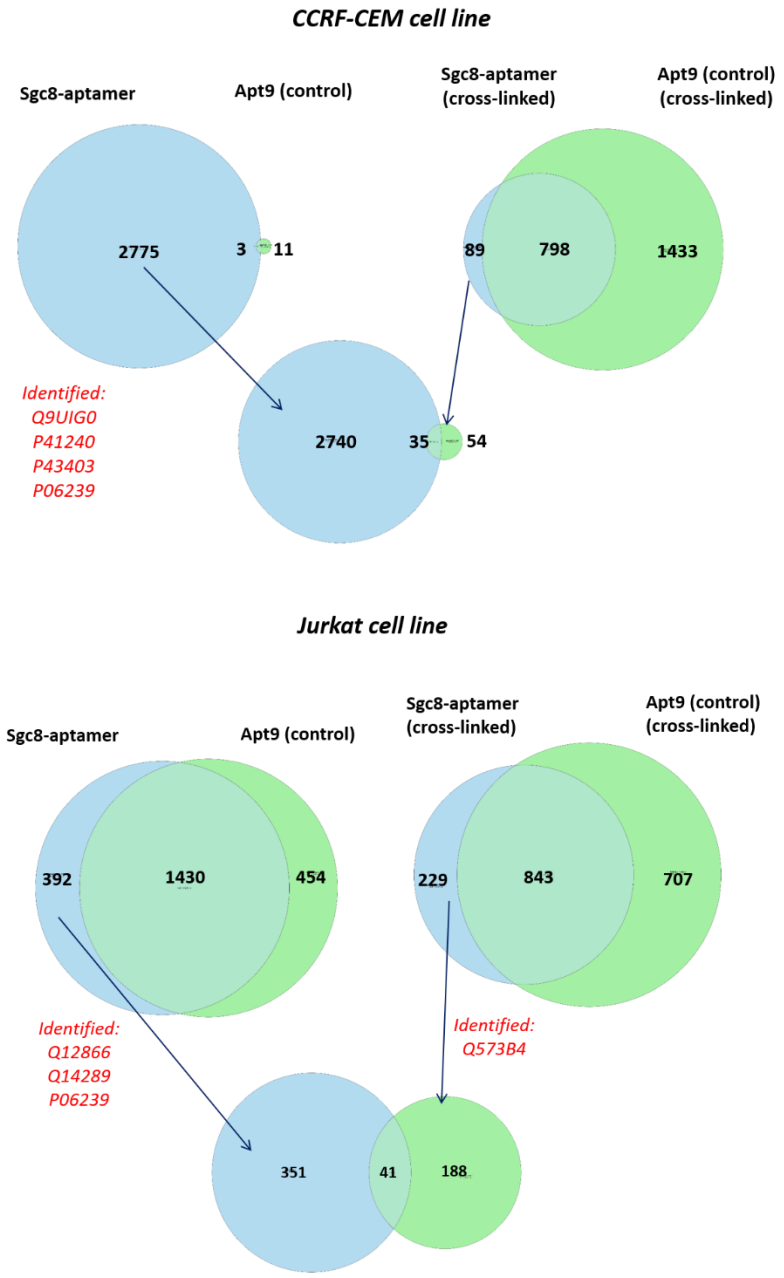

Figure 3.9. Venn diagrams, representing the amount of proteins identified with MS within each sample. In the following experiment we optimized all the previous conditions (including the incubation at 4 C°), and n-dodecyl-β-D-maltopyranoside was used as a detergent. MS results were obtained in triplicates for each sample, and only mutual proteins found in each of triplicates were used for further analyses.

Conclusions

In this study, the pull-down of aptamer-target complexes approach of Aptamer-facilitated Biomarker Discovery was used for the optimization of an aptamer target identification assay. Sgc8-aptamer has showed strong binding with CCRF-CEM and Jurkat cell lines, and it was used in order establish optimal conditions for its binding partner identification, since Sgc8-aptamer target was identified previously and confirmed with several validation assays.

It was revealed that Sgc8-aptamer recognized non-malignant human T lymphocytes, which could be associated with either its binding to the same target on healthy and malignant T cells, or Sgc8-aptamer displayed non-specific binding to another target molecule due to the electrostatic attraction. It is vital to conduct additional experiments with healthy T lymphocytes, such as experiments with Anti-PTK7 Antibody and the pull-down with MS analysis in order to clarify, whether they possess the same target as CCRF-CEM and Jurkat cell lines.

In order to optimize aptamer-target complexes pull-down technique of AptaBiD, we have compared three commonly used detergents in protein purification studies including digitonin, Triton X-100 and n-dodecyl-β-D-maltopyranoside since it is a well-known fact that a detergent plays a vital role in the aptamer target identification. Using N-dodecyl-β-D-maltopyranoside, we identified PTK7 in all samples, containing Sgc8-aptamer, except the sample with CCRF-CEM cells with formaldehyde cross-linking. Triton X-100 and digitonin could be utilized for the aptamer-target identification; however, we have identified a lot of irrelevant proteins, which could be related to their "harsher" extraction, whether n-dodecyl-β-D-maltopyranoside induced a gentle cell lysis. The results obtained suggest that the approach used requires further optimization, considering the amount of proteins identified within the samples, which could be due to either poor purification of samples, or Sgc8-aptamer possesses non-specific binding. Even though it has been

reported previously that Sgc8-aptamer can be internalized through the endocytosis once it binds PTK7, a lot of intracellular proteins identified could be related to the non-specific binding of Sgc8-aptamer with positively charged proteins. In order to improve that, cell fractionation with the membrane component isolation could be used for those aptamers, which target is a transmembrane protein. Additional positive control can be used, such as Anti-PTK7 Antibody during the pull-down in order to compare results obtained with Sgc8-aptamer. Considering that antibodies have greater selectivity and specificity of the binding than aptamers, this could help to reveal whether Sgc8-aptamer has poor specificity to its target, or the approach requires further major improvements. Moreover, an increased concentration of the masking DNA could be used prior to the incubation of an aptamer with the membrane component as well as increased amount of washing rounds of captured aptamer-target complexes performed, which in both cases should positively influence on the target isolation and identification

In addition, we aimed to evaluate the impact of cross-linking with 2% formaldehyde on our results. Considering the complexity of PTK7 internalization followed by endocytosis and lysosomal degradation, formaldehyde cross-linking did not improve our results, and mostly enhanced the pull-down of irrelevant and intracellular proteins. To improve this, photo cross-linking of an aptamer with a modified photoactive nucleobase with its target can be used instead, which would diminish the cross-linking of adjacent proteins via lysine residues, and would allow isolating the aptamer-target complexes with a greater efficiency.

Chapter IV: General Discussion and Conclusions

Aptamers have gained a great interest over the past two decades and have been utilized in various biological assays. Even though aptamers offer cheaper synthesis, low immunogenicity and flexibility with chemical modifications, they cannot currently fully substitute antibodies due to a number of reasons. First, antibodies possess higher natural affinity to their targets compared to aptamers, and non-specific binding of aptamers due to the electrostatic interactions with positively charged biomolecules limits their usage in a complex biological media. An antibody precisely binds its target (an epitope on the antigen) with an antigen-binding site, called paratope, through the specific "lock-key" interactions, while an aptamer binds its target through the formation of a stem-loop secondary structure, which can be easily affected by various factors, such as temperature and surroundings. In fact, there is only a little known about the aptamer interactions with its target as well as the stability of formed complexes under physiological conditions. Although these drawbacks of aptamers require further improvements and limit the aptamer widespread employment for antibody-based applications; aptamers, unlike antibodies, could be utilized in biomarker discovery through Cell-SELEX, including positive and counter selection rounds, which results in the development of aptamers, exclusively binding targets present on abnormal cells. In addition, aptamer-based fluorescent probes can be used for *in vitro* imaging applications, such as blood screening, which is cheaper compared to the antibody-based assays.

In the first part of this work, luminescent nanoparticles were synthesized for their further bioconjugation with Sgc8-aptamer, which showed previously strong binding with leukemia cells. Hence, the microemulsion method was used for Tb-doped silica-coated Tb-TCAS synthesis, and then, amino- and carboxyl groups were immobilized on their surface. Tb-TCAS-doped nanoparticles were used as they possess stronger luminescence intensity compared to other

lanthanide ions with TCAS as well as silica enhances Tb-TCAS luminescence through shielding Tb-TCAS complexes from water molecules. Despite all the advantages of Tb-TCAS doped nanoparticles, they absorb light in the far UV range with the maximum at 330 nm, which is not convenient for instrumental bioanalysis, and the excitation in the far UV range could be harmful to tissues or cells under analysis. In the future, another lanthanide-ligand system could be used, which absorbs light in the visible or near-IR range, such erbium or holmium complexes with fleroxacin, or upconverting nanoparticles. This would allow obtaining luminescent nanoparticles, which would be more suitable for biomedical applications.

Furthermore, in order to conjugate Sgc8-aptamer with luminescent nanoparticles, we utilized Michael addition - Schiff base reaction and confirmed that the bioconjugation was performed successfully. It has been shown that aptamer-conjugated nanoparticles indicate the presence of an aptamer with zeta potential analysis and UV spectroscopy; however, it is not clear, whether the aptamer was bound covalently to Tb-TCAS silica nanoparticles, or it was attracted through electrostatic interactions. In order to improve that, IR spectroscopy could be performed to show the formation of new bonds within aptamer-conjugated nanoparticles. In addition, SNs-NH_2 conjugated with Sgc8 aptamer possessed less intensive luminescence, compared to SNs-NH_2. This could be due to the electrostatic interactions between the negatively charged aptamer and positively charged amino groups at physiological pH, or due to the cross-linking of SNs-NH_2, induced by glutaraldehyde. Lastly, the conjugation of SNs-NH_2 nanoparticles with Sgc8-aptamer results in the formation of an unstable conjugate, which requires further reductive amination, and glutaraldehyde used as a cross-linker can polymerize in aqueous media and induce cross-linking of the adjacent SNs-NH_2. This suggests that the conjugation of SNs-COOH with the aptamer is

more favorable and allows obtaining aptamer-conjugated nanoparticles with greater luminescence intensity.

Then, using fluorescence microscopy, we showed that SNs-Sgc8 complexes can recognize leukemia cells showing bright luminescence under the excitation at 340 nm. However, it is also essential to elucidate with fluorescence microscopy if Sgc8-aptamer-conjugated nanoparticles bind leukemia cells non-specifically, or due to the cellular uptake. In order to improve that, an antibody blocking experiment could be performed along with the negative control cell line used. Sgc8-aptamer has non-competitive binding with PTK7, and according to the previously published results, it should not completely lose its binding with leukemia cells, upon the addition of Anti-PTK7 antibody. And lastly, in order to reveal, whether the aptamer-conjugated nanoparticles do not affect the cell viability, additional cytotoxicity tests could be performed, such as MTT assay.

Overall, despite all the advantages of aptamer-conjugated nanoparticles for their utilization as luminescent probes in biomedicine, a lot of improvements should be considered. The bioconjugation approach allows to couple nanomaterials with various biomolecules. In particular, nanoparticles, possessing functional groups, such as amino, carboxyl, hydroxyl or carbonyl groups can be conjugated with aptamers or antibodies; and, therefore, they could serve as diagnostic probes for a plethora of biomedical applications. Considering the reliability of antibodies, it would be more beneficial to conjugate an antibody with Tb-TCAS doped silica nanoparticles since aptamers are prone to non-specific binding and vulnerable to nuclease activity, which would allow to obtain antibody-based luminescent probes with higher affinity and stability.

In the second part of this study, I aimed to optimize the approach for aptamer-target identification, using AptaBiD. For that, of Sgc8-aptamer was chosen as its target has been already identified as a transmembrane protein, protein tyrosine kinase 7 (PTK7). Even though Sgc8-

aptamer binding was confirmed previously with leukemia cells, it was essential to validate it with different negative controls. In addition, non-malignant T lymphocytes have been used in order to reveal, whether the target of Sgc8-aptamer is only present on leukemia cells, or on both, healthy and malignant T cells. It was shown, that Sgc8-aptamer possesses stronger binding with leukemia cells; however, it binds to healthy T lymphocytes as well. As it was previously reported, PTK7 is overexpressed on malignant cells, and in order to improve the detection of leukemia cells with Sgc8-aptamer, PTK7 expression rate should be determined, which would allow improving the accuracy of the detection and distinguishing between malignant and non-malignant cells using Sgc8-aptamer. Also, an additional affinity probe to leukemia cells, coupled with Sgc8-aptamer could result in the more accurate and precise detection of malignant T lymphoblasts and could be considered as another improvement.

In order to optimize the aptamer-target identification approach, three commonly used detergents were tested along with the induced cross-linking with 2% formaldehyde. The approach used includes aptamer-target complexes pull-down with magnetic beads, followed by the in-solution digestion and sample preparation for MS analysis, which is less time-consuming and tedious, compared to the most popular method utilized for the following purpose with SDS-PAGE and subsequent in-gel digestion of samples. Nevertheless, our results have shown that this method requires further improvements due to the numerous proteins identified within samples, which is either as a result of the aptamer non-specific binding or due to the internalization of Sgc8-aptamer. If an aptamer has been selected to a transmembrane protein, which can be explored with fluorescence microscopy or the cell treatment with trypsin, cell fractionation with the isolation of a membrane component could be used for the identification of an aptamer-target. This would allow decreasing the number of irrelevant intracellular proteins, which may attract an aptamer through

electrostatic interactions. In addition, an increased number of washing steps of captured aptamer-target complexes along with the increased concentration of the masking DNA used for the incubation with cells, preceding the incubation with an aptamer could beneficially impact on the target identification.

Analysis of the results obtained with three non-ionic detergents revealed that n-dodecyl-β-D-maltopyranoside showed that the previously assigned target of Sgc8-aptamer has been identified almost in all samples with Sgc8-aptamer, excluding the sample with CCRF-CEM cells and formaldehyde cross-linking; however, it has not been identified within samples with the control aptamer, which could be associated with its gentle solubilization of membrane proteins, allowed for the identification of PTK7 in all samples. On the other hand, cross-linking with formaldehyde did not improve our results, which could probably be associated with the internalization of Sgc8-aptamer target, PTK7, followed by the endocytosis and subsequent lysosomal degradation. For future experiments, photocross-linking could be used, which excludes the non-specific cross-linking of adjacent proteins and their further pull-down and identification.

To conclude, the identification of internalizing aptamer-protein target complexes is a complicated and challenging task, and if the aptamer target is located on a cellular membrane, the membrane isolation with further target identification procedures should be performed before MS analysis, which would decrease the number of irrelevant proteins identified, and it will facilitate the analysis of post MS results.

Chapter V: Materials and Methods

Aptamer-conjugated Tb(III)-doped silica nanoparticles for efficient luminescent leukemia cells detection

Reagents and Materials

Tetraethyl orthosilicate (TEOS, 98%), ammonium hydroxide (28–30%), n-heptanol (98%), 3-aminopropyltriethoxysilane (99%), succinic anhydride (99%), N,N-dimethylformamide (DMF, 99.5%), β-alanine, fluorescamine and acetic acid were purchased from Acros Organics and used without further purification. Terbium (III) nitrate hexahydrate (99.9%), sulfo-NHS and glutaraldehyde (50 wt% in H_2O) were from Alfa Aesar. Triton X-100, cyclohexane (99%), NaH_2PO_4, Na_2HPO_4, NaCl, Dullbecco's phosphate buffered saline (PBS, 1X with Ca/Mg), BSA and 4-morpholineethanesulfonic acid hydrate (MES, 99%) were purchased from Sigma-Aldrich. N-(3-dimethylaminopropyl)-N'-ethylcarbodiimide hydrochloride (EDAC) was purchased from Fluka Analytical. $Na_2B_4O_7$ was purchased from EMD Chemicals, Inc.

DMF, Ethanol and TEOS were purified by distillation. The synthesis of *p*-sulfonatothiacalix[4]arene tetrasodium salt (TCAS) was carried out according to the classical procedure[87].

Oligonucleotides

Single-stranded DNA aptamers with conjugated FITC dye – FITC-Sgc8 (5'-FITC-TTT TTT TTT TAT CTA ACT GCT GCG CCG CCG GGA AAA TAC TGT ACG GTT AGA-3') and conjugated amino-group - -NH_2 -Sgc-8 (5'-NH_2-TTT TTT TTT TAT CTA ACT GCT GCG CCG CCG GGA AAA TAC TGT ACG GTT AGA-3') were purchased IDT DNA Technologies, USA.

Cell lines

All cell lines (CCRF-CEM, Raji, Jurkat) were purchased from American Type Culture Collection (ATCC) and grown in RPMI media 1640 (1X, Gibco by Life Technologies^{TM}) supplemented with 10% FBS (Gibco by Life Technologies^{TM}) and 1-2% of antibiotics (Streptomycin-Penicillin, Gibco by Life Technologies^{TM}, Ref. 15140-122). Cells were maintained in the cell culturing incubator with a humidified atmosphere at 37 ^{o}C with 5% CO_2.

Synthesis of amino-modified [Tb(TCAS)]-doped silica nanoparticles SNs-NH2 was performed according to the procedure published in[80,126]. Carboxyl-modified [Tb(TCAS)]-doped silica nanoparticles SNs-COOH were synthesized using the protocol published in[127]. The extent of the substitution of amino- to carboxyl-groups was measured using fluorescamine-based procedure at pH 9[128].

Bioconjugation of SNs-COOH by 5'-NH_2-Sgc8 aptamer was performed according to the protocol[94] using EDAC and sulfo-NHS. 1 mg of EDAC, 2.5 mg of sulfo-NHS, 0.05 ml of 5'-NH_2-Sgc8 aptamer (10 μM) were added to the dispersion of SNs-COOH (1 g L^{-1}, 1 mL) in MES (100 mM, pH = 5.65), and then incubated at room temperature with gentle shaking during 3 hours. After, nanoparticles were washed three times with PBS (C = 100 mM, pH = 7.4) and redispersed in PBS+BSA (0.05%) solution during 1 hour. Aptamer-conjugated nanoparticles SNs(COOH)-Sgc8 were washed with $Na_2B_4O_7$ (0.05 M, pH=9, with 1% BSA) and stored at 4^{o}C.

Synthesis of SNs-COH and their bioconjugation by 5'-NH2-Sgc8 aptamer SNs(COH)-Sgc8 were performed according to the protocol[94]. Dispersion of SNs-NH_2 (1 g L^{-1}, 1 mL) was washed two times with PBS (100 mM, pH=7.4, 1 ml). After the second wash, nanoparticles were suspended in 1 mL of 8% glutaraldehyde solution in PBS. The reaction was carried out for 6 hours at room temperature with gentle shaking (speed 600). SNs-COH were washed two times with PBS

(0.5 mL) and centrifuged. 1 ml of 5'-NH_2-Sgc8 aptamer solution (10 μM, in PBS) was added to washed nanoparticles (pH=7.4), and nanoparticles were left at room temperature with shaking for 4 hours. Afterwards, modified nanoparticles were washed two times with PBS, and quenching solution (30 mM glycine + 0.05% BSA in PBS) was added. After 30 minutes, SNs(COH)-Sgc8 nanoparticles were centrifuged again and suspended in storage buffer (PBS+ 0.05 % BSA) and placed at 4ºC.

The quantitative analysis of amino groups on the surface silica nanoparticles modified by APTES was based on the reported protocol using fluorescamine[128]. Asparagine solutions in the concentration range $6.25x10^{-3}$ –$1x10^{-1}$ mM in 50 mM of borate buffer (pH=9.0) and 0.924 M of fluorescamine were used as a standard to make the calibration curve. For the quantitative analysis of Sgc8-aptamer on the surface of Tb-doped silica nanoparticles, Sgc8-aptamer solutions in the concentration range 3.75 $x10^{-2}$ –1.5 μM in 50 mM of borate buffer (pH=9.0) were used. All samples were dispersed in in 50 mM of borate buffer (pH=9.0), and the concentration of nanoparticles in both cases was 0.05 g L^{-1}. Excitation of samples was performed at 390 nm, and emission was detected at 485 nm.

Nanoparticles size and morphology were studied using FEI Tecani G2 spirit Transmission Electron Microscope with a LaB6 emitter. The images were acquired under an accelerating voltage of 120 kV. Samples were ultrasonicated in absolute ethanol for 10 min, and then applied on 200 mesh copper grids with continuous formvar support films.

Zeta potential (ξ-potential) was measured using Zetasizer NanoZS (Malvern Instruments) instrument and Dispersion Technology Software (Nano Series, copyright 2008). All samples were diluted in bi-distilled water filtered through 0.45 μm Millipore nylon membrane filter (Millipore-

Q water purification system). Samples were ultrasonicated for 30 min using ultrasonication bath prior the measurements.

UV-Vis spectra were obtained with Cary Eclipse (Agilent) spectrophotometer. All samples were dispersed in Millipore-Q water. Tb-TCAS-COOH and Tb-TCAS-NH_2 concentration was 0.5 g L^{-1}, Sgc8 aptamer concentration was 10 µM.

Luminescence of amino- and carboxyl-modified [Tb(TCAS)]-doped nanoparticles was measured using Cary Eclipse fluorescence spectrophotometer. All samples were prepared in bi-distilled water (Millipore-Q water purification system) with concentration of Tb-TCAS nanoparticles 0.05 g/L. Samples were excited at 330 nm.

Flow cytometric analysis was performed in order to evaluate Sgc-8 aptamer binding to leukemia cells. Cells were centrifuged (200 *g*, 3 minutes, 4 C^o) and washed with PBS two times. Then, cells were incubated at 4 C^o with Sgc8 aptamer (200 nM), DNA library (200 nM) and Anti-PTK7 Antibody (5 µg/mL) for 30 minutes at dark. After incubation, samples were washed three times in order to wash away all the unbound sequences, and analyzed with Gallios Flow Cytometer (Beckman Coulter). Propidium iodide was used for detection of all the dead cells, and only viable single cell population was gated.

Fluorescence microscopy images were acquired with Nikon Ni-U ratiometric fluorescence microscope with dual excitation sources and UPLANS apo 60xw objective. Images were captured with Orca R2 (Hamamatsu) CCD camera and analyzed through ImagePro software (Media Cybernetics, Bethesda, MD, USA). Cells ($6x10^6$ cells) were washed with 10 mL of PBS two times, and incubated with SNs-COOH-Sgc8 and SNs-NH_2-Sgc8 nanoparticles (5 µg mL^{-1}). After incubation, samples were washed two times with PBS and added dropwise to the polylysine-

coated microscopy slides that allow better adhesion of suspension cells. After 10 minutes, glass slides were washed with PBS two times and sealed for further analysis.

Cell viability assay with Annexin V-FITC and Propidium Iodide was performed according to the published protocol[104]. Briefly, CCRF-CEM cells (8 10^6 cells) were incubated with different concentrations (0 µg mL^{-1}, 25 µg mL^{-1}, 50 µg mL^{-1} and 100 µg mL^{-1}) of SNs-COOH-Sgc8 nanoparticles. After 24 and 48 hours, cells were centrifuged and washed with 10 mL of PBS two times, and suspended in 100 µL of binding buffer. Then, 6 µL Annexin V-FITC/PI mixture was added to all samples and they were left at dark for 15 minutes at 4 C°. Finally, 400 µL of binding buffer were added to the samples, and they were analyzed with Gallios Flow Cytometer (Beckman Coulter).

Statistical analysis was performed using the OriginPro software.

Sgc8-aptamer molecular target confirmation using AptaBiD

Reagents and Materials

Phosphate buffer saline (PBS, pH=7.4, Gibco by Life Technologies™, 10010023), Triton X-100, (99%, Sigma-Aldrich, 9002-93-1), digitonin (99%, Sigma-Aldrich, 11024-24-1), n-dodecyl-β-D-maltopyranoside (Thermo Scientific™, 89902), formaldehyde solution (36.5-38% in H_2O, Sigma-Aldrich, 50-0-0), streptavidin-coated magnetic beads (Pierce™, 88817), Trypsin/Lis-C solution (200 ng/µl, Promega, V5072), HEPES (99%, Sigma-Aldrich, 7365-45-9), DTT (1,4-dithiothreitol, 97%, Sigma-Aldrich, 3483-12-3), urea (Thermo Scientific™, 15505035), TCEP (Tris(2-carboxyethyl)phosphine hydrochloride, Sigma-Aldrich, 51805-45-9), iodoacetamide (Sigma-Aldrich, 144-48-9), formic acid (98%, Sigma-Aldrich, 64-18-6), 0.1% formic acid in water (MS grade,

Pierce^{TM}, 85171), acetonitrile (99%, MS grade, Pierce^{TM}, 51101), TopTip (10-200 UL, Pierce^{TM}, 87782), Propidium Iodide/RNAse staining solution (FxCycle^{TM}, F10797), Anti-PTK7 Antibody-APC (Biolegend^{TM}, 357347), Anti-human CD4-PE/Cy7 antibody (Biolegend^{TM}, 357409) and Anti-CD3-FITC antibody(Biolegend^{TM}, 317305), Lymphocyte Separation Medium (LSM, Corning^{TM}, 25-072-CI).

Buffers and solutions

Cell lysis buffer (detergent at CMC in water), protein digestion buffer (8 M urea, detergent at CMC, 10 mM DTT and 100 mM HEPES, pH 8.0), alkylation buffer (500 mM iodoacetamide), reduction buffer (100 mM TCEP,) elution buffer (70% acetonitrile + 0.1% FA), washing buffer (0.1% formic acid in water).

Oligonucleotides

Single-stranded DNA aptamers with conjugated FAM dye - Sgc8-FAM (5'-FAM-TTT TTT TTT TAT CTA ACT GCT GCG CCG CCG GGA AAA TAC TGT ACG GTT AGA-3') and conjugated biotin - Sgc-8-Bio (5'-Bio-TTT TTT TTT TAT CTA ACT GCT GCG CCG CCG GGA AAA TAC TGT ACG GTT AGA-3'), N40-FAM DNA library (5'-FAM- CTC CTC TGA CTG TAA CCA CG (N1: 25/25/25/25) (N1) (N1) (N1) (N1) (N1) (N1) (N1) (N1) (N1) (N1) (N1) (N1) (N1) (N1) (N1) (N1) (N1) (N1) (N1) (N1) (N1) (N1) (N1) (N1) (N1) (N1) (N1) (N1) (N1) (N1) (N1) (N1) (N1) (N1) (N1) (N1) (N1) (N1) (N1) (N1) GCA TAG GTA GTC CAG AAG CC -3'), Apt9-Bio (5'-Bio-CTC CTC TGA CTG TAA CCA CGG CGC AAG CCG GGG TGT ACG TGT TAT ACG TGC GTG TAT CGA GCA TAG GTA GTC CAG AAG CC-3'), masking scrambled non-labelled DNA (5'-CTC CTC TGA CTG TAA CCA CGC TGT TCA CGA CCG TGT ACA CGT GTT GCG TAT TCG

TCC GAG TAC GCA TGT GTA AGA TGT CCG CAT AGG TAG TCC AGA AGC C-3') were purchased IDT DNA Technologies, USA.

Cell lines

All cell lines (CCRF-CEM, Raji, Jurkat) were purchased from American Type Culture Collection (ATCC) and grown in RPMI media 1640 (1X, Gibco by Life Technologies™) supplemented with 10% FBS (Gibco by Life Technologies™) and 1-2% of antibiotics (Streptomycin-Penicillin, Gibco by Life Technologies™, Ref. 15140-122). Cells were maintained in the cell culturing incubator with a humidified atmosphere at 37 ºC with 5% CO_2.

Human whole blood

Whole blood of healthy human was obtained from Stemcell Technologies. Whole blood leukocytes were isolated by standard procedures using Lymphoprep (Stemcell Technologies, 07801) gradient centrifugation to remove erythrocytes

Flow cytometric analysis was performed in order to evaluate Sgc-8 aptamer binding to leukemia cells. Cells were centrifuged (200 *xg*, 3 minutes, 4 C^o) and washed with PBS two times. Then, cells were incubated at 4 C^o with FAM-Sgc8 aptamer (200 nM), FAM-DNA library (200 nM) and APC-Anti-PTK7 Antibody (5 µg/mL) for 30 minutes at dark. After incubation, samples were washed three times in order to wash away all the unbound sequences, and analyzed with Gallios Flow Cytometer (Beckman Coulter). Propidium Iodide was used for detection of all the dead cells, and only viable single cell population was gated.

Human PMBC isolation and Flow cytometric analysis

3 mL of lymphocyte separation medium (LSM) was gently mixed and added to 15 mL centrifuge tube, and 2 mL of defibrinated blood were mixed with 2 ml of PBS (-Ca, -Mg), and diluted blood was carefully layered on the top of the LSM, creating a sharp blood-LSM interphase, avoiding mixing. Then, the tube was centrifuged at 400 g at room temperature for 20 min. The top layer with clear plasma was aspirated to within 2-3 mm above the lymphocyte layer and discarded. The lymphocyte layer was then again aspirated and diluted with PBS (approximately 3 volumes of the layer) into a new centrifuge tube, and centrifuged for 10 minutes at room temperature at 260 g. Afterwards, cells were washed in order to remove LSM and reduce amount of platelets. Samples with lymphocytes were washed again and diluted in 1 mL of PBS. Then, samples containing FAM-Sgc8 aptamer (200 nM), Anti-human CD4-PE/Cy7 antibody (5 µg/mL) and Anti-CD3-FITC antibody (5 µg/mL) were prepared and incubated at 4 C^{o} for 30 minutes at dark. After the incubation, samples were washed three times in order to wash away all the unbound sequences, and analyzed with Gallios Flow Cytometer (Beckman Coulter). Propidium iodide was used for detection of all the dead cells, and only viable single cell population was gated.

Aptamer protein target pull-down with magnetic beads

10 mL of cell suspension was added to 15 mL tube, and centrifuged with PBS (-Ca/-Mg) for 5 minutes at 3000 rpm. Then, after the supernatant was discarded, 1 mL of PBS (-Ca/-Mg) was added, and cell suspension was transferred to a 1.5 mL microtube, and centrifuged again using the same conditions. All samples were incubated with masking scrambled DNA oligonucleotide (non-binding, non-labeled random aptamer) at a final concentration of 2 µM by shaking at room temperature for 30 minutes at 270 rpm. Biotinylated aptamers were refolded by heating to 95 °C for 10 minutes, cooling

at room temperature for 10 minutes, and cooling at 4 C^o for 10 minutes. Then, samples were incubated with the biotinylated aptamer at a final concentration of 0.7 µM by shaking at 270 rpm for 30 minutes at room temperature. 20 µL of 14% formaldehyde was added to samples in order to induce cross-linking by shaking at 270 rpm for 30 minutes at room temperature. 20 µg/µL of streptavidin-coated magnetic beads was added to all samples and incubated for 30 minutes by shaking at 270 rpm for 30 minutes at 4 C^o to capture the aptamer-protein complexes. Then, beads were collected by a magnetic stand (10 minutes). Collected magnetic beads were incubated with 100 µL of lysis buffer by shaking for 30 minutes at 270 rpm. Then, collected magnetic beads were washed 2 times in 200 µl of cell lysis buffer, and 2 times in 200 µl of MS grade ddH_2O.

Protein reduction, alkylation and tryptic digestion

25 µL of the protein digestion buffer and 4 µL of protein reducing buffer were added to each sample. Incubation was performed for 45 minutes at room temperature, and then, 4 µL of freshly prepared protein alkylation buffer was added to samples, and they were incubated for 60 minutes in the dark at room temperature. 1.5 µL of trypsin/Lys-C Mix solution was added to samples and incubation was conducted overnight (16 hours) at room temperature. Then, 1 µL of 100% formic acid was added to protein samples. Final concentration of formic acid is typically between 0.5-1% in water. Samples were vortexed well, and then centrifuged for 30 s at high speed (10 000 RPM), and precipitate was transferred to new microtubes.

Desalting of digested samples

C18 tip was prepared by loading 50 µL of the elution buffer into the top of the C18 tip. Then, the elution buffer was pushed through the C18 material by a plastic syringe. TopTip (10-200 UL, Pierce™, 87782) was removed from the pipettor, and this washing procedure was repeated 2 times.

C18 column (10-200 UL, Pierce™, 87782) was equilibrated by loading 50 µL of the washing buffer onto the C18 tip and pushing/sucking the buffer through it. After, TopTip (10-200 UL, Pierce™, 87782) was removed from the pipettor, and this washing procedure was repeated 2 times. 75 µL of sample solution was loaded onto the C18 tip and slowly pushed over the C18 phase. The procedure was repeated 3 more times. The packed bed was washed 3 times with 50 µL of the washing solution in order to elute salts and other non-retained components. The packed bed was washed 3 times with 50 µL of eluting solution (while now collecting eluent). The eluent was combined in order to elute all of the adsorbed peptides. Solvent was evaporated using the Speed-Vac (Thermo Scientific™, SPD-210-230).

MS analysis

EASY nano-LC system coupled with Q Exactive Plus mass spectrometer (Thermo Scientific™) were used for the analysis of peptides with an Acclaim PepMap RSLC 75 µm IDx150 mm length separation column (Thermo Scientific™,). 2 µl of a sample were injected and separated by the following gradient (A – 0.1% formic acid in H_2O, B – 100% acetonitrile, 0.1% formic acid in H_2O) with the flow of 300 nl/min: 0.0-73.0 min 5-40% B, 73.0-76.0 min 40-100% B, 76.0-85.0 min 100% B, 85.0-91.0 min 100-0% B, 91-100.0 min 0% B. Nano-ESI conditions: spray voltage in positive mode – 2100 V; ion transfer tube temperature – 250 °C; S-lens RF level – 60. Full scan resolutions were set to 70 000 at m/z 200. Full scan target was 3×106 with a maximum fill time of 200 ms. Mass range was set to 350–1800 m/z. Target value for fragment scans was set at 1×105 and isolation width was set at 2 m/z. Resolution for HCD spectra was set to 17,500 at m/z 200, and normalized collision energy was set at 28. All data was acquired in data-depending mode using positive polarity. The raw data was processed using Proteome Discoverer (version 1.4.1.14, Thermo Scientific™). MS^2 spectra were searched with SEQUEST HT engine through the UniProt

database for Homo sapiens (Human) (http://www.uniprot.org). Peptides were generated from a tryptic digestion with up to two missed cleavages, carbamidomethylation of cysteines as fixed modifications, and oxidation of methionines and protein N-terminal acetylation as variable modifications. Precursor mass tolerance was 10 ppm and product ions were searched at 0.6 Da tolerances. Peptide spectral matches (PSM) were validated using a target decoy validation with FDR of 1%.

Bioinformatics analysis

Bioinformatics analysis was performed using the R programming language. Proteins were considered identified if they were found in at least two technical triplicates. Further analysis was done by comparing the presence of proteins in Sgc8-aptamer and control samples. Candidate proteins were annotated with Gene Ontology Cellular Component terms[129] and filtered for transmembrane proteins.

Table S1. Aptamers and their protein targets identified by AptaBiD

Target Protein	Cancer type / Cell line	Aptamer sequence (5'-3')	K_d, nM	Pull-down procedures	References
Vimentin	Human ovarian cancer / IGROV and HMVECs cells	V5:cgctcggatcgataagcttcgCATAGACCCAGCTGGTCCGGAAAATAAGATgtcacggatcctctagagcactg	N/A	Cross-linking with 1% formaldehyde and further pull-down of cell lysates after centrifugation with biotinylated aptamers and streptavidin-coated magnetic beads	Wang H. et al.[30]
Vimentin	Lung cancer tissue and circulating tumor cells	LC-18: CTCCTCTGAC TGTAACCACG TGCCCGAACGCGAGTTGAGT TCCGAGAGCT CCGACTTCTT GCATAGGTAG TCCAGAAGCC	38	Pull-down of cell lysates after centrifugation with biotinylated aptamers and streptavidin-coated magnetic beads.	Zamay G. et al.[28]
Vimentin	Mouse Erlich ascites adenocarcinoma cells	NAS24: CTC CTC TGA CTG TAA CCA CGC CTG GGA CAG CCA CAC AGA AGT GTA GAC CTC GCG GAA TCG GCA TAG GTA GTC CAG AAG CC	5.9	Pull-down of cell lysates after centrifugation with biotinylated aptamers and streptavidin-coated magnetic beads.	Zamay T.N. et al.[29]
Tenascin-C	Human glioblastoma / U251 cell line	GBI-10: ggctgttgtgagcctcctCCCAGAGGGAAGACTTTAGGTTCGGTTCACGTCCcgcttattcttactccc	N/A	Pull-down of cell lysates after centrifugation with biotinylated aptamers and streptavidin-coated magnetic beads.	Daniels D. et al.[25]
IHMC (Immunoglobulin Heavy Mu Chain)	Burkitt's lymphoma / Ramos cells	TD05: ACCGGGAGGAUAGTUCGGTGGCTGTTCAGGGUCTCCUCCCGGTG-S-S-T-PEG	N/A	Photocross-linking with further pull-down of cell lysates after centrifugation with biotinylated aptamers and streptavidin-coated magnetic beads	Malikaratchy P. et al.[13]

CD109	Nasopharyngal carcinoma / NPC 5-8F	S3: atccagagtgacgcagcaTCTGAGAATAGTGGTTTGCTGTATGGTGGGCGTTGAAAGAGGGGtggacacg gtggcttagt	12	Pull-down of cell lysates with biotinylated aptamers and streptavidin-coated sepharose beads.	Jia W. et al.[24]
PTK7 / protein tyrosine kinase	T-cell acute lymphoblastic leukemia (T-all) / CCRF-CEM cell line	Sgc8: ATCTAACTGCTGCGCCGCCGGGAAAATACTGTACGGTTAGA	0.8	Pull-down of cell lysates after centrifugation with biotinylated aptamers and streptavidin-coated magnetic beads.	Shangguan D. et al.[97]
Siglec-5	Acute myelogenous leukemia / NB4 AML cell line	K19: gacgcttactcaggtgtgactcgAAGGGGTTGGGTGGGTTTATACAAATTAATTAATATTGTATGGTATA TTTcgaaggacgcagatgaagtctc	12.37	Pull-down of cell lysates after centrifugation with biotinylated aptamers and streptavidin-coated magnetic beads.	Yang M. et al.[23]
Selectin L Integrin α4	Human acute T-cell leukemia / Jurkat 6E1 cell line	Sgc–3b:TTTACTTATTCAATTCCCGTGGGAAGGCTATAGAGGGGCCAGTCTATGAATAAGTTT Sgc-4e: TTTATCACTTATTCAATTCGAGTGCGGATGCAAACGCCAGACAGGGGGACAGGAGATAAGT GATTT	N/A	Cross-linking with 2% formaldehyde and further pull-down of cell lysates after centrifugation with biotinylated aptamers and streptavidin-coated magnetic beads	Bing T. et al.[31]
Rat homologue of mouse pigpen protein	Adenovirys-12 SV40 transformed endothelial cells / YPEN-1 cell line	AptamerIII.1:taccagcttattcaattAGGCGGTGCATTGTGGTTGGTAGTATACATGAGGTTTGGTTGAG ACTAGTCGCAAGATATagatagtaagtgcaatct	N/A	Pull-down of cell lysates after centrifugation with biotinylated aptamers and streptavidin-coated magnetic beads.	Blank M. et al.[130]

EFFR vIII	Primary glioblastoma / U87MG cell line	Apt32:gcaatggtacggtacttccTGAATGTTGTTTTTTCTCTTTTCTATAGTAcaaaagtgcacgctactttgctaa	0.62	Pull-down of cell lysates after centrifugation with biotinylated aptamers and streptavidin-coated magnetic beads.	Tan Y. et al.[131]
HCV envelope glycoprotein E2	Murine colon carcinoma / CT26 cell line, HCV positive	ZE2: gcggaattctaatacgactcactatagggaacagtccgagccGAATGAGGAATAATCTAGCTCCTTCGCTGAgggtcaatgcgtcata	1.05	N/A	Chen F. et al.[132]
ALPPL-2	Pancreatic carcinoma / Panc-1 and Capan-1 cell lines	SQ-2: auaccagcuuauucaauuGCCUGAAAAGCUAUCGCCCAAUUCGCAGUGAUAUCCUUUAagauaguaagugcaaucu	22.5 - 24.74	Pull-down of cell lysates after centrifugation with biotinylated aptamers and streptavidin-coated magnetic beads.	Dua P. et al.[26]
c-kit	Burkitt's lymphoblastoma / BJAB	Kit-129: gcagcacagaggtcagatgGCTCAACGCGGGACGGCTCTCCCATTGACcctatgcgtgctaccgtgaa	12.21	N/A	Meyer S. et al.[133]
Filamin A α-subunit of mitochondrial ATP synthase	Ehrlich ascites adenocarcinoma cells	AS14: ctcctctgactgtaaccacgCTCCTCTGACTGTAACCACGAAGGTGTCGGCCTTAGTAAGGCTACAGCCAAGGGAACGTAGCATAGGTAGTCCAGAAGCCgcataggtagtccagaagcc AS9:ctcctctgactgtaaccacgCTCCTCTGACTGTAACCACGACTGAGCTTTGGTGGGTCGAGCTATGTGCTGCCTCTTCACGCATAGGTAGTCCAGAAGCCgcataggtagtccagaagcc	3.8 0.75	Pull-down of cell lysates after centrifugation with biotinylated aptamers and streptavidin-coated magnetic beads.	Kolovskaya O.S.et al.[27]
CD279 (PD-1)	Murine mastocytoma – P815 cell line	MP7.1: gacgatagcggtgacggcacagacgGTACAGTTCCCGTCCCTGCACTACAcgtatgccgcttccgtccgtcgctc	167	As SELEX was performed using PD-1 recombinant chimera consisting of the mPD-1 extracellular domain fused to a histidine-tagged	Prodeus A. et al.[33]

				human Fc domain as a target and there were no pull-down procedures performed.	
CD274 (PD-L1)	Murine colon carcinoma - CT26 cell line and murine Lewis lung carcinoma – LL/2 cell line	aptPD-L1: ACG GGC CAC ATC AAC TCA TTG ATA GAC AAT GCG TCC ACT GCC CGT	72	As SELEX was performed using PD-L1 protein as a target there were no pull-down procedures performed.	Lai W-T., et al.[34]

References

1 Kim, Y., Liu, C. & Tan, W. Aptamers generated by Cell SELEX for biomarker discovery. *Biomark Med* **3**, 193-202, doi:10.2217/bmm.09.5 (2009).

2 Siegel, R. L., Miller, K. D. & Jemal, A. Cancer Statistics, 2017. *CA Cancer J Clin* **67**, 7-30, doi:10.3322/caac.21387 (2017).

3 Etzioni, R. *et al.* The case for early detection. *Nat Rev Cancer* **3**, 243-252, doi:10.1038/nrc1041 (2003).

4 Pepe, M. S. *et al.* Phases of biomarker development for early detection of cancer. *J Natl Cancer Inst* **93**, 1054-1061 (2001).

5 Gorenstein, A. S. a. D. G. Vol. S1:001 1-5 (Translational Medicine, 2011).

6 Kelly, D. J. & Ghosh, S. RNA profiling for biomarker discovery: practical considerations for limiting sample sizes. *Dis Markers* **21**, 43-48 (2005).

7 Meyer, H. E. & Stühler, K. High-performance proteomics as a tool in biomarker discovery. *Proteomics* **7 Suppl 1**, 18-26, doi:10.1002/pmic.200700183 (2007).

8 Rifai, N., Gillette, M. A. & Carr, S. A. Protein biomarker discovery and validation: the long and uncertain path to clinical utility. *Nat Biotechnol* **24**, 971-983, doi:10.1038/nbt1235 (2006).

9 Diamandis, E. P. Mass spectrometry as a diagnostic and a cancer biomarker discovery tool: opportunities and potential limitations. *Mol Cell Proteomics* **3**, 367-378, doi:10.1074/mcp.R400007-MCP200 (2004).

10 Norton, S. M., Huyn, P., Hastings, C. A. & Heller, J. C. Data mining of spectroscopic data for biomarker discovery. *Curr Opin Drug Discov Devel* **4**, 325-331 (2001).

11 Bledi, Y., Inberg, A. & Linial, M. PROCEED: A proteomic method for analysing plasma membrane proteins in living mammalian cells. *Brief Funct Genomic Proteomic* **2**, 254-265 (2003).

12 Oh, P. *et al.* Subtractive proteomic mapping of the endothelial surface in lung and solid tumours for tissue-specific therapy. *Nature* **429**, 629-635, doi:10.1038/nature02580 (2004).

13 Mallikaratchy, P. *et al.* Aptamer directly evolved from live cells recognizes membrane bound immunoglobin heavy mu chain in Burkitt's lymphoma cells. *Mol Cell Proteomics* **6**, 2230-2238, doi:10.1074/mcp.M700026-MCP200 (2007).

14 Kingsmore, S. F. Multiplexed protein measurement: technologies and applications of protein and antibody arrays. *Nat Rev Drug Discov* **5**, 310-320, doi:10.1038/nrd2006 (2006).

15 Nelson, B. P. Multiplexed antibody arrays for the discovery and validation of glycosylated protein biomarkers. *Bioanalysis* **1**, 1431-1444, doi:10.4155/bio.09.119 (2009).

16 Ayoglu, B. *et al.* Systematic antibody and antigen-based proteomic profiling with microarrays. *Expert Rev Mol Diagn* **11**, 219-234, doi:10.1586/erm.10.110 (2011).

17 Gold, L. *et al.* Aptamer-based multiplexed proteomic technology for biomarker discovery. *PLoS One* **5**, e15004, doi:10.1371/journal.pone.0015004 (2010).

18 Chang, Y. M., Donovan, M. J. & Tan, W. Using aptamers for cancer biomarker discovery. *J Nucleic Acids* **2013**, 817350, doi:10.1155/2013/817350 (2013).

19 Berezovski, M. V., Lechmann, M., Musheev, M. U., Mak, T. W. & Krylov, S. N. Aptamer-facilitated biomarker discovery (AptaBiD). *J Am Chem Soc* **130**, 9137-9143, doi:10.1021/ja801951p (2008).

20 Fang, X. & Tan, W. Aptamers generated from cell-SELEX for molecular medicine: a chemical biology approach. *Acc Chem Res* **43**, 48-57, doi:10.1021/ar900101s (2010).

21 Weihong Tan, X. F. XIII, 352 (Springer-Verlag Berlin Heidelberg Berlin, 2015).

22 Ye, M. *et al.* Generating aptamers by cell-SELEX for applications in molecular medicine. *Int J Mol Sci* **13**, 3341-3353, doi:10.3390/ijms13033341 (2012).

23 Yang, M. *et al.* Developing aptamer probes for acute myelogenous leukemia detection and surface protein biomarker discovery. *J Hematol Oncol* **7**, 5, doi:10.1186/1756-8722-7-5 (2014).

24 Jia, W. *et al.* CD109 is identified as a potential nasopharyngeal carcinoma biomarker using aptamer selected by cell-SELEX. *Oncotarget* **7**, 55328-55342, doi:10.18632/oncotarget.10530 (2016).

25 Daniels, D. A., Chen, H., Hicke, B. J., Swiderek, K. M. & Gold, L. A tenascin-C aptamer identified by tumor cell SELEX: systematic evolution of ligands by exponential enrichment. *Proc Natl Acad Sci U S A* **100**, 15416-15421, doi:10.1073/pnas.2136683100 (2003).

26 Dua, P. *et al.* Alkaline phosphatase ALPPL-2 is a novel pancreatic carcinoma-associated protein. *Cancer Res* **73**, 1934-1945, doi:10.1158/0008-5472.CAN-12-3682 (2013).

27 O.S., K. Vol. 8 (ed Zamay A.S. Zamay T.N., Glazyrin Y.E., Spivak E.A., Zubkova O.A., Kadkina A.V., Erkaev E.N., Zamay G.S., Savitskaya A.G., Trufanova L.V.,

Petrova L.L., Berezovski M.V.) 60-72 (Biochemistry (Moscow) Supplement Series A: Membrane and Cell Biology, 2014).

28 Zamay, G. S. *et al.* DNA Aptamers for the Characterization of Histological Structure of Lung Adenocarcinoma. *Mol Ther Nucleic Acids* **6**, 150-162, doi:10.1016/j.omtn.2016.12.004 (2017).

29 Zamay, T. N. *et al.* DNA-aptamer targeting vimentin for tumor therapy in vivo. *Nucleic Acid Ther* **24**, 160-170, doi:10.1089/nat.2013.0471 (2014).

30 Wang, H. *et al.* Morph-X-Select: Morphology-based tissue aptamer selection for ovarian cancer biomarker discovery. *Biotechniques* **61**, 249-259, doi:10.2144/000114473 (2016).

31 Bing, T., Shangguan, D. & Wang, Y. Facile Discovery of Cell-Surface Protein Targets of Cancer Cell Aptamers. *Mol Cell Proteomics* **14**, 2692-2700, doi:10.1074/mcp.M115.051243 (2015).

32 Seddon, A. M., Curnow, P. & Booth, P. J. Membrane proteins, lipids and detergents: not just a soap opera. *Biochim Biophys Acta* **1666**, 105-117, doi:10.1016/j.bbamem.2004.04.011 (2004).

33 Prodeus, A. *et al.* Targeting the PD-1/PD-L1 Immune Evasion Axis With DNA Aptamers as a Novel Therapeutic Strategy for the Treatment of Disseminated Cancers. *Mol Ther Nucleic Acids* **4**, e237, doi:10.1038/mtna.2015.11 (2015).

34 Lai, W. Y., Huang, B. T., Wang, J. W., Lin, P. Y. & Yang, P. C. A Novel PD-L1-targeting Antagonistic DNA Aptamer With Antitumor Effects. *Molecular Therapy-Nucleic Acids* **5**, 9, doi:10.1038/mtna.2016.102 (2016).

35 Meisenheimer, K. M. & Koch, T. H. Photocross-linking of nucleic acids to associated proteins. *Crit Rev Biochem Mol Biol* **32**, 101-140, doi:10.3109/10409239709108550 (1997).

36 Jensen, O. N. *et al.* Direct observation of UV-crosslinked protein-nucleic acid complexes by matrix-assisted laser desorption ionization mass spectrometry. *Rapid Commun Mass Spectrom* **7**, 496-501, doi:10.1002/rcm.1290070619 (1993).

37 Bennett, S. E., Jensen, O. N., Barofsky, D. F. & Mosbaugh, D. W. UV-catalyzed Cross-linking of *Escherichia coli* Uracil-DNA Glycosylase to DNA. *Journal of Biological Chemistry* **269**, 21870-21879 (1994).

38 Ole N. Jensen, D. F. B., Mark C. Young, Peter H. von Hippel, Stephen Swenson, Steven E. Seifried. Vol. 5 27-37 (Techniques in Protein Chemistry, 1994).

39 Connor, D. A., Falick, A. M. & Shetlar, M. D. UV light-induced cross-linking of nucleosides, nucleotides and a dinucleotide to the carboxy-terminal heptad repeat peptide of RNA polymerase II as studied by mass spectrometry. *Photochem Photobiol* **68**, 1-8 (1998).

40 David L. Wong, J. G. P., Norbert O. Reich. Vol. 26 645-649 (Nucleic Acids Research, 1998).

41 Golden, M. C., Resing, K. A., Collins, B. D., Willis, M. C. & Koch, T. H. Mass spectral characterization of a protein-nucleic acid photocrosslink. *Protein Sci* **8**, 2806-2812, doi:10.1110/ps.8.12.2806 (1999).

42 Jemal, A. *et al.* Cancer statistics, 2008. *CA Cancer J Clin* **58**, 71-96, doi:10.3322/CA.2007.0010 (2008).

43 Xie, Y., Davies, S. M., Xiang, Y., Robison, L. L. & Ross, J. A. Trends in leukemia incidence and survival in the United States (1973-1998). *Cancer* **97**, 2229-2235, doi:10.1002/cncr.11316 (2003).

44 Emrani, A. S., Danesh, N. M., Ramezani, M., Taghdisi, S. M. & Abnous, K. A novel fluorescent aptasensor based on hairpin structure of complementary strand of aptamer and nanoparticles as a signal amplification approach for ultrasensitive detection of cocaine. *Biosens Bioelectron* **79**, 288-293, doi:10.1016/j.bios.2015.12.025 (2016).

45 Song, K. M., Lee, S. & Ban, C. Aptamers and their biological applications. *Sensors (Basel)* **12**, 612-631, doi:10.3390/s120100612 (2012).

46 Shangguan, D. *et al.* Aptamers evolved from live cells as effective molecular probes for cancer study. *Proc Natl Acad Sci U S A* **103**, 11838-11843, doi:10.1073/pnas.0602615103 (2006).

47 Shangguan, D., Tang, Z., Mallikaratchy, P., Xiao, Z. & Tan, W. Optimization and modifications of aptamers selected from live cancer cell lines. *Chembiochem* **8**, 603-606, doi:10.1002/cbic.200600532 (2007).

48 Danesh, N. M., Lavaee, P., Ramezani, M., Abnous, K. & Taghdisi, S. M. Targeted and controlled release delivery of daunorubicin to T-cell acute lymphoblastic leukemia by aptamer-modified gold nanoparticles. *Int J Pharm* **489**, 311-317, doi:10.1016/j.ijpharm.2015.04.072 (2015).

49 Taghdisi, S. M. *et al.* Double targeting, controlled release and reversible delivery of daunorubicin to cancer cells by polyvalent aptamers-modified gold nanoparticles. *Mater Sci Eng C Mater Biol Appl* **61**, 753-761, doi:10.1016/j.msec.2016.01.009 (2016).

50 Sefah, K. *et al.* Molecular recognition of acute myeloid leukemia using aptamers. *Leukemia* **23**, 235-244, doi:10.1038/leu.2008.335 (2009).

51 Zhao, N. *et al.* Oligonucleotide aptamer-drug conjugates for targeted therapy of acute myeloid leukemia. *Biomaterials* **67**, 42-51, doi:10.1016/j.biomaterials.2015.07.025 (2015).

52 Yang, L. *et al.* Aptamer-conjugated nanomaterials and their applications. *Adv Drug Deliv Rev* **63**, 1361-1370, doi:10.1016/j.addr.2011.10.002 (2011).

53 Vasilescu, A. *et al.* Surface Plasmon Resonance based sensing of lysozyme in serum on Micrococcus lysodeikticus-modified graphene oxide surfaces. *Biosens Bioelectron* **89**, 525-531, doi:10.1016/j.bios.2016.03.040 (2017).

54 Abnous, K., Danesh, N. M., Sarreshtehdar Emrani, A., Ramezani, M. & Taghdisi, S. M. A novel fluorescent aptasensor based on silica nanoparticles, PicoGreen and exonuclease III as a signal amplification method for ultrasensitive detection of myoglobin. *Anal Chim Acta* **917**, 71-78, doi:10.1016/j.aca.2016.02.036 (2016).

55 Estévez, M.-C., O'Donoghue, M. B., Chen, X. & Tan, W. Highly fluorescent dye-doped silica nanoparticles increase flow cytometry sensitivity for cancer cell monitoring. *Nano Res.* **2**, 448–461 (2009).

56 Chen, X. *et al.* Using aptamer-conjugated fluorescence resonance energy transfer nanoparticles for multiplexed cancer cell monitoring. *Anal Chem* **81**, 7009-7014, doi:10.1021/ac9011073 (2009).

57 Herr, J. K., Smith, J. E., Medley, C. D., Shangguan, D. & Tan, W. Aptamer-conjugated nanoparticles for selective collection and detection of cancer cells. *Anal Chem* **78**, 2918-2924, doi:10.1021/ac052015r (2006).

58 Cornell, B. A. *et al.* A biosensor that uses ion-channel switches. *Nature* **387**, 580-583, doi:10.1038/42432 (1997).

59 Ramezani, M., Mohammad Danesh, N., Lavaee, P., Abnous, K. & Mohammad Taghdisi, S. A novel colorimetric triple-helix molecular switch aptasensor for ultrasensitive detection of tetracycline. *Biosens Bioelectron* **70**, 181-187, doi:10.1016/j.bios.2015.03.040 (2015).

60 Benson, J. *et al.* Direct patterning of gold nanoparticles using flexographic printing for biosensing applications. *Nanoscale Res Lett* **10**, 127, doi:10.1186/s11671-015-0835-1 (2015).

61 Wei, L. *et al.* Colorimetric assay for protein detection based on "nano-pumpkin" induced aggregation of peptide-decorated gold nanoparticles. *Biosens Bioelectron* **71**, 348-352, doi:10.1016/j.bios.2015.04.072 (2015).

62 Ye, X. *et al.* Iodide-Responsive Cu-Au Nanoparticle-Based Colorimetric Platform for Ultrasensitive Detection of Target Cancer Cells. *Anal Chem* **87**, 7141-7147, doi:10.1021/acs.analchem.5b00943 (2015).

63 Wang, H. *et al.* Immunophenotyping of acute leukemia using an integrated piezoelectric immunosensor array. *Anal Chem* **76**, 2203-2209, doi:10.1021/ac035102x (2004).

64 Tan, L. *et al.* In vitro study on the individual and synergistic cytotoxicity of adriamycin and selenium nanoparticles against Bel7402 cells with a quartz crystal microbalance. *Biosens Bioelectron* **24**, 2268-2272, doi:10.1016/j.bios.2008.10.030 (2009).

65 Pan, Y. *et al.* Selective collection and detection of leukemia cells on a magnet-quartz crystal microbalance system using aptamer-conjugated magnetic beads. *Biosens Bioelectron* **25**, 1609-1614, doi:10.1016/j.bios.2009.11.022 (2010).

66 Jiang, X. C. & Yu, A. B. Silver nanoplates: a highly sensitive material toward inorganic anions. *Langmuir* **24**, 4300-4309, doi:10.1021/la7032252 (2008).

67 Li, H., Hu, H. & Xu, D. Silver decahedral nanoparticles-enhanced fluorescence resonance energy transfer sensor for specific cell imaging. *Anal Chem* **87**, 3826-3833, doi:10.1021/ac5045274 (2015).

68 Zhang, M. *et al.* A disposable electrochemiluminescence device for ultrasensitive monitoring of K562 leukemia cells based on aptamers and ZnO@carbon quantum dots. *Biosens Bioelectron* **49**, 79-85, doi:10.1016/j.bios.2013.05.003 (2013).

69 Khoshfetrat, S. M. & Mehrgardi, M. A. Amplified detection of leukemia cancer cells using an aptamer-conjugated gold-coated magnetic nanoparticles on a nitrogen-doped graphene modified electrode. *Bioelectrochemistry* **114**, 24-32, doi:10.1016/j.bioelechem.2016.12.001 (2017).

70 Siegel, R. L., Miller, K. D. & Jemal, A. Cancer statistics, 2018. *CA Cancer J Clin* **68**, 7-30, doi:10.3322/caac.21442 (2018).

71 Chari, R. V. Targeted cancer therapy: conferring specificity to cytotoxic drugs. *Acc Chem Res* **41**, 98-107, doi:10.1021/ar700108g (2008).

72 Barth, B. M. *et al.* Targeted indocyanine-green-loaded calcium phosphosilicate nanoparticles for in vivo photodynamic therapy of leukemia. *ACS Nano* **5**, 5325-5337, doi:10.1021/nn2005766 (2011).

73 Jayasena, S. D. Aptamers: an emerging class of molecules that rival antibodies in diagnostics. *Clin Chem* **45**, 1628-1650 (1999).

74 Bagalkot, V., Farokhzad, O. C., Langer, R. & Jon, S. An aptamer-doxorubicin physical conjugate as a novel targeted drug-delivery platform. *Angew Chem Int Ed Engl* **45**, 8149-8152, doi:10.1002/anie.200602251 (2006).

75 Tang, J. *et al.* Aptamer-conjugated PEGylated quantum dots targeting epidermal growth factor receptor variant III for fluorescence imaging of glioma. *Int J Nanomedicine* **12**, 3899-3911, doi:10.2147/IJN.S133166 (2017).

76 Chen, M., Bi, S., Jia, X. & He, P. Aptamer-conjugated bio-bar-code Au-Fe3O4 nanoparticles as amplification station for electrochemiluminescence detection of tumor cells. *Anal Chim Acta* **837**, 44-51, doi:10.1016/j.aca.2014.05.035 (2014).

77 Deng, N. *et al.* Aptamer-conjugated gold functionalized graphene oxide nanocomposites for human α-thrombin specific recognition. *J Chromatogr A* **1427**, 16-21, doi:10.1016/j.chroma.2015.12.018 (2016).

78 Liu, Q. *et al.* Aptamer-conjugated nanomaterials for specific cancer cell recognition and targeted cancer therapy. *NPG Asia Mater* **6**, doi:10.1038/am.2014.12 (2014).

79 Tan, J. *et al.* Aptamer-Functionalized Fluorescent Silica Nanoparticles for Highly Sensitive Detection of Leukemia Cells. *Nanoscale Res Lett* **11**, 298, doi:10.1186/s11671-016-1512-8 (2016).

80 Fedorenko, S. V. *et al.* Cellular imaging by green luminescence of Tb(III)-doped aminomodified silica nanoparticles. *Mater Sci Eng C Mater Biol Appl* **76**, 551-558, doi:10.1016/j.msec.2017.03.106 (2017).

81 Runowski, M. *et al.* Synthesis and organic surface modification of luminescent, lanthanide-doped core/shell nanomaterials (LnF3@SiO2@NH2@organic acid) for

potential bioapplications: spectroscopic, structural, and in vitro cytotoxicity evaluation. *Langmuir* **30**, 9533-9543, doi:10.1021/la501107a (2014).

82 Min, Y. *et al.* Recent Advance of Biological Molecular Imaging Based on Lanthanide-Doped Upconversion-Luminescent Nanomaterials. *Nanomaterials (Basel)* **4**, 129-154, doi:10.3390/nano4010129 (2014).

83 Kang, X. *et al.* Lanthanide-doped hollow nanomaterials as theranostic agents. *Wiley Interdiscip Rev Nanomed Nanobiotechnol* **6**, 80-101, doi:10.1002/wnan.1251 (2014).

84 Mukhametshina, A. R. *et al.* Tb(III)-doped silica nanoparticles for sensing: effect of interfacial interactions on substrate-induced luminescent response. *Langmuir* **31**, 611-619, doi:10.1021/la503074p (2015).

85 Iki, N., Ohta, M., Horiuchi, T. & Hoshino, H. Exceptionally long-lived luminescence emitted from Tb(III) ion caged in an Ag(I)-Tb(III)-thiacalix[4]arene supramolecular complex in water. *Chem Asian J* **3**, 849-853, doi:10.1002/asia.200700298 (2008).

86 Parker, D., Dickins, R. S., Puschmann, H., Crossland, C. & Howard, J. A. Being excited by lanthanide coordination complexes: aqua species, chirality, excited-state chemistry, and exchange dynamics. *Chem Rev* **102**, 1977-2010 (2002).

87 Iki, N. *et al.* 2219-2225 (J. Chem. Soc., Perkin Trans. 2, 2001).

88 Tamba, B. I. *et al.* Silica nanoparticles: preparation, characterization and in vitro/in vivo biodistribution studies. *Eur J Pharm Sci* **71**, 46-55, doi:10.1016/j.ejps.2015.02.002 (2015).

89 Veeranarayanan, S. *et al.* FITC labeled silica nanoparticles as efficient cell tags: uptake and photostability study in endothelial cells. *J Fluoresc* **22**, 537-548, doi:10.1007/s10895-011-0991-3 (2012).

90 Mustafina, A. R. *et al.* Novel highly charged silica-coated Tb(III) nanoparticles with fluorescent properties sensitive to ion exchange and energy transfer processes in aqueous dispersions. *Langmuir* **25**, 3146-3151, doi:10.1021/la8032572 (2009).

91 Fatema, U. K., Rahman, M. M., Islam, M. R., Mollah, M. Y. A. & Susan, M. A. B. H. Silver/poly(vinyl alcohol) nanocomposite film prepared using water in oil microemulsion for antibacterial applications. *J Colloid Interface Sci* **514**, 648-655, doi:10.1016/j.jcis.2017.12.084 (2018).

92 Ye, Z., Tan, M., Wang, G. & Yuan, J. Preparation, characterization, and time-resolved fluorometric application of silica-coated terbium(III) fluorescent nanoparticles. *Anal Chem* **76**, 513-518, doi:10.1021/ac030177m (2004).

93 Mandal, D., Ghosh, M., Maiti, S., Das, K. & Das, P. K. Water-in-oil microemulsion doped with gold nanoparticle decorated single walled carbon nanotube: scaffold for enhancing lipase activity. *Colloids Surf B Biointerfaces* **113**, 442-449, doi:10.1016/j.colsurfb.2013.09.047 (2014).

94 (Fishers IN: Bangs Laboratory Inc., 2002).

95 Niknejad, H. & Mahmoudzadeh, R. Comparison of Different Crosslinking Methods for Preparation of Docetaxel-loaded Albumin Nanoparticles. *Iran J Pharm Res* **14**, 385-394 (2015).

96 Mukhametshina, A. R. *et al.* The energy transfer based fluorescent approach to detect the formation of silica supported phosphatidylcholine and phosphatidylserine containing bilayers. *Colloids Surf B Biointerfaces* **115**, 93-99, doi:10.1016/j.colsurfb.2013.11.035 (2014).

97 Shangguan, D. *et al.* Cell-specific aptamer probes for membrane protein elucidation in cancer cells. *J Proteome Res* **7**, 2133-2139, doi:10.1021/pr700894d (2008).

98 Zembruski, N. C., Stache, V., Haefeli, W. E. & Weiss, J. 7-Aminoactinomycin D for apoptosis staining in flow cytometry. *Anal Biochem* **429**, 79-81, doi:10.1016/j.ab.2012.07.005 (2012).

99 Fakhri, A. Assessment of Ethidium bromide and Ethidium monoazide bromide removal from aqueous matrices by adsorption on cupric oxide nanoparticles. *Ecotoxicol Environ Saf* **104**, 386-392, doi:10.1016/j.ecoenv.2013.12.017 (2014).

100 Kim, I. Y., Joachim, E., Choi, H. & Kim, K. Toxicity of silica nanoparticles depends on size, dose, and cell type. *Nanomedicine* **11**, 1407-1416, doi:10.1016/j.nano.2015.03.004 (2015).

101 Sun, L. *et al.* Cytotoxicity and mitochondrial damage caused by silica nanoparticles. *Toxicol In Vitro* **25**, 1619-1629, doi:10.1016/j.tiv.2011.06.012 (2011).

102 Rim, K. T., Koo, K. H. & Park, J. S. Toxicological evaluations of rare earths and their health impacts to workers: a literature review. *Saf Health Work* **4**, 12-26, doi:10.5491/SHAW.2013.4.1.12 (2013).

103 Shimada, H., Nagano, M., Funakoshi, T. & Kojima, S. Pulmonary toxicity of systemic terbium chloride in mice. *J Toxicol Environ Health* **48**, 81-92, doi:10.1080/009841096161483 (1996).

104 Rieger, A. M., Nelson, K. L., Konowalchuk, J. D. & Barreda, D. R. Modified annexin V/propidium iodide apoptosis assay for accurate assessment of cell death. *J Vis Exp*, doi:10.3791/2597 (2011).

105 Wang, N. *et al.* Visible absorption spectra of the 4f electron transitions of neodymium, praseodymium, holmium and erbium complexes with fleroxacin and their analytical application. *Anal Sci* **18**, 591-594 (2002).

106 Hemmer, E. *et al.* Upconverting and NIR emitting rare earth based nanostructures for NIR-bioimaging. *Nanoscale* **5**, 11339-11361, doi:10.1039/c3nr02286b (2013).

107 Yazdian-Robati, R., Arab, A., Ramezani, M., Abnous, K. & Taghdisi, S. M. Application of aptamers in treatment and diagnosis of leukemia. *Int J Pharm* **529**, 44-54, doi:10.1016/j.ijpharm.2017.06.058 (2017).

108 Lin, Y. *et al.* PTK7 as a novel marker for favorable gastric cancer patient survival. *J Surg Oncol* **106**, 880-886, doi:10.1002/jso.23154 (2012).

109 Chen, R. *et al.* A meta-analysis of lung cancer gene expression identifies PTK7 as a survival gene in lung adenocarcinoma. *Cancer Res* **74**, 2892-2902, doi:10.1158/0008-5472.CAN-13-2775 (2014).

110 Jung, P. *et al.* Isolation of Human Colon Stem Cells Using Surface Expression of PTK7. *Stem Cell Reports* **5**, 979-987, doi:10.1016/j.stemcr.2015.10.003 (2015).

111 Shin, W. S. *et al.* Soluble PTK7 inhibits tube formation, migration, and invasion of endothelial cells and angiogenesis. *Biochem Biophys Res Commun* **371**, 793-798, doi:10.1016/j.bbrc.2008.04.168 (2008).

112 Citartan, M., Gopinath, S. C., Tominaga, J., Tan, S. C. & Tang, T. H. Assays for aptamer-based platforms. *Biosens Bioelectron* **34**, 1-11, doi:10.1016/j.bios.2012.01.002 (2012).

113 Lee, K. H. & Zeng, H. Aptamer-Based ELISA Assay for Highly Specific and Sensitive Detection of Zika NS1 Protein. *Anal Chem* **89**, 12743-12748, doi:10.1021/acs.analchem.7b02862 (2017).

114 Guskov, A. S. a. A. Vol. 7 16 (Crystals, 2017).

115 Chae, P. S. *et al.* A new class of amphiphiles bearing rigid hydrophobic groups for solubilization and stabilization of membrane proteins. *Chemistry* **18**, 9485-9490, doi:10.1002/chem.201200069 (2012).

116 Zhang, Z. & Chen, J. Atomic Structure of the Cystic Fibrosis Transmembrane Conductance Regulator. *Cell* **167**, 1586-1597.e1589, doi:10.1016/j.cell.2016.11.014 (2016).

117 Moharram, S. A., Shah, K. & Kazi, J. U. T-cell Acute Lymphoblastic Leukemia Cells Display Activation of Different Survival Pathways. *J Cancer* **8**, 4124, doi:10.7150/jca.21725 (2017).

118 Ashani, Y. & Catravas, G. N. Highly reactive impurities in Triton X-100 and Brij 35: partial characterization and removal. *Anal Biochem* **109**, 55-62 (1980).

119 McPherson, A. & Gavira, J. A. Introduction to protein crystallization. *Acta Crystallogr F Struct Biol Commun* **70**, 2-20, doi:10.1107/S2053230X13033141 (2014).

120 Xiao, Z., Shangguan, D., Cao, Z., Fang, X. & Tan, W. Cell-specific internalization study of an aptamer from whole cell selection. *Chemistry* **14**, 1769-1775, doi:10.1002/chem.200701330 (2008).

121 Shnitsar, I. & Borchers, A. PTK7 recruits dsh to regulate neural crest migration. *Development* **135**, 4015-4024, doi:10.1242/dev.023556 (2008).

122 Wehner, P., Shnitsar, I., Urlaub, H. & Borchers, A. RACK1 is a novel interaction partner of PTK7 that is required for neural tube closure. *Development* **138**, 1321-1327, doi:10.1242/dev.056291 (2011).

123 Chae, P. S. *et al.* Maltose-neopentyl glycol (MNG) amphiphiles for solubilization, stabilization and crystallization of membrane proteins. *Nat Methods* **7**, 1003-1008, doi:10.1038/nmeth.1526 (2010).

124 Slotboom, D. J., Duurkens, R. H., Olieman, K. & Erkens, G. B. Static light scattering to characterize membrane proteins in detergent solution. *Methods* **46**, 73-82, doi:10.1016/j.ymeth.2008.06.012 (2008).

125 Drabik, A. *et al.* Advances in the Study of Aptamer-Protein Target Identification Using the Chromatographic Approach. *J Proteome Res* **17**, 2174-2181, doi:10.1021/acs.jproteome.8b00122 (2018).

126 Mukhametshina, A. *et al.* Luminescent nanoparticles for rapid monitoring of endogenous acetylcholine release in mice atria. *Luminescence* **33**, 588-593, doi:10.1002/bio.3450 (2018).

127 An, Y., Chen, M., Xue, Q. & Liu, W. Preparation and self-assembly of carboxylic acid-functionalized silica. *J Colloid Interface Sci* **311**, 507-513, doi:10.1016/j.jcis.2007.02.084 (2007).

128 Chen, Y. & Zhang, Y. Fluorescent quantification of amino groups on silica nanoparticle surfaces. *Anal Bioanal Chem* **399**, 2503-2509, doi:10.1007/s00216-010-4622-7 (2011).

129 Ashburner, M. *et al.* Gene ontology: tool for the unification of biology. The Gene Ontology Consortium. *Nat Genet* **25**, 25-29, doi:10.1038/75556 (2000).

130 Blank, M., Weinschenk, T., Priemer, M. & Schluesener, H. Systematic evolution of a DNA aptamer binding to rat brain tumor microvessels. selective targeting of endothelial regulatory protein pigpen. *J Biol Chem* **276**, 16464-16468, doi:10.1074/jbc.M100347200 (2001).

131 Tan, Y. *et al.* DNA aptamers that target human glioblastoma multiforme cells overexpressing epidermal growth factor receptor variant III in vitro. *Acta Pharmacol Sin* **34**, 1491-1498, doi:10.1038/aps.2013.137 (2013).

132 Chen, F., Hu, Y., Li, D., Chen, H. & Zhang, X. L. CS-SELEX generates high-affinity ssDNA aptamers as molecular probes for hepatitis C virus envelope glycoprotein E2. *PLoS One* **4**, e8142, doi:10.1371/journal.pone.0008142 (2009).

133 Meyer, S. *et al.* Development of an efficient targeted cell-SELEX procedure for DNA aptamer reagents. *PLoS One* **8**, e71798, doi:10.1371/journal.pone.0071798 (2013).